



Investigation on the Emulsification and Microencapsulation of Olive Oil

Doctoral (Ph.D.) dissertation by

Donia CHAABANE

DOI: 10.54598/005560

Under the supervision of

Dr. András Koris and

and

Dr. Krisztina Albert

Hungarian University of Agriculture and Life Sciences

Institute of Food Science and Technology

Department of Food Engineering

Budapest, 2023

The PhD School

Name: Doctoral School of Food Science

Discipline: Food science

Head: **Dr. Livia Simonné Sarkadi**
Professor, DSc,
Hungarian University of Agriculture and Life Sciences

Institute of Food Science and Technology

Department of Nutrition

Supervisors: **Dr. András Koris**
Full Professor, PhD,
Hungarian University of Agriculture and Life Sciences

Institute of Food Science and Technology

Department of Food Process Engineering

Dr. Krisztina Albert
Assistant Professor, PhD,
Hungarian University of Agriculture and Life Sciences

Institute of Food Science and Technology

Department of Food Engineering

Approval signature of Head of the doctoral school and supervisors:

The candidate has fulfilled all the conditions prescribed by the Doctoral School of Hungarian University of Agriculture and Life Sciences, the comments and suggestion at the thesis workshop were taken into consideration when revising the thesis, so the dissertation can be submitted to a public debate.

.....

Signature of Head of PhD School

.....

Signature of Supervisor

.....

Signature of Supervisor

Contents

Abbreviations	6
1. INTRODUCTION.....	1
2. LITERATURE REVIEW	5
2.1. Main composition of olive oil	5
2.2. Oxidative deterioration of olive oil	6
2.2.1. Hydrolysis	7
2.2.2. Lipid oxidation	8
2.2.3. Photosensitized oxidation.....	9
2.3. Microencapsulation	9
2.4. Emulsification	10
2.4.1. Membrane emulsification technology	11
2.4.2. ME process controlling parameters	13
2.5. Emulsifier	15
2.6. Wall material (matrix)	17
2.7. Technologies to prepare olive oil microcapsule.....	19
2.7.1. Spray drying	21
2.7.2. Freeze drying.....	23
2.7.3. Coacervation.....	24
2.7.4. Extrusion	25
2.7.5. Microencapsulation by ionic gelation	26
2.8. Characterization of microencapsulated olive oil	27
2.9. Applications of microencapsulated olive oil	30
2.9.1. Foods	30
2.9.2. Pharmaceuticals.....	30
2.9.3. Cosmetics	31
2.10. Summary	32

3. MATERIALS AND METHODS	33
3.1. Materials.....	33
3.1.1. Bioactive compound: olive oil	33
3.1.2. Wall materials	33
3.1.3. Solvents and chemicals	33
3.2. Methods.....	34
3.2.1. Charecteristics of olive oil.....	34
3.2.2. Emulsions preparation.....	37
3.2.3. Emulsion characterisation	41
3.2.4. Emulsion dehydration (ED)	43
3.2.5. Powder characterization	44
3.2.6. Preparation of olive oil beads by gelation of sodium alginate or emulsification - external gelation method	47
4. RESULTS AND DISCUSSION	50
4.1. Characterization of olive oil.....	50
4.2. Membrane emulsification of olive oil by different combinations of wall materials: Preliminary study	51
4.2.1. Formulation and preparation of olive oil emulsion.....	51
4.2.2. Size and morphology.....	53
4.2.3. Emulsification results.....	54
4.2.4. Emulsions stability	56
4.2.5. Summary	57
4.3. Effect of change of emulsification method and wall material composition on microencapsulation of olive oil	58
4.3.1. Formulation of the emulsions.....	59
4.3.2. Emulsions stability	60
4.3.3. Emulsion droplet size and span	60
4.3.4. Encapsulation Efficiency.....	62

4.3.5. Particle size and span	63
4.3.6. Moisture content.....	64
4.3.7. Morphology of OOM	64
4.2.8. Summary: Comparison of Emulsification Methods for OOM Properties.....	65
4.4. Effect of change of the drying method and wall material composition on the microencapsulation of extra virgin olive oil	65
4.4.1. Description of the formulation of the feeding emulsions.....	66
4.4.2. Emulsion characterization	66
4.4.3. Powder analysis.....	70
4.4.4. Process intensification by using CFME coupled with SD to the optimum sample	80
4.4.4.3. Stability to oxidation of microencapsules	81
4.4.5. Summary	84
4.5. Investigation of microencapsulation of olive oil by external gelation to obtain alginate/olive oil capsules	85
4.5.1. Optimization of the process parameters for preparation of capsules with high oil phase content	86
4.5.2. Summary: Modeling and optimization of the emulsions for the preparation of capsules with high oil phase content	98
5 CONCLUSIONS AND RECOMMENDATIONS	100
6 NEW SCIENTIFIC RESULTS	103
7 SUMMARY	104
Appendices	107
Annex 1 References	107
Annex 2	119
ACKNOWLEDGEMENT	124

Abbreviations

Wall materials

MD	maltodextrin
DE	dextrose equivalent
GA	gum arabic
CMC	carboxymethylcellulose
WPI	whey protein isolate
Tween-80	polyoxyethylene sorbitan monooleate
Tween-20	polyoxyethylene sorbitan monolaurate

General terms

CFME	cross flow membrane emulsification
D ₃₂	particle mean diameter
D ₄₃	volume mean diameter
ED	Emulsion dehydration
FD	freeze drying
FSEM	field emission scanning electron microscope
GC-MS	gas chromatography-mass spectrometry
HPLC	high-performance liquid chromatography
IP	Induction period
MANOVA	multivariate analysis of variance
ND	Not determined
OO	Olive oil
OOE	Olive oil emulsion
OOM	Olive oil microcapsule
RC	Retention capacity
RSH	rotor stator homogenization
RT	room temperature
SD	spray drying
SPSS	statistics software
T _g	glass-transition temperature
TMP	transmembrane pressure

Response surface methodology

A	Sodium alginate concentration %
B	Olive oil concentration %
C	Homogenization rate rpm
ANOVA	analysis of variance
BBD	Box-Behnken design
DOE	design of expert
RSM	response surface methodology
SS	sum of squares
Std. Dev.	standard deviation
C.V. %	coefficients of variation
R ²	coefficient of determination
df	degree of freedom

1. INTRODUCTION

Olive oil is obtained from the fruit of the olive tree (*Olea europea L.*). It is widely produced in Spain, Italy, Tunisia, Greece, and Turkey. For a long time, in the diet of mentioned countries, three main grades of olive oil, such as refined, virgin, and extra virgin olive oil were received a great importance (Gunstone, 2011). Olive oil is highly appreciated for its fine taste and aroma as well as for its nutritional properties (Espí et al., 2021). Presently, olive oil is used to prepare ketogenic diet. Due to its unique biological importance, application of olive oil is not limited within diet chart and to prepare cuisines. Its application to develop biopharmaceuticals and cosmetics is noteworthy (Onsaard & Onsaard, 2019). Olive oil offers antioxidant, anti-inflammatory and antibacterial activities. It reduces the risk of several chronic and acute metabolic disorders, including cardiovascular diseases, Alzheimer's disease, cancer, type 2 diabetes, obesity and rheumatoid arthritis (Dahl et al., 2016). Therefore, acceptance of olive oil is not limited to the Mediterranean region. In present era, it crosses the boundary of mentioned countries and received popularity around the globe (Gaforio et al., 2019). Olive oil is enriched with monounsaturated fatty acids (ω -6 and ω -3 fatty acids), phenolic antioxidant compounds, vitamin E and vitamin K. Composition of olive oil may differ by several reasons, such as zone of cultivation, latitude, climate, quality of soil, genetic variety and maturity of olive fruits (Boskou, 2007). Dietary fat plays a major role in human nutrition and diet. Nutritional benefits of olive oil are primarily related to the fatty acid composition. Virgin olive oil contains two main fractions, such as saponifiable fraction (98.5–99.5%) and unsaponifiable fraction (0.5–1.5%). Saponifiable fraction consists of monoglycerides, diglycerides, triglycerides, free fatty acids and phospholipids. Unsaponifiable fraction of olive oil is enriched with essential ingredients of sterols, hydrocarbons, tocopherols, coloring pigments, phenols and triterpenes (Šarolić et al., 2014). Olive oil triacylglycerols are mainly represented by monounsaturated fatty acids (oleic acid), together with balanced ratio of saturated fatty acids and polyunsaturated fatty acids (mainly linoleic acid). Among the composition of the total fatty acid, monounsaturated fatty acids, saturated fatty acids and polyunsaturated fatty acids are 56–87%, 8–25% and 8–22%, respectively. Some polyunsaturated fatty acids with 18 carbons (C18) are known as essential fatty acids. Those are linoleic acid (18:2, ω -6) in an amount of 3.5–21% and α -linolenic acid (18:3, ω -3) in an amount up to 0.9% (Dahl et al., 2016; Gaforio et al., 2019). They are precursors of long-chain polyunsaturated fatty acids such as arachidonic acid (20:4 ω -6), or eicosapentaenoic (20:5 ω -3) and docosahexaenoic (22:6 ω -3) (Fig. 1).

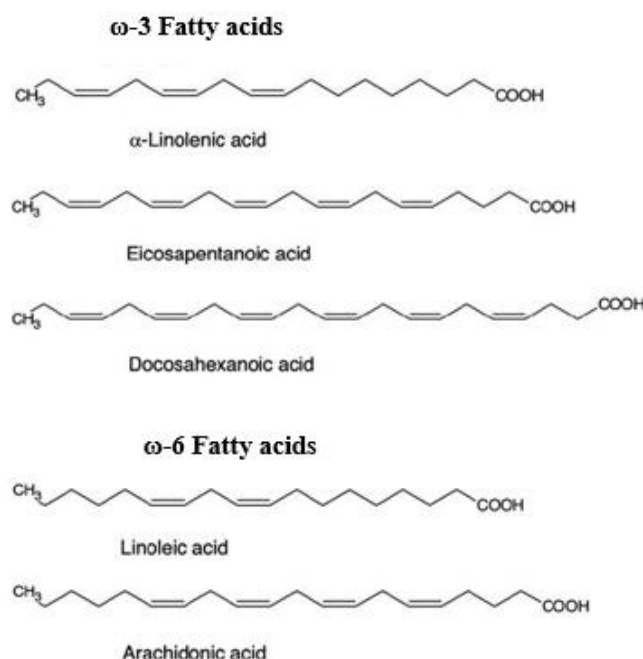


Figure 1. Different types of ω -3 and ω -6 fatty acids in olive oil and there metabolites (self-developed the concept was adopted from (Viola & Viola, 2009)).

The ratio ω -6/ ω -3 in olive oil is highly satisfied, since the World Health Organization (WHO) has recommended this ratio to be within 5:1 to 10:1 (Šarolić et al., 2014; Viola & Viola, 2009). ω -3 and ω -6 fatty acids play an important role in development of cell membrane, regulate fluidity of cell membrane and activities of precursor molecules of many physiological elements, those are involved in controlling inflammatory reactions, blood pressure, mortal cardiac diseases and cancer (la Lastra et al., 2005). In addition, total content of antioxidants (phenols) in olive oil is abundant (~500–1000 mg/kg) compared to other edible vegetable oils (Koidis & Boskou, 2014). Different types of polyphenols present in olive oil are represented in Fig. 2 (Dimitrios, 2006). Antioxidants are substances that prevent or slow down the process of oxidation in foods, biopharmaceuticals and cells within the body. The considerable amount of phenolic compounds, such as hydroxytyrosol and oleuropein are responsible for the unique taste and high stability of olive oil during storage and cooking (Šarolić et al., 2014). In olive oil, concentration of vitamin E (α -tocopherol) and vitamin K (phytonadione) are abundant. Tocopherols are methyl-substituted chromanols with a three-isoprene moiety in the side chain. Other tocopherols, such as α -, β -, γ -, and δ -tocopherols differ from one another by the number and position of methyl groups in the phenolic part of the chromane (benzodihydropyran) ring. The α -homologue contains three methyl groups. The β and γ homologues are dimethylated positional isomers. δ -tocopherol is monomethylated. They play an effective role in the inhibition of lipid oxidation in foods and biological systems (Psomiadou et al., 2000).

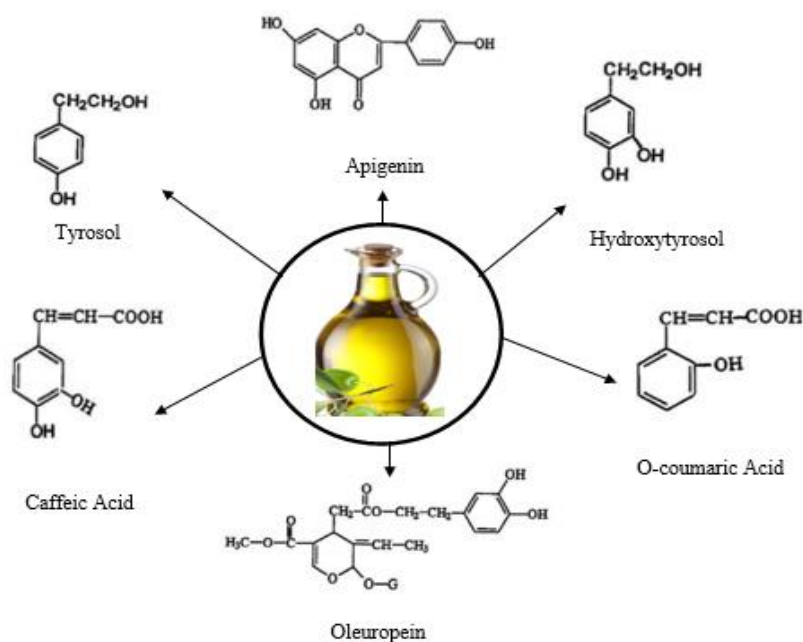


Figure 2: Different types of polyphenols present in olive oil (self-developed the concept was adopted from (Dimitrios, 2006))

Chemically, the vitamin K family comprises 2-methyl-1,4-naphthoquinone (3-) derivatives and includes two natural vitamers, such as vitamin K1 (phylloquinone) and vitamin K2 (menaquinone). They play a significant role in blood clotting, bone metabolism, level of calcium in blood and absorption of vitamin D in body (Otles & Cagindi, 2007). However, olive oil is enriched with antioxidant, often due to oxidation of fatty acid, sensory and nutritional properties of olive oil are altered (Morales and Przybylski, 2013). Oxidation of fatty acids leads to the formation of hydroperoxides carboxylic acids, aldehydes, ketones, and short chain alkenes and alkanes. They are responsible to reduce the shelf life of olive oil and consequently, unpleasant taste and odor are generated (Koidis & Boskou, 2014). One of the solutions to preserve the functional values of olive oil is its microencapsulation. It prevents the oxidation and increases the shelf life of olive oil (Calvo et al., 2012).

In the literature research part of my PhD work, information about olive oil composition and its oxidative deterioration was discussed. Then, different technologies of the microencapsulation of olive oil and biochemical characteristics of the microcapsule are discussed. In later exercise, applications of microencapsulated olive oil in food, cosmetic and biopharmaceutical industries are represented. Considering above-mentioned concerns, the objective of my PhD work is to find the most promising encapsulation materials and techniques for development of microcapsule systems that can be utilized for effective protection and gastrointestinal delivery

of bioactive and, simultaneously, can be well-adapted for industrial applications, thereby for developing novel functional foods. In order to solve these research problems, the following tasks were set to accomplish:

- As a preliminary study, I focused on emulsion preparation by cross flow membrane emulsification technology using a combination of maltodextrin (MD) with different other wall materials such as gum arabic (GA) alone, gum arabic with whey protein isolate (WPI) and gum arabic with carboxymethylcellulose (CMC).
- The second task was to study the effects of emulsification technologies, such as homogenization by rotor–stator homogenizer (RSH) and crossflow membrane emulsification (CFME) along with the effect of wall materials composition (MD, CMC and GA) on microencapsulation of olive oil by freeze drying method.
- The third task was to study the effects of change of the drying technology such as spray-drying and freeze-drying along with the wall materials composition (MD and WPI) to show up the more effective drying method.
- The final task was to study the emulsification/external gelation of olive oil to increase the oil load of the capsules. This method is an ionic gelation of olive oil emulsified with sodium alginate by a calcium chloride solution.
- The evaluation and comparison of the differently formed oil-loaded capsule systems regarding encapsulating wall materials and technique for their efficiency in delivery systems were based on the following physical and chemical aspects:
 - ✓ Particle size in both emulsion and powder
 - ✓ Morphology in both emulsion and powder
 - ✓ Encapsulation efficiency
 - ✓ Emulsion stability
 - ✓ Zeta potential
 - ✓ Span value
 - ✓ Powder solubility
 - ✓ Powder moisture contents
 - ✓ Accelerated rancimat test
 - ✓ Retention capacity for the gelation method

2. LITERATURE REVIEW

2.1. Main composition of olive oil

Olive oil is predominantly composed of the saponifiable fraction (98,5–99,5%) which consists of triacylglycerols, di- and monoacylglycerols, free fatty acids and phospholipids. An unsaponifiable fraction (0.5-1.5%) consists of a mixture of sterols, hydrocarbons, tocopherols, pigments, phenolic and volatile compounds. All these molecules contribute to the valuable characteristics of the extra VOO (Gaforio et al., 2019).

Table 1. Fatty acids composition of olive oil as determined by the codex standard.

Fatty acid	Carbon number	Allowed range (%)
lauric	C12:0	Not present in discernible amounts
myristic	C14:0	< 0.1
palmitic	C16:0	7.5-20.0
palmitoleic	C16:1	0.3-3.5
heptadecanoic	C17:0	< 0.5
heptadecenoic	C17:1	< 0.6
stearic	C18:0	0.5-5.0
oleic	C18:1	55.0-83.0
linoleic	C18:2	3.5-21.0
linolenic	C18:3	**
arachidic	C20:0	0.8
eicosenoic	C20:1	Not specified
behenic	C22:0	< 0.3
erucic	C22:1	Not present in discernible amounts
ligniceric	C24:0	< 1.0

Fatty acids are the most important components in olive oil. The fatty acid composition (Table 1) of olive oil consists of the following fatty acids: palmitic (C16:0), palmitoleic (C16:1), stearic (C18:0), oleic (C18:1), linoleic (C18:2), linolenic (C18:3), myristic (C14:0), heptadecanoic (C17:0) and eicosanoic (C20:1) acids are found in trace amounts. Fatty acid composition is influenced by many factors such as the zone of production, the latitude, the climate, the variety, and the maturation stage of the fruit. For example, Greek, Italian and Spanish olive oils have a low amount of linoleic and palmitic acids and big amounts of oleic

acid. Meanwhile, Tunisian olive oils have higher percentages of linoleic and palmitic acids and a lower percentage of oleic acid (Dimitrios, 2006).

Triacylglycerols (TAGs) are glycerol esters of fatty acids where the fatty acids are bound in groups of three together with a unit of glycerol (Figure 3). About 95–98% of olive oil consists of TAGs. The carbon chains may be different lengths and they may be saturated, monounsaturated, or polyunsaturated.

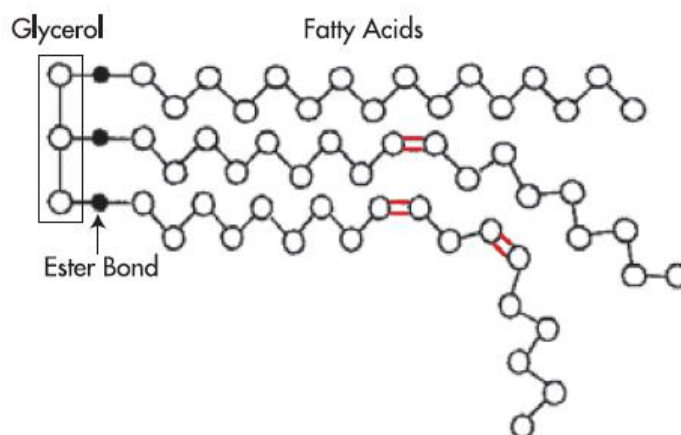


Figure 3 : Triacylglycerol (oil) molecule with three different fatty acids attached (Mailer et al., 2006).

Only when the fatty acids are bound in these small units, the olive oil is considered as good quality oil. A triacylglycerol unit may lose one fatty acid to become a diacylglycerol – if it loses two fatty acids, it is a monoacylglycerol. The fatty acid which is lost from the triacylglycerol is then called a free fatty acid (FFA). Triacylglycerols are created by three saturated fatty acids and glycerol. Under the influence of lipase enzymes this very vulnerable composition breaks and changes into glycerol and free fatty acids. This increases the acidity of the oil and creates what we call rancidity. This chemical reaction is the most serious damage that olive oil experiences (Morales and Przybylski, 2013).

Saturated triacylglycerols such as PPP, SSS, PSP, SPS etc. are never found in olive oil. In olive oil, the triacylglycerols found by Dimitrios. (2006) in significant proportions are OOO (40-59%), POO (12-20%), OOL (12.5-20%), POL (5.5-7%) and SOO (3-7%).

Unfortunately, the presence of unsaturation giving all the benefits for the olive oil also makes it sensitive to environmental attack, and more particularly to oxidative deterioration.

2.2. Oxidative deterioration of olive oil

The main processes leading to the deterioration of lipids are hydrolytic rancidity (lipolysis) and oxidative rancidity (oxidation). In olive oil, the former usually begins while the oil is in the

fruit, whereas the latter mainly occurs during the extraction process and storage. Oxidation can occur either in the dark (autooxidation) or in the presence of light (photo-oxidation) (Morales and Przybylski, 2013).

2.2.1. Hydrolysis

Lipolysis or hydrolysis is caused by the release of free fatty acids (FFAs) from glycerides. Hydrolytic rancidity is extremely important in determining how a product tastes; it is unlikely to be of any nutritional significance because fats are in any case enzymatically hydrolyzed in the small intestine before they are absorbed. Olive oil lipolysis results from microbial and enzymatic lipolysis. Olive oil lipolysis is the most important cause of negative changes and happens by enzymatic, microbial, and chemical reaction pathways (Morales and Przybylski, 2013).

2.2.1.1. Enzymatic pathway

The degradation of lipids in plant tissues is performed by a process often called the polyunsaturated fatty acid (PUFA) cascade. Typically, the decomposition of unsaturated fatty acids requires different enzymes as shown in Figure 4. The sequence begins with the hydrolysis of various acylglycerides by lipases, lipolytic acyl hydrolases and phospholipases, and free PUFAs are released. Lipoxygenases then convert unsaturated fatty acids into two main hydroperoxides, namely 9 and 13 isomers, which are unstable. In the last step of the cascade, lyases, isomerases, and dehydrogenases degrade hydroperoxides into a variety of volatile and nonvolatile products. The flavor components formed, such as aldehydes, ketones, and alcohols, can be directly responsible for the off-flavor occurrence in oils (Morales and Przybylski, 2013). In olives the formation of 13-hydroperoxides from linoleic and linolenic acids is promoted, leading to the formation of C6 aldehydes and alcohols, which are the main contributors to VOO sensory perception. Free unsaturated fatty acids, particularly linoleic and linolenic in plants, are the preferred substrates for oxidation by lipoxygenases.

2.2.1.2. Microbial pathway

Microbial enzymes cannot be excluded as an additional deterioration factor. The microorganisms present in the olive fruit liberate the enzyme lipase responsible for microbial lipolysis. The formation of small amounts of hydroperoxides can have an accelerating effect on oxidation in the finished oil. Free radicals formed from the decomposition of hydroperoxides can escalate further oxidation, causing earlier-than-expected off-flavor formation and lowering oil storage stability (Morales and Przybylski, 2013).

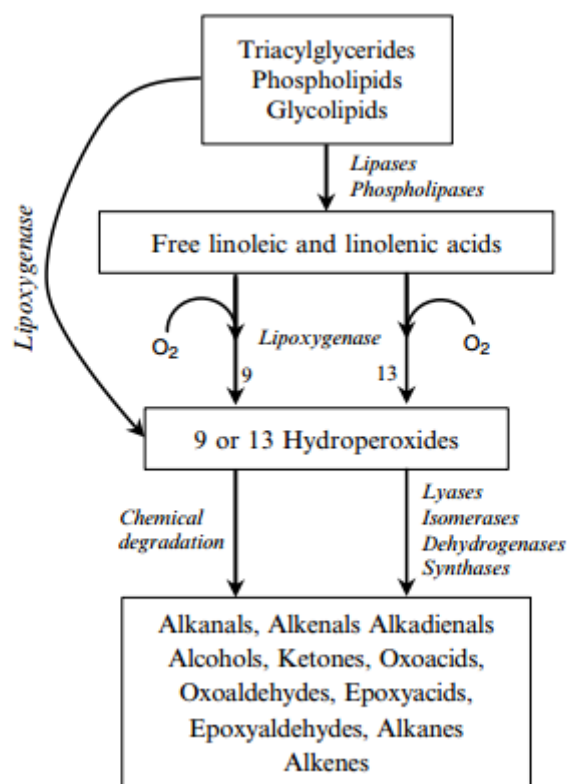


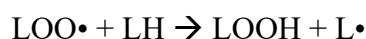
Figure 4: Enzymatic oxidation of unsaturated fatty acids. Numbers with lipoxxygenase represent enzymes producing specific isomers of hydroperoxide (Morales and Przybylski, 2013).

2.2.2 Lipid oxidation

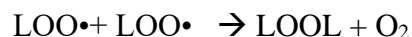
The reaction of oxygen with unsaturated fatty acids (LH) involves a free radical mechanism of lipid oxidation which is usually divided into three stages: initiation, propagation, and termination. The oxidation of lipids is accelerated by many factors such as light, temperature, enzymes, metals, metalloproteins, pigments, and microorganisms. In the initiation stage free radicals are formed directly from fatty acids in the presence of initiators such as temperature, light, other free radicals, and heavy metals. The resulting lipid free radicals ($L\bullet$) react with oxygen to form peroxy radicals ($LOO\bullet$). Formed at this propagation stage, peroxy radicals react with another molecule of lipid (LH), forming a lipid radical and a hydroperoxide ($LOOH$) which is a fundamental primary product of auto-oxidation. During the termination stage, radicals react with each other and form non-radical products. Any reaction that prevents the propagation of peroxidation or removes free radicals from the system plays a key role in the termination mechanism (Frankel, 1984):



Propagation $L\cdot + O_2 \rightarrow LOO\cdot$



Termination $L\cdot + L\cdot \rightarrow LL$



Metallic ion catalysts in the presence of small amounts of hydroperoxides are the most important initiators of lipid oxidation. Transition metals such as iron and copper catalyze both the initiation and decomposition of hydroperoxides.

2.2.3. Photosensitized oxidation

The mechanism of photosensitized oxidation consists of the transfer of energy from light to the photosensitizer (chlorophylls and pheophytins), which in turn can react directly with a lipid (RH), forming radicals ($R\cdot$) that in turn initiate autoxidation. Exposure of olive oil to light can cause the formation of hydroperoxides when both oxygen and the photosensitizer are present. This non free radical process favors the oxygen activation into the singlet state. Singlet oxygen has been found to react with linoleic acid about 1500 times faster than normal oxygen. Therefore, this reactive component is defined as the most important initiator in the free radical autoxidation of vegetable oils. This process is propagated by the free radical mechanism discussed earlier, and similar hydroperoxides are formed (Frankel, 1984).

To protect the oil from all the deterioration mechanisms listed above, we will proceed to encapsulate olive oil to preserve it. Thus, emulsifying technology is a key step for obtaining the dried form of olive oil.

2.3. Microencapsulation

Microencapsulation is an emerging technology, which is used to protect bioactive compounds within capsule and control their release in environment. In this process, a small droplet of liquid or solid particles are surrounded by coating within a thin film, known as a wall material or matrix (Bakry et al. 2016; Poshadri and Kuna 2010; Rodríguez et al. 2016). Different techniques have been adopted for the microencapsulation of food grade bioactive compounds. They can be classified into three categories. Those are herein: 1. physical methods: spray drying, lyophilization, supercritical encapsulation and solvent evaporation 2. physico-chemical methods: coacervation, ionic gelation, and molecular inclusion 3. chemical methods: interfacial polymerization and molecular inclusion complexation (Ozkan et al., 2019). For the

microencapsulation of olive oil, the first step is the preparation of aqueous emulsion of olive oil with matrix. Subsequently, dehydration of emulsion by spray drying or freeze drying or complex coacervation. Extrusion and emulsification coupled with external gelation could be also used for microencapsulation of olive oil.

2.4. Emulsification

Emulsion preparation plays a key role in encapsulation efficiency. Basically, an emulsion consists of at least two immiscible liquids (hydrophilic and hydrophobic). Here one of the liquids being dispersed as small spherical droplets into other (Bakry et al., 2016; Fang & Bhandari, 2010; Rodríguez et al., 2016). Emulsion instabilities could be expressed either by flocculation, a reversible aggregation of droplets or by coalescence, an irreversible fusion of droplets (Aronson, 1989). To maintain the stability of emulsion, and avoid the coalescence and flocculation of droplets, one or more surface active agents (emulsifiers) are generally used (Zanatta et al., 2017). The emulsion stability is controlled by many factors, such as ratio of oil and water, and presence of emulsifier (Nakashima et al., 2000). Technologies to prepare the emulsion can be classified into two categories, conventional and emerging. Conventional methods rely on stirring equipment, colloid mill, homogenizer and ultrasonic or micro-fluidizer. These technologies are high energy consuming, since they utilize a strong shearing stress, which may result in coalescence of the dispersed phase. Emulsion prepared through conventional technologies may be polydisperse. Unfortunately, it is difficult to maintain the uniform size of droplets. Emulsion preparation through emerging technologies does not consume significant external thermal or mechanical energy. Therefore, they may be considered as low energy consuming technologies. Emulsification of two immiscible liquids can be prepared by controlling phase inversion temperature, membrane emulsification and spontaneous way (Nazari et al., 2019). In many cases, biological or chemical emulsifier is used to stabilize emulsion as well as increase the efficiency of emulsion (T. T. Liu & Yang, 2011; Yang et al., 2020). Table 2 summarized the different emulsification technologies.

Table 2 : Summary of different emulsification technologies (Yakdhane et al., 2021)

Emulsification Techniques		Description	Reference
High-Energy consuming methods	Ultrasound generator	Due to the ultrasound (physical shear force), fine droplets are created. At a certain range of sound, a source pressure amplitude cavitation takes place and Pandit, 2008) emulsification of the immiscible liquids occurs.	(Gaikwad &

Low-Energy Techniques	High pressure homogenizer	In a homogenizer, with the help of a pump the liquid is pressed with high pressure to a narrow channel, which offers shear force on immiscible liquids. It creates cavitation and leads to emulsion with a small droplet size.	(Stang et al., 2001)
	Phase inversion temperature	Due to the change in factors, such as temperature or pH, the activity of the emulsifier in terms of its hydrophilic-lipophilic balance is affected. It helps create the emulsion.	(Friberg et al., 2011)
	Membrane emulsification	Membrane emulsification is performed with the porous membrane. Hydrophilic liquid (oil) in a dispersed phase is pressed through the membrane pores to a continuous phase, generally hydrophilic liquid and the emulsion is formed in a continuous phase.	(Charcosset et al., 2004)
	Spontaneous emulsification	In spontaneous emulsification, the immiscible liquids, such as oil and water along with the emulsifier create the emulsion without an external energy source.	(Lopez-Montilla et al., 2002; Solans et al., 2016)

2.4.1. Membrane emulsification technology

In recent years, membrane emulsification (ME) has been explored as a promising method to produce uniform emulsion with controlled droplet size. It consists of using a porous membrane to produce emulsion droplets under certain conditions. The dispersed phase is pressed through the membrane pores under pressure and thus, droplets are formed at the membrane surface (Charcosset et al., 2004; Gijssbertsen-Abrahamse, 2003; Joscelyne & Trägårdh, 2000; Piacentini et al., 2014). This method was invented by (Nakashima et al., 2000). Membrane emulsification technologies are classified into two categories dead-end or premix ME technology and CFME technology. Premix ME technology consists of pressing a coarse pre-mixed emulsion through the porous membrane to reduce the droplet size of the pre-emulsion. Subsequently, the droplets are deformed and detached by the flow of the emulsion through the pore tips of the membrane (Lambrich & Schubert, 2005). Figure 5 describes the premix ME process.

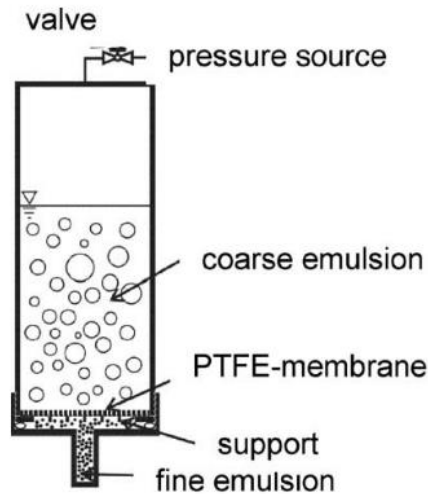


Figure 5: Premix membrane emulsification process, PTFE : Polytetrafluoroethylene membrane (Lambrich & Schubert, 2005).

However, in cross-flow ME to-be-dispersed phase (oil) is pressed through the membrane and forms droplets at the pore openings in the membrane surface. Subsequently, the droplets are detached by the continuous phase (water and wall materials) flowing across the membrane surface (Gijsbertsen-Abrahamse, 2003). Figure 6 describes the droplet detachment in cross flow ME process.

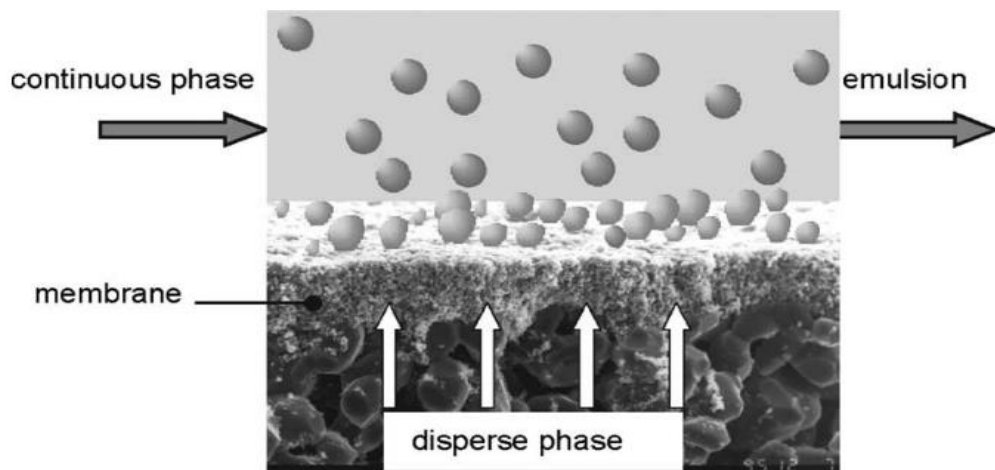


Figure 6: Droplet detachment at the cross-flow membrane interface (Lambrich & Schubert, 2005).

The advantage of CFME is the ability to produce monodisperse emulsions, with narrow droplet size (1 – 10 μm) and emulsions with shear sensitive substances with relatively low energy input. Lower energy inquired implies that less shear stress is exerted on the ingredients which could

assure the protection of the microencapsulated bioactive. Monodispersity of the emulsions prepared by ME technology implies its various applications in the food, cosmetic and pharmaceutical industries such as making low-fat spreads, anti-cancer drugs and pigments obtained by encapsulated metal oxides (Gijsbertsen-Abrahamse, 2003).

However, the disadvantage of this process is the low disperse phase flux ($0.01 - 0.1 \text{ m}^3 \text{ m}^{-2} \text{ h}^{-1}$) resulting in low operating time (Joscelyne & Trägårdh, 2000). Many researchers tried to increase the flux through application of high-pressure driving force. This led either to droplet coalescence or jetting of the dispersed phase. Therefore, because of the higher throughput of the disperse phase, coalescence may happen by the fact that neighboring pores are forming droplets simultaneously. Figure 7 describes the phenomenon of droplet coalescence. The jetting of the disperse phase means that the pores of the membrane generate a liquid jet instead of single droplet (Lloyd et al., 2015).

Another disadvantage is the low number of active pores (pores at which droplets are formed) in the membrane. It has been reported that only 3-40% of the membrane pores are active (Gijsbertsen-Abrahamse, 2003). As membranes have asymmetric pore size distribution, this could result in a wide droplet size range. Besides, the composition of the wall materials contained in the continuous phase may adsorb to the pores of the membrane and consequently block the pores. That's why regular and intensive cleaning of the membrane is compulsory (Lambrich & Schubert, 2005).

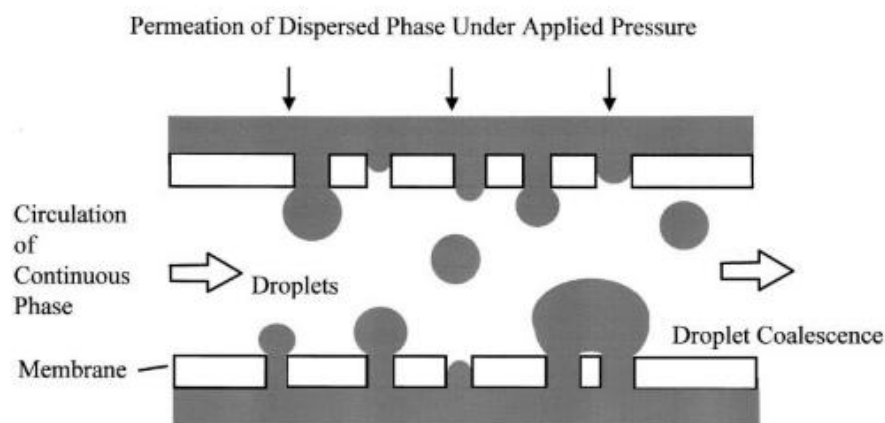


Figure 7: Droplet coalescence in cross-flow membrane emulsification process (Joscelyne & Trägårdh, 2000).

2.4.2. ME process controlling parameters

ME is influenced by several parameters including membrane pore size and distribution, membrane porosity, membrane surface type, emulsifier type and concentration, dispersed phase

flux, velocity of the continuous phase and transmembrane pressure (Joscelyne & Trägårdh, 2000). These parameters are classified by Charcosset, 2009 (Figure 8) into membrane parameters, phase parameters and process parameters. Membrane parameters include mean pore size, pore size distribution, pore shape, number of active pores, porosity, wettability, permeability K and thickness L . Phase parameters include interfacial tension, emulsifier type and concentration, viscosity, and density of continuous and dispersed phase. Process parameters include wall shear stress, transmembrane pressure, temperature, membrane module configuration. They influence the emulsifying process (droplet size distribution, dispersed phase flux, dispersed phase percentage).

All these different parameters presented in figure 8 influence droplets detachment by the effect of the forces acting on the droplets at the membrane pore interface. Therefore, to produce monodisperse droplets with controlled size at a reasonable dispersed phase flux, an appropriate attention should be given through the selection of each parameter in order to answer to specific industrial requests.

The forces acting on the droplet are presented by Piacentini et al. (2014) as the detaching forces which take droplets off the pore such as drag force (F_D), buoyancy (F_{BG}), inertial (F_I), lift (F_L) and static pressure forces (F_{SP}), and the retaining forces which keep holding droplets on the pore such as the interfacial tension (F_γ). The forces acting on a droplet at the membrane pore interface are presented in figure 9. The continuous phase flowing parallel to the membrane surface results on (F_D) while (F_{BG}) is coming from the density difference between the continuous phase and the dispersed phase. The dispersed phase flow moving out from the pore outlet creates the (F_I) force. The asymmetric velocity profile of the continuous phase near the droplet gives the F_L . The pressure difference between the dispersed phase and the continuous phase at the membrane surface results on the (F_{SP}). Finally, (F_γ) is coming from the effects of dispersed phase adhesion around the edge of the pore opening.

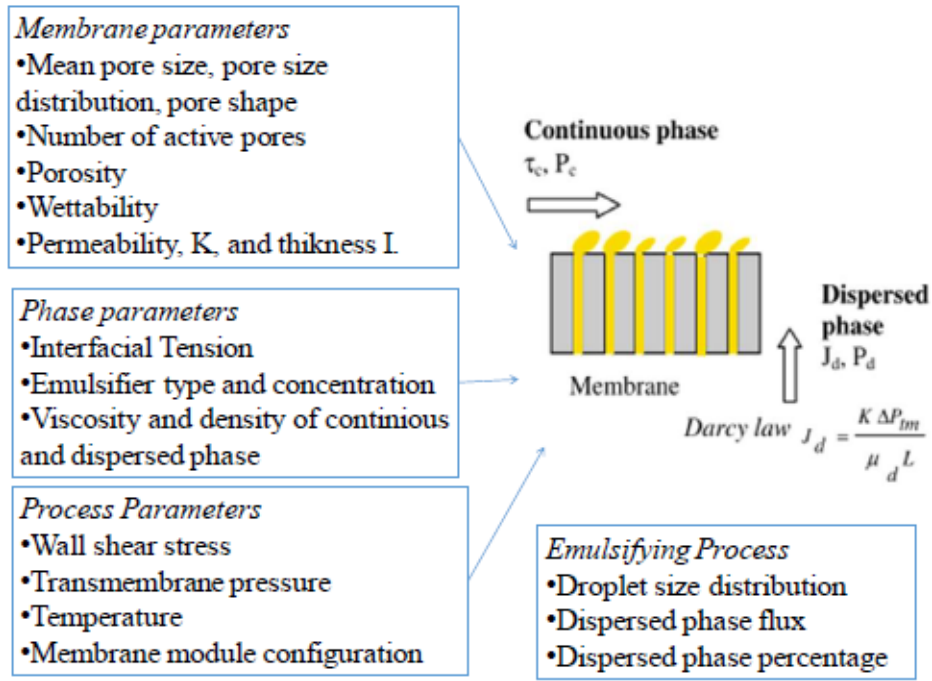


Figure 8: Membrane emulsification process control parameters (Charcosset, 2009).

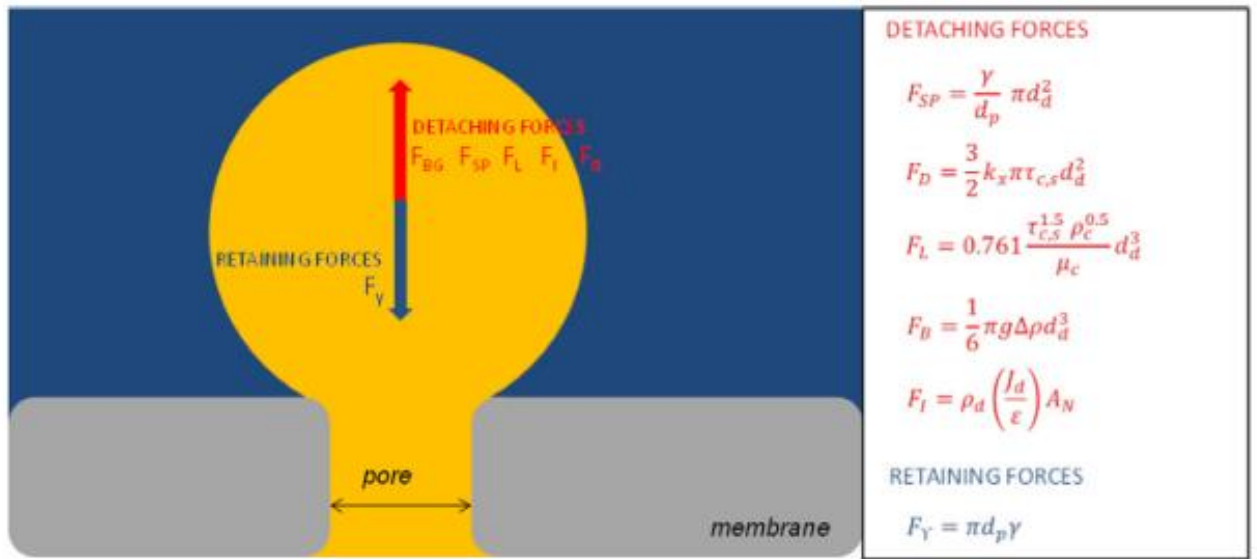


Figure 9: Forces acting on a droplet at the membrane pore interface (Piacentini et al., 2014).

2.5. Emulsifier

Emulsifier is a surface-active agent, also known as "emulgent". It has a great influence to prepare aqueous emulsification of olive oil with matrix. Emulsifiers are amphiphilic by nature with hydrophilic and hydrophobic functional groups in their conformational structure (Kinyanjui et al., 2003). The emulsifier reduces the interfacial surface tension among hydrophobic and hydrophilic compounds and makes them miscible (Dickinson, 2009). Emulsifiers such as oxidized fatty acids from hydrolyzed castor oil also offer antimicrobial and

antiadhesive properties (Nabilah et al., 2020). Selection of an appropriate emulsifier to prepare stable emulsion is one of the important efforts to formulate emulsion-based product. Furthermore, to find out the suitable concentration of selected emulsifier to prepare stable emulsion is a considerable important issue. The hydrophile–lipophile balance and concentration of emulsifier influence the stability of the emulsion and encapsulation efficiency (Yang et al., 2020). As emulsification process is a considerable important issue to prepare microcapsule, different emulsifiers, such as lecithin, saponins, Tweens, Spans are commonly used in food, cosmetic and biopharmaceutical industries (McClements & Jafari, 2018). For the preparation of olive oil microcapsule, emulsifier lecithin (Calvo et al., 2012) (Figure 10 (A)) and tween 20 (Koç et al., 2015) (Figure 10 (B)) have been used. Often novel or improved functional activities (enhanced nutritional property, flavor and improved texture) can be obtained using mixture of emulsifiers instead of using single emulsifier (McClements & Jafari, 2018). The mechanism of olive oil-water emulsion in presence of emulsifier is represented in Figure 10 (C). During the emulsification process, the hydrophilic group of emulsifier binds with water or the wall material and the hydrophobic group binds with the olive oil (Dickinson, 2009).

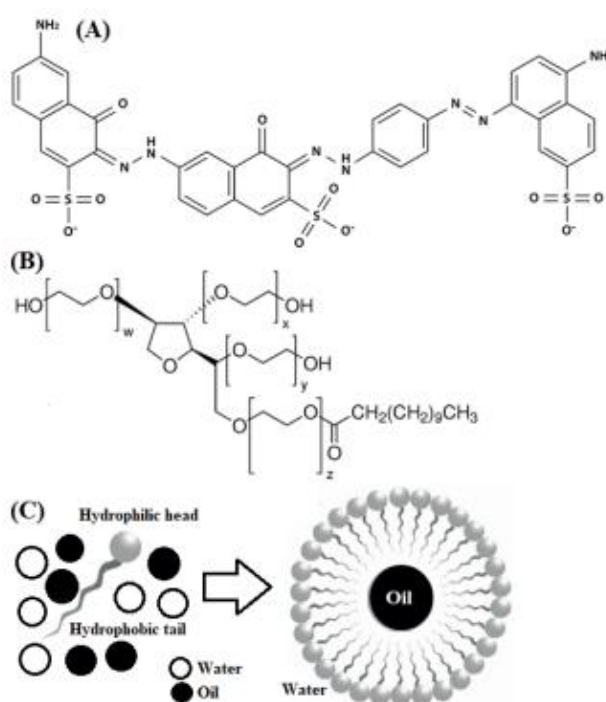


Figure 10: Emulsifier: Soya lecithin (A), Tween 20 (B), Mechanism of oil-water emulsion in presence of emulsifier (C) (self-developed, concept was adopted from (Kinyanjui et al., 2003) and (Dickinson, 2009)).

2.6. Wall material (matrix)

For microencapsulation of any bioactive compound, selection of a suitable coating material, basically a film-forming agent or matrix or wall material is an important task (Jafari et al., 2008). Wide variety of natural and synthetic biopolymers are used for microencapsulation of olive oil. It has been reported that the size and shape of microcapsule depend on characteristics of wall material, method and unit operation (Onsaard & Onsaard, 2019). Wall material could act as a barrier and it may protect the encapsulated bioactive compound against oxygen, water, light and contact with other ingredients. Furthermore, characteristics of the wall material influences the controlled release of encapsulated bioactive compound to environment (Calvo et al., 2012). Criteria to select wall material for microencapsulation purpose are soluble in water, a tendency to form a fine and dense network during drying, high glass transition temperature of the oil and matrix to avoid stickiness of microcapsule and resist the leakage of oil during dehydration or drying (Bae & Lee, 2008; Gharsallaoui et al., 2007). There is no wall material that can meet all the mentioned properties. Often combination of different wall materials has been used to prepare microcapsule (Hogan et al., 2001; Jafari et al., 2008). Several wall materials, such as gelatin (Calvo et al., 2010; Devi et al., 2012), arabic gum (Calvo et al., 2010; Silva et al., 2013), sodium caseinate (Calvo et al., 2012), MD, CMC (Calvo et al., 2012; Silva et al., 2013), sodium alginate (Devi et al., 2012; Sun-Waterhouse et al., 2011), WPI (Koç et al., 2015), soy protein isolate, pea protein isolate, defatted milk powder and octenylsuccinic anhydride-modified starch (Zhao & Tang, 2016) and purple potato starch (Lei et al., 2018) are used for encapsulation of olive oil. Table 3 presents an overview of the biochemical characteristics of different wall materials along with their advantages and disadvantages.

Table 3: Characteristics of the matrix used for the microencapsulation (Yakdhane et al., 2021)

Matrix	Source	Characteristics	Advantages	Disadvantages	Reference
Gum Arabic	Extracted from <i>Acacia senegal</i> (L.) or <i>Acacia seyal</i> (L.).	<ol style="list-style-type: none"> 1. It is a mixture of polysaccharides, oligosaccharides, and glycoproteins. 2. Hydrolysis of polysaccharides produce arabinose, galactose, rhamnose, and glucuronic acid. 3. It is soluble in water. 	<ol style="list-style-type: none"> 1. Well accepted film-forming ability. 2. It has an emulsifying property due to the presence of protein. 3. Low viscosity in aqueous solution. 4. Stable in aqueous emulsion. 5. High solubility in aqueous solution. 	<ol style="list-style-type: none"> 1. Expensive. 2. Variable availability and quality. 3. Limited potentiality to prevent oxidation of the encapsulated item. 	(Anandha ramakrish nan & Padma Ishwarya, 2015; Fang & Bhandari, 2012)

			6. Good retention of flavour.	
Maltodextrin	Enzymatically derived from corn (<i>Zea mays</i>), potato (<i>Solanum tuberosum</i> L.), rice (<i>Oryza sativa</i>), and wheat (<i>Triticum aestivum</i> L.) starches.	Maltodextrin consists of D-glucose, linked with $\alpha(1\rightarrow4)$ glycosidic bond. Maltodextrin can be of variable length according to the degree of polymerization. Typically, it varies from 3 to 17 glucose units. Maltodextrins are classified according to the dextrose equivalent. The higher value of dextrose equivalent signifies a shorter glucose chain, higher solubility, higher sweetness, and lower heat resistance.	<ol style="list-style-type: none"> 1. Low cost. 2. High potentiality to prevent oxidation of the encapsulated item. 3. Easily digestible in the intestine. 4. Highly soluble in water. 5. Low viscosity with a high solid content in the emulsion. 6. Heat resistance. 	<ol style="list-style-type: none"> 1. Poor emulsifying property. 2. Poor flavour retention. 3. Sometimes offer allergenic activity. <p>(Anandha ramakrishnan & Padma Ishwarya, 2015)</p>
Modified starch	Native starch is collected from corn (<i>Zea mays</i>), potato (<i>Solanum tuberosum</i> L.), rice (<i>Oryza sativa</i>), and wheat (<i>Triticum aestivum</i> L.) starches.	It is prepared by physical, enzymatic, or chemical treatment of native starch, which changes according to the property of the native starch.	<ol style="list-style-type: none"> 1. Well soluble in water. 2. Low viscosity. 3. Excellent volatile compound retention. 4. Excellent emulsifying property. 5. Provide stability in emulsion. 6. Heat stable. 7. Odourless and tasteless. 8. Low cost. 	<p>(Anandha ramakrishnan & Padma Ishwarya, 2015; Fang & Bhandari, 2012; Mishra, 2015)</p> <p>Provide allergenicity to food due to the presence of gluten.</p>
Methyl cellulose	Methyl cellulose is not present in the plant cell wall. After the collection of natural cellulose from the plant cell wall, methyl cellulose is produced by the heat treatment of native cellulose with a sodium hydroxide solution and treating with methyl chloride.	Different types of methyl cellulose are produced by etherification of different numbers of the hydroxyl group. It has an amphiphilic property.	<ol style="list-style-type: none"> 1. Stable viscosity over a wide range of pH (pH 3–11). 2. Heat stable. 3. Odorless and tasteless. 4. High emulsifying property due to its amphiphilic structure. 5. Satisfactory film-forming ability. 	<p>Low solubility with a higher degree of polymerization.</p> <p>(Mishra, 2015; Shahidi & Han, 1993)</p>
Whey protein	Dairy milk	1. Whey protein is a mixture of α -lactalbumin (molecular weight: 14.2 kDa, isoelectric point: 4.2), β -globulin (molecular weight: 18.3	<ol style="list-style-type: none"> 1. High solubility in aqueous solution. 2. Satisfactory film-forming ability. 	<ol style="list-style-type: none"> 1. Coagulate at lower pH of the emulsion. 2. Heat sensitive. <p>(Anandha ramakrishnan & Padma</p>

		kDa, isoelectric point: 5.2–5.4), serum albumin (molecular weight: 66 kDa, isoelectric point: 4.9–5.1), lactoperoxidase (molecular weight: 78 kDa, isoelectric point: 9.6), lactoferrin (molecular weight: 78 kDa, isoelectric point: 8), immunoglobulin G (molecular weight: 150 kDa, isoelectric point: 6.5–9.5), immunoglobulin A (molecular weight: 320 kDa, isoelectric point: 4.5–6.5), and immunoglobulin M (molecular weight: 900 kDa, isoelectric point: 4.5–6.5). 2. All whey proteins may denature with the heat treatment ~70 °C for 20 min, but do not aggregate due to renneting or acidification of milk.	3. Efficient to protect from oxidation. 4. Good emulsifying property due to its amphiphilic structure.	3. Provide allergenicity to food.	Ishwarya, 2015)
Sodium caseinate	Dairy milk	Casein is a phospho protein. Different types of casein proteins, such as α _{s1} -casein, α _{s2} -casein, β-casein, and κ-casein are present in the casein fraction of milk. Casein is produced by the neutralisation of acid precipitated casein with sodium hydroxide.	1. Highly soluble in aqueous solution. 2. Good film-forming ability. 3. High denaturation temperature. 4. Good emulsifying property due to the presence of hydrophilic and hydrophobic amino acids in the protein structure.	1. Coagulate at a lower pH of the emulsion. 2. Provide allergenicity to food.	(Anandha ramakrish nan & Padma Ishwarya, 2015)
Vegetable proteins, such as lentil, chickpea, flaxseed, soy, pea proteins, etc.	Proteins from lentil (<i>Lens culinaris</i>), chickpea (<i>Cicer arietinum</i>), flaxseed (<i>Linum usitatissimum</i>), soybean (<i>Glycine max</i>), pea (<i>Pisum sativum</i>).	Proteins from different plant sources have a unique amino acid sequence. Due to that, they offer a variety of biochemical activities.	1. Inexpensive and available throughout the year. 2. Highly soluble in aqueous solution. 3. Good film-forming ability. 4. Efficient to protect from oxidation. 5. Good emulsifying property due to its amphiphilic structure.	1. Coagulate at a lower pH of the emulsion. 2. Heat sensitive. 3. Some vegetable proteins, such as chickpea and soy-based proteins may provide allergenicity to the food product.	(Fang and Bhandari, 2012.) (Karaca et al., 2013) (Mishra, 2015)

2.7. Technologies to prepare olive oil microcapsule

To prepare microcapsule of olive oil, several drying technologies to dehydrate the emulsion have been used. These are spray drying (Bakry et al., 2016; Ozkan et al., 2019; Paulo & Santos, 2020), freeze drying or lyophilization (Fang and Bhandari, 2012; Ozkan et al., 2019; Paulo and Santos, 2020) and coacervation (Devi et al., 2012; Ozkan et al., 2019; Poshadri and Kuna, 2010; Desai and Jin Park, 2005). Furthermore, extrusion have been used for microencapsulation of olive oil (Desai and Jin Park, 2005; Kaushik et al., 2015; Poshadri and Kuna, 2010). The

principles, advantages, and disadvantages of mentioned unit operations are mentioned in Table 4.

Table 4: Microencapsulation techniques : Principles, steps, advantages and disadvantages

Process	Principle	Steps	Advantages	Disadvantages	Ref
Spray drying	Due to high heat, the water content is evaporated. Subsequently, due to high heat, the phase of the matrix is altered, and solidification of the matrix takes place around the bioactive compound.	1. Preparation of the dispersion or emulsion. 2. Transfer the emulsion into the nozzle for drying.	1. Rapid 2. Continuous operation, 3. Simple 4. Economic 5. Reproducible 6. Easy to scale up	1. Limited number of wall materials available which are expected to have good water solubility. 2. Difficult to control the size and shape of particles. 3. Lower oxidative stability of microcapsules due to the high temperature during drying. 4. Loss of particle in the drying vessel.	(Bakry et al., 2016) (Ozkan et al., 2019) (Paulo & Santos, 2020)
Freeze drying or Lyophilization	Reducing the surrounding pressure. Providing heat to emulsion to sublimate the frozen water. Solid frozen water is transferred to gas phase.	1. Freezing 2. Sublimation (primary drying) 3. Desorption (secondary drying) 4. Storage	1. Low operating temperature 2. Absence of oxidizing atmosphere (air) 3. Prolonged and superior quality product	1. Long process time (more than 20 hours). 2. High capital cost. 3. High operating costs 4. Difficult to control the distribution of particle size.	(Fang and Bhandari, 2012) (Ozkan et al., 2019) (Paulo and Santos, 2020)
Coacervation	Liquid-liquid phase separation of a single or a mixture of two oppositely charged polymers in aqueous solution triggered by electrostatic interactions, hydrogen bonding, hydrophobic interactions, polarization-induced attractive interactions as well as chemical or	1. Formation of three immiscible chemical phases. 2. Deposition of the coating. 3. Solidification of the coating.	1. High loading capacity. 2. Low temperature. 3. Reduced thermal degradation 4. Compatibility for control release of bioactive.	1. High cost of particle isolation. 2. Complex technique	(Devi et al., 2012) (Ozkan et al., 2019) (Poshadri and Kuna, 2010) (Desai and Jin Park, 2005)

	enzymatic cross-linking agent.						
Extrusion	Mixing molten carrier with oil and allow the emulsion to pass through a die or nozzle at high pressure. Molten carrier creates a thin film around bioactive compound at ambient temperature and within cross-linking agent.	1. Preparation of molten coating solution. 2. Dispersion of core into molten polymer. 3. Cooling or passing of core-coat mixture through dehydrating liquid.	1. Impermeability to oxygen 2. Very long shelf life of the encapsulated compound. 3. Good barrier properties of the matrix. 4. Low surface oil	1. Expensive (double than spray drying). 2. Large particle size (150-2000 μm). 3. High shear force is generated using screw extruders at high pressure which affects the stability of core material.	(Desai and Jin Park, 2005) (Kaushik et al., 2015) (Poshadri and Kuna, 2010)		

2.7.1. Spray drying

In several decades, spray-drying has been successfully used in the food industry to prepare microcapsule. The first attempt was to encapsulate flavor using gum acacia as wall material (Shahidi & Han, 1993). Consequently, different types of oils were successfully encapsulated using this technique (Bae & Lee, 2008; Chan et al., 2000; Xu et al., 2020). Its application to formulate cosmetics (Xu et al., 2020), pharmaceuticals (Liu and Yang 2011) and pesticides (López et al., 2014) have also been published. Preparation of microcapsule by spray drying process involves some steps. The emulsion, prepared by olive oil and aqueous solution of matrix is transferred to nozzle of spray dryer. Due to high heat, phase of wall material is changed, and a layer is created on the surface of droplet of olive oil (Bakry et al., 2016; Gharsallaoui et al., 2007). Schematic diagram of spray dryer is represented in Figure 11.

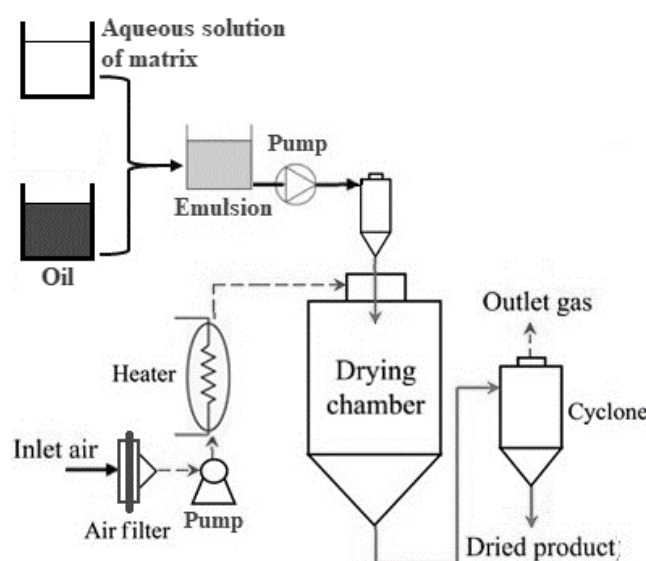


Figure 11 : Schematic representation of spray drying process (self-developed, concept was adopted from(Fang and Bhandari 2012)).

Wall materials, such as polysaccharides (alginate, carboxymethylcellulose, arabic gum, maltodextrin, hydrophobically modified starch) and proteins (whey protein, soy protein, sodium caseinate, gelatin) are used to prepare microcapsule by spray drying technique (Calvo et al., 2010; Koç et al., 2015; Zhao & Tang, 2016). It has been reported that the size of the microcapsule, prepared by spray drying process ranges within 10–400 μm (Yakdhane et al., 2021). The particle size of microcapsule is influenced by the type of atomizer, such as centrifugal wheel atomizer and spray pressure nozzle. If the spray pressure nozzle is used, the particle size of spray-dried product is increased with increase of the nozzle orifice diameter and decreased by the atomization pressure. When the centrifugal wheel atomizer is used, larger wheel diameter and speed provide a smaller size of the particle (Jafari et al., 2008; Yakdhane et al., 2021). Furthermore, different process parameters in emulsion preparation and drying process influence the particle size of microcapsule. Microencapsulation efficiency is reduced with larger oil droplets in emulsion. In the emulsion, viscosity is directly proportional to the droplet size and inversely proportional to the emulsion stability (Bae & Lee, 2008). The particle size of microcapsule increases with the increase in the emulsion flow in spray drying process. In spray dryer, high inlet air temperature and low difference between inlet and outlet air temperatures produce slightly larger particle (Jafari et al., 2008). In practice, particle size of microcapsule is controlled to some extent based on the mentioned parameters. To conclude, spray-drying microencapsulation process steps are first the choice of the wall material, second the emulsification technology and third the spray drying technology. Its efficiency depends on many factors in each step which are listed in figure 12.

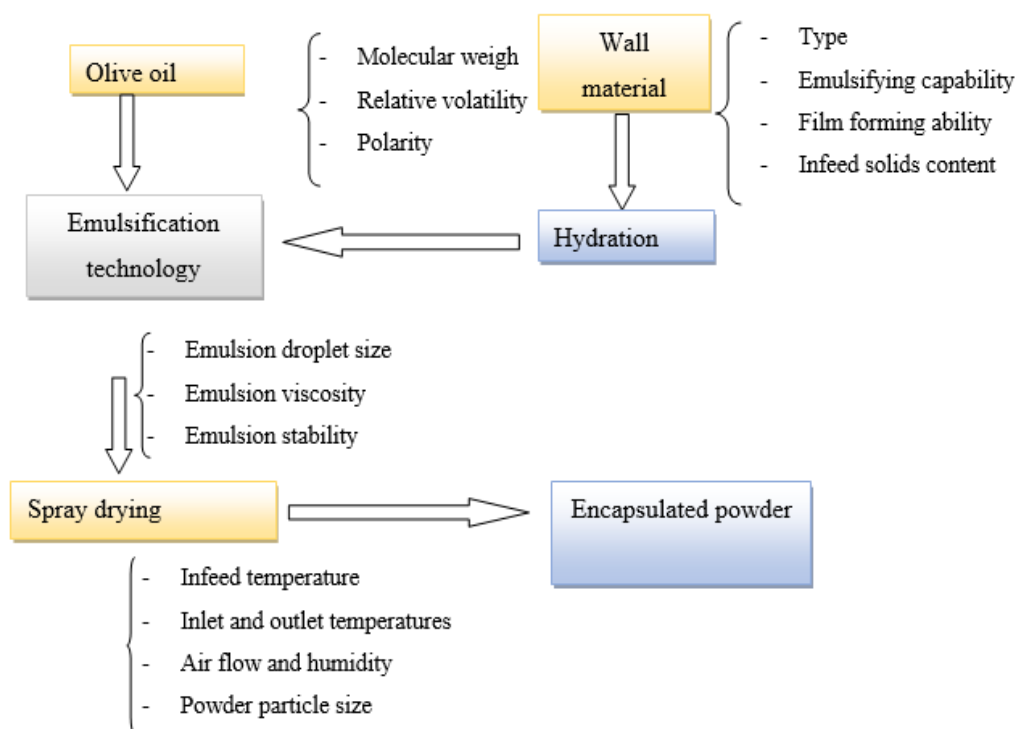


Figure 12: Flow diagram of spray drying microencapsulation with factors affecting the encapsulation efficiency (self-developed, concept was adopted from (Jafari et al., 2008)).

2.7.2. Freeze drying

Freeze-drying is also known as lyophilization or cryodesiccation. It is popularly used in food and biopharmaceutical industries for the dehydration of heat-sensitive bioactive compounds, including olive oil and aromas. Freeze drying process controls the moisture content in the final food product. Chances of thermal deterioration of bioactive compounds are less in case of lyophilization process. Therefore, food products, produced by this technology provide a better organoleptic property (Desai & Jin Park, 2005). Freeze dryer is quite expensive compared to spray dryer. Emulsion of oil and water is frozen between -90°C and -40°C . In this process, the reduction of surrounding pressure takes place and enough heating to emulsion is applied to allow the frozen water to sublime from the solid state to vapor state. Therefore, in this process, transformation of water from a solid phase to vapor phase directly takes place at a minimal operational temperature. Freezing of emulsion with faster rate may lead to aggregation of the freeze-drying products (Bakry et al., 2016). Therefore, it is difficult to control the particle size of microcapsule during freeze drying. After freeze drying, dried material is crushed into fine powder (Ozkan et al., 2019) and subsequently, sieving may consider to maintain the particle size of microcapsule. In this process, the properties of microcapsules are influenced by the

system pressure and temperature. In addition, the operational time of drying is important to achieve a stable moisture content in the dried powder (Yakdhane et al., 2021). Wall materials, such as maltodextrin, carboxymethyl cellulose and sodium caseinate are used to prepare olive oil microcapsule by freeze drying process (Calvo et al., 2012). Depending on process parameters, size of the microcapsule, prepared by freeze drying process ranges within 20–5000 μm (Yakdhane et al., 2021). Schematic diagram of freeze dryer is represented in Figure 13.

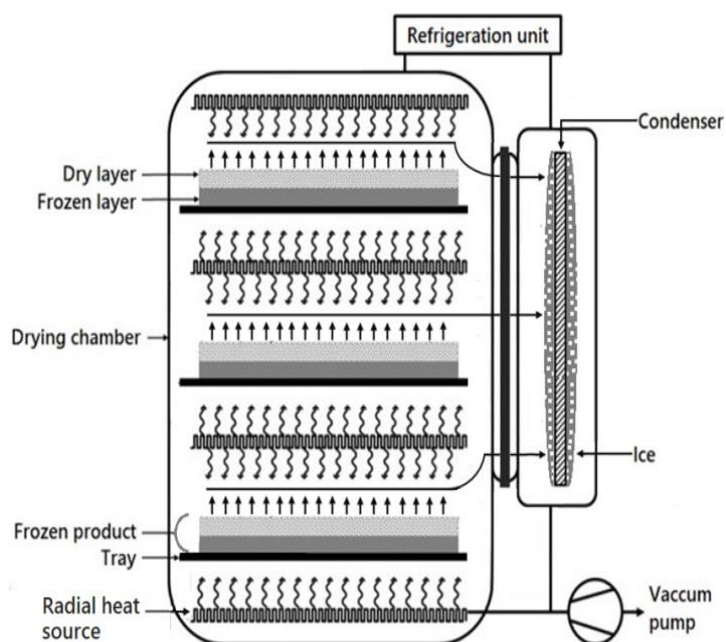


Figure 13 : Schematic representation of freeze-drying process (self-developed, concept was adopted from (Fang and Bhandari 2012)).

2.7.3. Coacervation

Coacervation is generally defined as a liquid – liquid phase separation of a single or a mixture of two oppositely charged polymers in aqueous solution. In this process, the application of cross-linking agents including glutaraldehyde or transglutaminase is noteworthy. Among two phases, concentration of polymer is abundant in coacervate phase, whereas concentration of polymer is poor in equilibrium solution (Ozkan et al., 2019). This process could be either simple or complex. The simple process involves only one type of polymer with addition of hydrophilic agent to the colloidal solution. Meanwhile, the complex process involves the interaction of two or more different types of polymers (Desai and Jin Park, 2005; Kaushik et al., 2015). In this process, oil is usually dispersed in polymer in aqueous/ buffer solution and subsequently, due to pH adjustment, polymer turns to coacervate and form a coating over oil droplets. The next step is cooling of the overall solution to increase the hardness of coating and encapsulate the oil within matrix (Rutz et al., 2017). Several wall materials have been used in simple

coacervation process. Those are gelatin, alginate, chitosan, glucan and cellulose derivative (Ozkan et al., 2019). For complex coacervation of omega-3 oil gelatin or whey proteins and oppositely charged gum arabic, sodium polyphosphate or carboxymethylcellulose have been used (Devi et al., 2012). Size of the microcapsule, prepared by coacervation process ranges within 2–500 μm (Jyothi et al., 2010). The particle size of microcapsule can be controlled by controlling the temperature, speed of stirring, viscosity of emulsion, concentration and type of polymer, and amount of emulsifier (Rodríguez et al., 2016). As an example, larger size of microcapsule is produced due to high concentration of polymer. Contradictorily, lower size of microcapsule is produced due to high stirrer speed (Jyothi et al., 2010). Schematic diagram of coacervation process is represented in Figure 14.

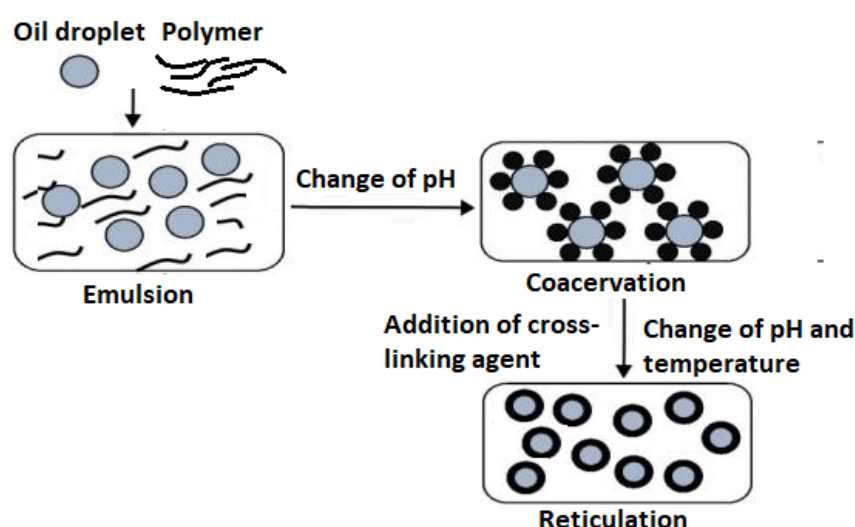


Figure 14: Schematic representation of coacervation process (self-developed, concept was adopted from (Rutz et al., 2017)).

2.7.4. Extrusion

Extrusion technique has been exclusively used for microencapsulation of oil in a carbohydrate matrix (Sun-Waterhouse et al., 2011). Extrusion technology, used for microencapsulation of oil can be classified in 3 categories, such as melt injection, melt-extrusion and centrifugal extrusion. The principals of melt extrusion and melt injection are similar. In melt extrusion, the driving force to prepare the matrix/ wall is a rotating screw without hardening bath, whereas, pressure is a driving force in melt injection process (Bakry et al., 2016). Centrifugal extrusion is most common than others. It is performed with low temperature comparing to spray drying method (Desai & Jin Park, 2005). In this process, heated aqueous polymer solution flows through the outer tube and oil flows through the inner tube and finally both two fluids are discharged into a moving stream (Kaushik et al., 2015). For microencapsulation of olive oil by

extrusion process, glutaraldehyde (Devi et al., 2012) and calcium alginate (Sun-Waterhouse et al., 2011) were successfully used. Gelatin, sodium alginate, carraghenan, starches, cellulose derivatives, gum acacia and polyethylene glycol can be used for coating by extrusion process (Poshadri & Kuna, 2010). Size of the microcapsule, prepared by coacervation process ranges within 150-2000 μm (Desai & Jin Park, 2005). The particle size of microcapsule, produced by extrusion process can be controlled by the diameter of hole in nozzle, external force in nozzle for detachment and flow rate of oil and wall material. Under fixed operating parameters in extrusion process, microcapsule with similar diameter can be produced (Kaushik et al., 2015). Schematic representation of extrusion process is represented in Figure 15.

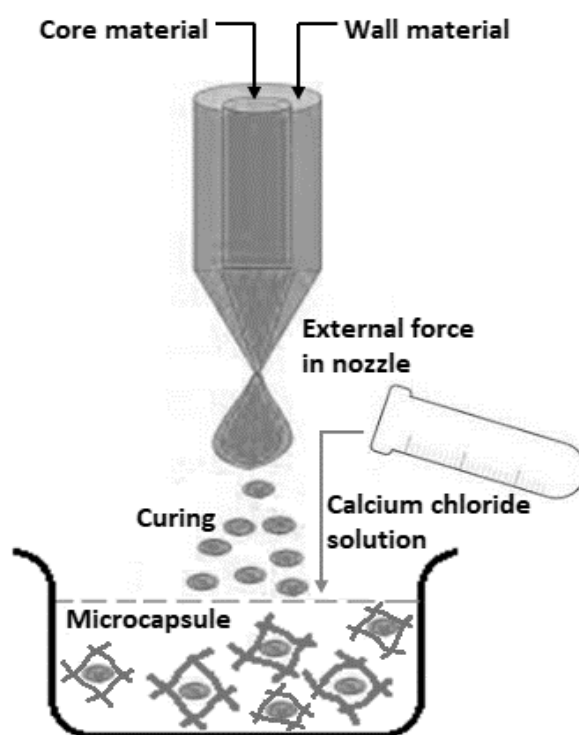


Figure 15: Schematic representation of co-extrusion process (self-developed, concept was adopted from (Risch, 1988)).

2.7.5. Microencapsulation by ionic gelation

This process starts from an aqueous polymeric solution, where ions with a low molecular mass interact with oppositely charged polyelectrolytes forming an insoluble gel (Kurozawa & Hubinger, 2017). Coagulation processes based on alginate beads are commonly used to encapsulate bioactive extracts and compounds for food applications (Dias et al., 2015). This process is based on the chemical reaction between the water-soluble sodium alginate and polyvalent cation, calcium, to form water-insoluble alginate beads or capsules (Chan et al. 2000). Sodium alginate food additive is commonly used due to its low cost and non-toxicity.

This co-polymer is extracted from brown seaweed or kelp. It is composed of two monomeric units D-mannuronic acid and L-guluronic acid. Alginate gel microspheres have been conventionally prepared via extrusion by dropping an alginate solution through a needle into a CaCl_2 solution (external gelation) (Sun-Waterhouse et al., 2011). It has been used by many researchers as an encapsulating material for the microencapsulation of oils (Chan et al. 2000; Devi et al. 2012; Fioramonti et al. 2017; Sun-Waterhouse et al. 2011). Emulsification/internal gelation was processed as an alternative technique to extrusion/external gelation in the encapsulation of several compounds (Reis et al., 2006). Microencapsulation by ionic gelation process has many advantages, such as its simplicity, low cost, the use of aqueous solutions without using special equipment, high temperature or organic solvents, better control of the particle size through variations in the precursor concentration, and the possibility of encapsulating a wide variety of substances. Also, it can be conducted under mild, nontoxic conditions to preserve bioactive compounds. Nevertheless, it has some disadvantages such as the need for a gelling bath, the time-consuming process, and low-scale reproducibility and the complex nature of the formulations (Carvalho Da Silva et al. 2022). Poirieux and co-authors have investigated the optimization of conditions for obtaining alginate/olive oil capsules by ionic gelation of emulsions containing sodium alginate and olive oil for application in dairy industry. They selected the following parameters as optimal for capsules preparation: medium viscosity alginate -1.37%; olive oil concentration- 30%; homogenization rate - 20000 rpm (Poirieux et al., 2017).

2.8. Characterization of microencapsulated olive oil

Physical and biochemical characteristics of olive oil microcapsule can be represented by particle size, particle morphology, color, moisture content, water activity, oxidative stability, encapsulation efficiency (EE) and release of bioactive compounds from the matrix (Onsaard & Onsaard, 2019). Characteristics of olive oil microcapsule depend on several factors, such as wall material, emulsifier, ratio of oil and wall material, and encapsulation technique (Calvo et al., 2010). EE, one of the major characteristics is generally estimated by measuring total oil by destructive method and surface oil. Often, high-performance liquid chromatography (HPLC) or gas chromatography (GC) (Calvo et al., 2012) is adopted for this purpose. Fourier transform infrared (FTIR) spectroscopy is used to understand the modulation of functional groups of fatty acids of oil, matrix, and emulsifier in microcapsule. Differential scanning calorimetry (DSC) and thermogravimetric analyzer (TGA) are used to understand the changes of phase and mass of wall material, oil, emulsifier, and microcapsule, accordingly. DSC curve is produced based

on heat flow versus temperature or time, and TGA curve is produced based on change of mass versus temperature or time (Devi et al., 2012; Lei et al., 2018; Silva et al., 2013). The mean particle size and their distribution are generally evaluated by the dynamic light scattering analytical instrument (Zhao & Tang, 2016). Particle morphology, such as surface characteristics, dispersed or agglomeration of particles and surface functionalization of microcapsule is determined by the Scanning Electron Microscopy (SEM) (Koç et al., 2015; Onsaard & Onsaard, 2019). Zeta potential (ζ -potential) is the electrokinetic potential of solute in colloidal dispersion, which reflects the stability of microcapsule. To understand the zeta potential is an important issue because it represents the fate of microcapsule in food matrix or intestinal tract. It is measured by the zeta potential analyzer (Onsaard & Onsaard, 2019). The moisture content influences the shelf life of the microcapsule and it is measured by the evaporation of water in a hot air oven moisture analyzer (Onsaard & Onsaard, 2019). Evaluating the oxidative stability of oil is a considerable important factor. It is measured by determining the peroxide value, antioxidant activity by 2,2'-azinobis 3-ethylbenzothiazoline-6-sulfonic acid (ABTS) radical scavenging assay (Calvo et al., 2012). The shelf life of the microencapsulated olive oil can be determined by using accelerated oxidation tests, such as rancimat assay, oxidative stability index OSI (Calvo et al., 2010) and absorbance constants, such as K232 and K270 (Calvo et al., 2012). K232 represents the average oxidation rate of the components of olive oil and K270 represents the percentage reduction of olive oil resistance from oxidation. Those are measured by the wavelength 232 nm and 270 nm, respectively. The higher values of them represents the poor quality of fat (Calvo et al., 2010). Summarized information about physical and biochemical characteristics of olive oil microcapsule, prepared by different technologies are represented in Table 5.

Table 5: Process conditions for producing OOM and their characteristics Wall.

Process	Wall material	Emulsifier	Cross-linker	Results	Ref
Spray drying	A: Gelatin + Gum Arabic + Maltodextrin (MD)	-	-	Encapsulation efficiency (EE)	A 42.35%
	B: Sodium caseinate (SC) + Lactose				B 52.98 %
	C: SC + MD				C 38.52 %
	D: MD + modified starch				D 33.43 %
				Encapsulation yield (EY)	A 51.20 %
					B 49.49 %
					C 51.21 %
					D 33.44 %

Freeze drying	A: SC + MD	Lecithin	-	EE	A 36.90 %	(Calvo et al., 2012)
	B: Carboxymethyl-cellulose (CMC) + MD			EY	B 69.09 % A 97.67 % B 99.79 %	
Co-extrusion	Sodium alginate	-	Calcium chloride	EE 60.6 % The encapsulated olive oil had a peroxide value PV < 14 meq/kg, p-anisidine value p-AV < 2.5 and free fatty acid FFA content <0.14%, indicating acceptable oil quality.		(Sun-Waterhouse et al., 2011)
Complex coacervation + Freeze drying	Gelatin A + Sodium alginate	-	Glutaraldehyde	EE 89.37 %, Loading capacity (LC) 187.79 % Maximum coacervation occurred when gelatin to sodium alginate ratio was 3.5:1, glutaraldehyde concentration 1.25 mmol.		(Devi et al., 2012)
Spray drying	MD	Tween 20	-	EE 69.07 %, when concentration of wall material MD and emulsifier are 99 % and 1 %, respectively.		(Koc et al., 2015)
Spray drying	MD	Soy protein isolate (SPI), Pea protein isolate (PPI), Defatted milk powder, Octenylsuccinic anhydride-modified starch (OSA)		EE SPI 87 % PPI 82.5 % Defatted milk powder 77.5 % OSA 88 % Microencapsulation remarkably improved the UV- or heat-stability, as well as the in vitro bio-accessibility of CoQ10. Improvement of the water solubility and bioavailability of CoQ10.		(Zhao & Tang, 2016)
Porous starch technique: drying under vacuum	Purple Potato starch	-	-	Loading ratio efficiency 29 % when oil to wall ratio is 4:1 Peroxide value PV 8 mmol/Kg		(Lei et al., 2018)
Freeze drying	A: MD + CMC B: Alginate (ALG)+ (MD) C: 12.5 g/100 g MD + 7.5 g/100 g GA Gum Arabic D: 10 g/100 g MD + 8.5 g/100 g GA	-	-	Particle size Glass transition temperature (Tg)	A 81.4 µm B 161 µm C 41.3 µm D 14.8 µm A - B - C 146.60 °C D 147.54 °C	(Silva et al., 2013)

2.9. Applications of microencapsulated olive oil

Microencapsulated olive oil has been used in food, pharmaceutical and cosmetic formulations. In subsequent section, information is provided in comprehensive way.

2.9.1. Foods

Microencapsulated olive oil was used in the food industry for many reasons. For general wellbeing, popularity and demand of antioxidant-enriched food catapulted to wide range of communities (Bakry et al., 2016). Antioxidant enriched foods not only reduce the risks of metabolic dysfunction, but its contribution to provide stability of nutrients against oxidative deterioration in food matrix (Devi et al., 2012) and preserve different sensory parameters (Sun-Waterhouse et al., 2011). Recently, oxidative stability of spray dried powder (microcapsule) containing fish oil and extra virgin olive oil blend (1:1 weight ratio), using sugar beet pectin as wall material has been investigated. It has been reported that the addition of olive oil into the formulation can improve the oxidative stability of microencapsulated fish oil and thereby prolong the shelf life of formulation (Sudheera et al., 2011). Presently, the ketogenic diet has been receiving lots of attention. Triacylglycerol in ketogenic diet converts to ketone bodies in the hepatocyte mitochondria (ketogenesis). Subsequently, these ketone bodies provide energy (ATP) through ketolysis in heart and muscle cells. Due to the presence of monounsaturated (such as oleic acid (18:1 ω -9)) and polyunsaturated fatty acids (such as ω -3 and ω -6 fatty acid fatty acids) in olive oil, its importance in formulation of ketogenic diet is significant (Ludwig, 2020). Due to fashionable organoleptic property of olive oil, its importance in cooking recipe is well known from past (Moldão-Martins et al., 2004). Emulsion of olive oil with lemon juice at the ratio (1:1) was microencapsulated by freeze-drying process and used successfully in instant salad sauce (Silva et al., 2013). Application of encapsulated olive oil in yogurt and spread cheese has been also reported (Poirieux et al., 2017).

2.9.2. Pharmaceuticals

From old age, application of olive oil was not limited within food recipes. Olive oil has been used as a pharmaceutical because it is considered as safe, biocompatible and non-toxic (Jos, 2018). In the 19th century, olive oil was administered as laxative and to treat poisoning. It was used in combination with fats and resins to develop skin ointment. Additionally, it could be administered by mouth, for the treatment of an inflammation of the intestinal tube, colic, diarrhea and disparity (Gorini et al., 2019). Due to the presence of different bioactive compounds, such as polyunsaturated fatty acids, vitamins and antioxidants with unique biochemical properties, olive oil has a great role in formulation of pharmaceuticals (E. Martins

et al., 2017). In pharmaceutical industry, encapsulated olive oils are used as therapeutics to modulate the oxidative stress that is related to cardiovascular diseases, arteriosclerosis and cancer (E. Martins et al., 2017). Coenzyme Q10 (CoQ10) is a hydrophobic compound with a high molecular weight, resulting the lower oral bioavailability. Microcapsule of olive oil with CoQ10 has been developed by combination of emulsification and drying techniques in sequential way for elderly individuals as oral food supplement due to their health consideration (Zhao & Tang, 2016). Polar phenolic compounds in olive oil, mainly hydroxytyrosol and its derivatives offer unique biological activities. It has been proven that their dietary intake reduces the risk of cardiovascular disease and cancer. Scavenging activity of these compounds against superoxide anion, hydrogen peroxide and reactive oxygen species has been demonstrated (Dimitrios, 2006).

2.9.3. Cosmetics

At end of the 19th century, olive oil started to be used within cosmetics in Mediterranean countries. As example, olive oil was used in hair care and to counter wrinkles in Egyptian culture. The first cold cream was developed by olive oil, bee wax and water in Greece. In Greek culture, olive oil was used to highlight the esthetic perfection of the body of athletes and to prepare them through thermal massage (Gorini et al., 2019). Several phenolic compounds, such as hydroxytyrosol, catechin, rutin, verbascoside, luteolin and oleuropein in olive oil act as an antioxidant. Their successful implementation in cosmetics have been proven (Kashaninejad et al., 2017). When cosmetics enriched with antioxidant are applied into the skin, they enter to the outermost layer of skin, i.e., epidermis, which is mostly composed of keratinocytes. In cosmetic industry, olive oil is largely used due to their antioxidant, nourishing and moisturizing properties (Badiu et al., 2010). Antioxidant protects the keratinocytes from oxidative damage and nourish cells and tissues (Luz et al., 2021). Vitamin E in olive oil protects skin from free radicals, responsible for the aging of skin (Danby et al., 2013). In combination with vitamin A, vitamin E stimulates cell regeneration. It is considered as useful remedy against wrinkles and is also applied in treatment to prevent stretch marks (Gorini et al., 2019; Viola & Viola, 2009). Presently, microcapsule of olive oil has been applied into the cosmetics with the same aid (Jos, 2018; Luz et al., 2021; Rodríguez et al., 2016). In some cases, visible microcapsules are intentionally added in skin and hair creams, shower soaps and household cleaners to make the product more visually attractive (Barbulova et al. 2015). Microencapsulated oil is also found in body deodorants and perfumes (E. Martins et al., 2017).

2.10. Summary

This literature review was an attempt to illustrate microencapsulation of olive oil as a unique approach to conserve the biochemical properties of bioactive compounds of olive oil, such as monounsaturated fatty acids (ω -9), polyunsaturated fatty acids (ω -3 and ω -6 fatty acids), vitamins and phenolic antioxidants, from oxidation and change of environmental condition. As a result, the quality and biological activity of olive oil are not deteriorated in the food matrix during processing, cooking and storage. Therefore, several applications of microencapsulated olive oil in food, pharmaceutical and cosmetic industries have received high status. In this part, I provided information about different techniques to prepare olive oil microcapsule, characterization of OOM, and application of encapsulated olive oil in food, pharmaceutical and cosmetic industries in a comprehensive way. The method selection to prepare microcapsule depends according to the situation and product interest. Furthermore, different process parameters influence the characteristics of olive oil microcapsule. In addition, it was shown that microcapsule, produced by extrusion technique has homogeneous diameter. Presently, olive oil microcapsule (Extra Virgin Olive Oil Cold-Pressed 1000 Milligrams 120 Sgels) is produced by Swanson Ltd, USA and available in market.

3. MATERIALS AND METHODS

3.1. Materials

3.1.1. Olive oil

A commercial Extra virgin olive oil (unrefined and unblended) was purchased from a local supermarket in Budapest, Hungary from the brand Bertolli. Olive oil was stored in glass bottle in dark storage room at RT. It was selected for microencapsulation by spray drying, freeze-drying and for microencapsulation by gelation of alginate as it contains bioactive compounds. It has a high content of triacylglycerols. Triacylglycerols (TAGs) are glycerol esters of fatty acids where the fatty acids are bound in groups of three together with a unit of glycerol (Figure 3). About 95–98% of olive oil consists of TAGs (Mailer et al., 2006).

3.1.2. Wall materials

Maltodextrin (MD, DE=5) was procured from Applichem panreac itw companies, Gum arabic was purchased from Bi-Bor Kft, carboxymethylcellulose (E466) was procured from Gréta-tortadekoracio- hungary. Maltodextrin (MD, DE= 19) and whey protein isolate (WPI 90) were purchased from Buda Family Kft., Austria. Tween 20 and tween 80 (Sigma Aldrich, France) were used as stabilizers. Tween 80 is an artificial additive made from sorbitol, oleic acid and ethylene oxide. In the food industry, it is known as E433 as an emulsifier. The maximum daily intake volume is 25 mg.kg⁻¹ (Martins, 2012) .

Sodium alginate food additive E401 was purchased from Naturguru Kft Hungary. The molecular weight of E401 is 10 000-600 000 and its viscosity ranged from 40 to 100 mPas. Sodium alginate powder was dispersed in distilled water under magnetic stirring at 65°C for 15 minutes, to produce alginate solutions of desired concentrations 0.5%, 1% and 1.5 %. The solutions were left standing for 24h to disengage bubble before use.

The characteristics of the MD, GA, CMC and WPI were presented in table 3 from section 2.6.

3.1.3. Solvents and chemicals

Solvents and standards for chromatography purpose such as methanol, isopropanol, ethanol, diethyl ether, n-hexane and potassium hydroxide were purchased from Sigma Aldrich, USA. All other chemicals with analytical grade such as cyclohexane (1% (w/v)), acetic acid, chloroform, potassium iodide, sodium thiosulphate, Folin–Ciocalteu reagent, pyridine, 5 α -cholestane, heptane and trifluoroacetamide were purchased from Fluka, Germany.

Milli-Q ultrapure deionized (DI) water (18.2 M Ω ·cm) was obtained from Milli-Q Synergy/Elix water purification system (Merck-Millipore, France) and used in all experiments. Ultrasil P3-11 was purchased from Ecolab-Hygiene Kft (Ecolab-Hygiene Kft, Budapest, Hungary). Citric

acid (99%) was purchased from Reanal Kft (Reanal Kft, Budapest, Hungary). Ultrasil and citric acid were used to clean the membrane emulsification machine.

Hexane was used to extract oil from the surface of microcapsules. It was purchased from (Sigma Aldrich, France). It is a colorless liquid with a slightly disagreeable odor. It is highly flammable, and its vapors can be explosive.

Concerning the gelation of sodium alginate, Calcium chloride dihydrate, $\text{CaCl}_2 \cdot 2\text{H}_2\text{O}$ (Thomasker, Hungary), was used as gelling ions for crosslinking.

3.2. Methods

3.2.1. Characteristics of olive oil

3.2.1.1. Extinction coefficients

Extra virgin olive oil in cyclohexane (1% (w/v)) was considered to determine extinction coefficients, such as K232 and K270 by a UV spectrophotometer (Thermo ScientificTM, Waltham MA, USA). Absorbances of solution were measured with wavelengths 232 nm and 270 nm (Karoui et al., 2020). Three parallel measurements were performed.

3.2.1.2. Peroxide value (PV)

To understand the PV of extra virgin olive oil, 1.5 g of olive oil was dissolved in 25 ml of solvent mixture (chloroform and acetic acid (2:3, v/v)) in a volumetric flask. Then 1 ml of saturated potassium iodide was added and the solution was shaken for 1 min and left in the dark for 5 min at a temperature of 25 °C. Subsequently, 75 ml of DI water was added. The titration of the liberated iodine was done with 0.01 N sodium thiosulphate solution and 1% aqueous starch solution as an indicator. The PV is expressed in terms of milliequivalents of active oxygen per kilogram of olive oil (meq O_2 /kg of oil).

$$PV = \frac{V \times T \times 1000}{m} \quad (1)$$

Where V is the number of ml of the standardized sodium thiosulphate solution used for the test, T is the exact molarity of sodium thiosulfate solution and m is the weight in g of the test portion (Ghanbari Shendi et al., 2018). Three parallel measurements were performed.

3.2.1.3. Total phenolic content

The content of total phenolics in extra virgin olive oil was determined by the Folin–Ciocalteu method following the extraction method described by the International Olive Council (Method COI/T.20/Doc. No 29, 2009), 5 g of olive oil was mixed with 5 ml of methanol and water (80:20 (v/v)) and shaken for 30 min (Mousavi et al., 2021). Subsequently, mixture was considered for

centrifugation with rotor speed $1700\times g$ for 5 min in a laboratory centrifuge (HERMLE Labortechnik, Wehingen, Germany). 1 ml of extract was mixed with 1.5 ml of sodium carbonate (20% w/v) and 0.25 ml of Folin–Ciocalteu reagent in a 10 ml volumetric flask. The final volume was maintained by DI water. Samples were stored for 90 min at room temperature $\sim 25^{\circ}\text{C}$ in dark conditions. The spectrophotometric analysis was performed with wavelength (λ) 725 nm considering gallic acid (GA) as standard. A UV-Vis spectrophotometer (Thermo Scientific TM, Waltham MA, USA) was used for the colorimetric analysis (Dini et al., 2020). Three parallel measurements were performed.

3.2.1.4. Tocopherol composition

Sample preparation for the analysis of tocopherols in extra virgin olive oil was performed prior to inject in the column LiChrospher Si60 column (inner diameter 25 cm, length 4.6 mm and particle size $5\text{ }\mu\text{m}$) (Merck, Darmstadt, Germany), fitted in an Agilent 1200 high performance liquid chromatography (HPLC) system equipped with a fluorescent detector (Agilent Technologies, Santa Clara, CA, USA). Sample preparation method is herein. 0.15 g of olive oil was diluted in 10 ml of n-hexane followed by centrifugation with rotor speed $25000\times g$ for 10 min. Supernatant was transferred to a chromatographic vial and $20\text{ }\mu\text{L}$ of sample was injected into the HPLC system. Chromatographic separation was performed by the isocratic mixture of isopropanol: hexane 0.5:99.5 (v/v) mobile phase, operated with $0.7\text{ ml}\cdot\text{min}^{-1}$ flow rate. Fluorescence detector was set to excitation and emission wavelengths of 296 nm and 330 nm, respectively. Peaks were identified on the basis of retention times of standards α -, β -, γ - and δ -tocopherol separately and their concentrations were calculated using respective external calibration curves (Czaplicki et al., 2011). Three parallel measurements were performed.

3.2.1.5. Sterol composition

For the analysis of sterols in extra virgin olive oil, 0.2 g of olive oil was dissolved in 1 ml of n-hexane and 0.2 ml of a 5α -cholestane solution ($0.4\text{ mg}\cdot\text{g}^{-1}$) as an internal standard. Subsequently, sample mixture was saponified by adding 0.5 ml of ethanolic potassium hydroxide solution (20 ml of ethanol and 50% (w/v) potassium hydroxide) at RT for 2 h. Unsaponifiable fraction was extracted with diethyl ether. Subsequently, extract was transferred into a sample vial and dried under nitrogen stream. The extract was further dissolved in 1.5 ml of hexane and transferred into a sample vial followed by drying under nitrogen stream. In next step for sample derivatization purpose, the residue was re-dissolved in $100\text{ }\mu\text{L}$ of pyridine and $100\text{ }\mu\text{L}$ N,O-bis (trimethylsilyl) trifluoroacetamide (BSTFA) with 1% trimethylchlorosilane

(TMCS) and heated in 60°C for 1 h. Subsequently, 1 ml of heptane was added in dried sample and the obtained mixture was analyzed using a ZB-5ms capillary column (inner diameter 30 m, length 0.25 mm and film thickness 0.25 μm) (Phenomenex, Torrance, CA, USA) in a GC-MS system (QP2010 PLUS, Shimadzu, Kyoto, Japan). Separation of sterols was performed by a carried gas helium at a flow rate 1 $\text{ml}\cdot\text{min}^{-1}$. 1 μL of sample was injected in a splitless mode and the injector temperature was 230 °C. The column temperature in GC was programmed as follows: initial temperature 50°C for 2 min, a subsequent increase to temperature 230°C at the rate of 15°C. min^{-1} , to 310°C at the rate of 3°C. min^{-1} 10 min hold. The inlet pressure was maintained at 28.5 psi. The interface temperature of GC-MS was 240°C. The temperature of ion source and electron energy were 220°C and 70 eV, respectively. The total ion current (TIC) mode was used for quantification (100–600 m/z range). The identification of the peaks was based on comparison of their mass spectra with standard compounds and their quantifications were carried out using internal standard method (Roszkowska et al., 2015). Three parallel measurements were performed.

3.2.1.6. Fatty acid composition

Acid value (titratable acidity) was measured to understand the amount of free fatty acids in extra virgin olive oil. For that purpose, olive oil in isopropanol (10% (w/v)) was neutralized by 0.1 N of potassium hydroxide solution. Here, oleic acid (C18:1) was considered as a basis because it is the predominant fatty acid in extra virgin olive oil (Japir et al., 2017). Fatty acids composition was determined as methyl esters by an Agilent 6850 gas chromatography system (Santa Clara, CA, USA) using a capillary column DB-23 (inner diameter 0.25 mm, length 60 m and film thickness 0.25 μm) and a hydrogen flame ionization detector (FID). Fatty acid methyl esters (FAME) was made according to Mousavi et al. 2021. Briefly, 0.1 g of extra virgin oil was dissolved in 2 ml n-heptane, where 0.2 ml of 2 N methanolic potassium hydroxide was used as catalyst. Temperatures of injector and detector were set at 230 and 280 °C, respectively. The injection volume was 1 μl and helium was employed as carrier gas with a flow rate of 1 $\text{ml}\cdot\text{min}^{-1}$ and the split ratio was 1:50. The oven temperature was programmed as follows: 140°C during 2 min, increased to 240°C at a rate of 4°C. min^{-1} which was held for 15 min, then 240°C for 42 min (Yorulmaz & Konuskan, 2017). Fatty acids in extra virgin olive oil were identified by comparing retention times of standers. Individual methylated standards were used for the saturated, monounsaturated, cis polyunsaturated fatty acids and the trans t-palmitoleic C16:1 $\Delta 9\text{t}$, elaidic C18:1 $\Delta 9\text{t}$, brassidic C20:1 $\Delta 13\text{t}$. For linoleic acid isomers, the mixture linoleic

acid cis/trans isomers (50% of C18:2 Δ 9t,12t; 20% of C18:2 Δ 9c,12t and C18:2 Δ 9t,12c; 10% of C18:2 Δ 9c,12c) were used (Ansorena et al., 2013).

3.2.2. Emulsions preparation

3.2.2.1. Emulsion prepared by membrane emulsification machine

The emulsions were produced using a laboratory membrane emulsification machine designed and constructed at the Department of Food Engineering at Hungarian University of Agriculture and Life Sciences, Faculty of Food Science. The device is a continuous, crossflow device, as illustrated in Figure 17, by designating the main units. The basic materials of this experiment are the dispersion phase measuring vessel (25 ml) and the continuous phase container (1000 ml). To improve the emulsion quality in terms of droplet size distribution and stability, a mechanical device, named turbulence static promoter, was inserted to the membrane module. The static promoter was made of stainless steel (SS316), it is a double helix-shaped-ribbon reducer (helix reducer) (Figure 16) with the width of 5.8 mm, thickness of 1.6 mm and the length of one complete turn in the spiral was 24 mm (Koris et al., 2011).

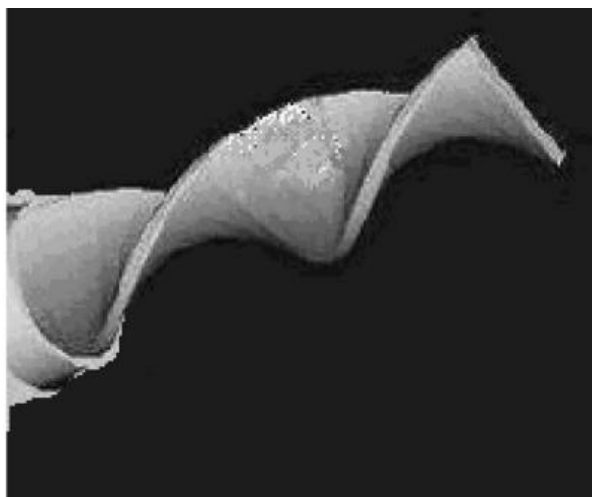


Figure 16: Geometry of the helix reducer (Koris et al., 2011).

The dispersed phase pressure was guaranteed by compressed air with compressor, and it was injected from the outer surface of the membrane. The peristaltic pump and recirculation channel were fitted to recirculate the continuous phase. A rotameter was placed at the exit side of the membrane for measuring the flow rate of continuous phase. Microcapsules were prepared by tubular ceramic porous membrane, pore size 1.4 μm (PALL Austria Filter GmbH). The membrane material was α alumina and the active membrane surface area was 50 cm^2 . The flux of the dispersed phase was examined during the emulsion preparation, and the time of the dispersion phase of the oily phase was measured by a stopwatch from the dispersion phase measuring vessel. The flux, which is expressed on ($\text{dm}^3\text{m}^{-2}\text{h}^{-1}$) can be determined from the

measured time and volume data by knowing the surface of the membrane. The dispersed phase flux through the membrane is:

$$\text{Flux } (J_d) = \frac{G_d}{r_d \cdot A} \quad (2)$$

where A is the membrane surface area (50 cm²), r_d the dispersed phase density (olive oil density is 0.917 Kg/L), and G_d, the mass flowrate of the dispersed phase through the membrane determined from the stopwatch.

The dispersed phase flux, J_d, which is expressed on (dm³m⁻²h⁻¹) is related to the transmembrane pressure ΔP_{tm} according to Darcy's law:

$$J_d = \frac{K \Delta P_{tm}}{\eta L} \quad (3)$$

where K is the membrane permeability, L the membrane thickness, and η the dispersed phase viscosity.

The dispersed phase flux is an important parameter for the membrane emulsification process. Therefore, increasing transmembrane pressure increases the flux of dispersed phase through the membrane, according to Darcy's law. At high fluxes, the average droplet size and the size distribution tend to increase because of increased droplet coalescence at the membrane surface (Charcosset 2009).

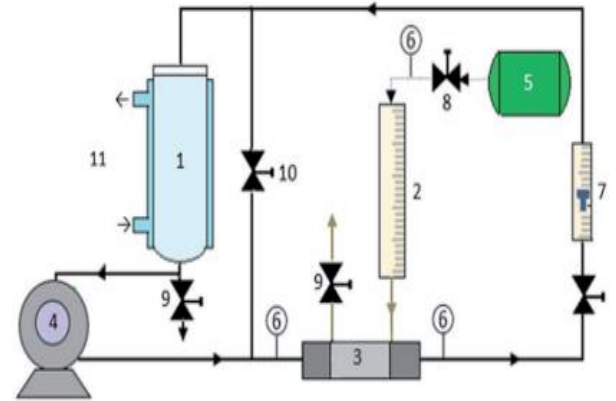
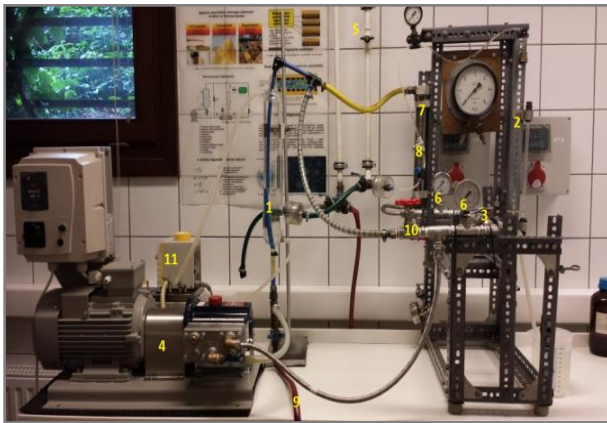


Figure 17: Experimental set-up for the crossflow membrane emulsification process; (1) Continuous phase tank, (2) Graduated disperse phase tank, (3) Membrane module, (4) Peristaltic pump, (5) Compressor, (6) Pressure meter, (7) Rotameter, (8) Pressure controller, (9) valve, (10) valve, (11) thermostat connection (Albert et al. 2018).

The principle of operation is set in figure 17: The continuous phase is recirculated by the pump (4) from the 1 L volume container (1) on the inside of the diaphragm. The recirculation volume

of the retentate can be read from the rotameter (7). The input of the membrane (3) On the output side, pressure gauges (6) are indicated by pressure gauges (6), based on the transmembrane differential pressure formula. The pressure of the dispersion phase is provided by compressed air produced by a compressor (5). From the dispersed phase tank (2) the material to be dispersed comes to the outer side of the membrane, which can be adjusted with the pressure control valve (8). The resulting product can be removed from the system via drain valves (9). Signal 11 indicates that the continuous medium can be heated by means of a thermostat connected to the tank, but if cold water circulates, it is possible to cool the system to avoid warming. Tank 1 must be filled with the continuous phase necessary for the next experiment to moisturize the surface of the membrane.

The membrane machine cleaning is a necessary step before and after each operation. To start cleaning the membrane should be placed in the module (using the screwdriver and the screws). Five cleaning cycles are proceeded to clean the machine. The first cycle with water in which I fill the continuous phase tank with 1 liter of distilled water and put the pump on for 45 min. The pressure should be regulated from 2 to 4 bars with the pressor meters (6) and the flow rate is regulated to 200 Lh^{-1} with the rotameter (7). The second cycle with ultrasil 1% in which I dissolve 15g ultrasil in 1,5 L water under a heat of 70°C . The solution is filled into the the continuous phase tank and the operation lasts for 45 min. The third cycle lasts 45 min and I use water in order to eliminate the remaining ultrasil from the membrane and the other parts of the machine. The fourth cycle is done with citric acid 1% in which I dissolve 15 g citric acid in 1,5 L water under a heat of 70°C . The solution is filled into the continuous phase tank and the pump is put on for 45 min. Finally, the fifth cycle of cleaning was performed with water to eliminate the citric acid residue from the membrane and the other parts.

The last step in the cleaning process is to measure the water flux in the membrane in relation with the TMP to know if the membrane is clean. I started each experiment by measuring the flux of the DI water. The water flux characterizes the permeability of the membrane and shows whether the cleaning after using the membrane was sufficiently effective. To determine it, I measured using a stopwatch the time required to collect a given volume of permeate and calculated its value using equation (1), knowing the surface area of the membrane ($A = 0,5 \text{ m}^2$). The water flux can be increased according to equation (1) by increasing the driving force. During the measurement of the water flux, the pressure was increased gradually by 0.5 bar, so that the values were 1; 1.5; 2; 2.5; 3 bar, and the measurement was always carried out at room temperature. The water flow rate was set to a constant 200 Lh^{-1} using the rotameter (7). The flux values were then plotted as a function of TMP in an Excel sheet and a linear trend line was

fitted to the dots, with the origin as the starting point. The membrane is considered to be clean if the correlation coefficient is > 0.96 . If this is not the case, the cleaning must be repeated according to the procedure mentioned above. Figure 18 shows an example of the verification of membrane purity.

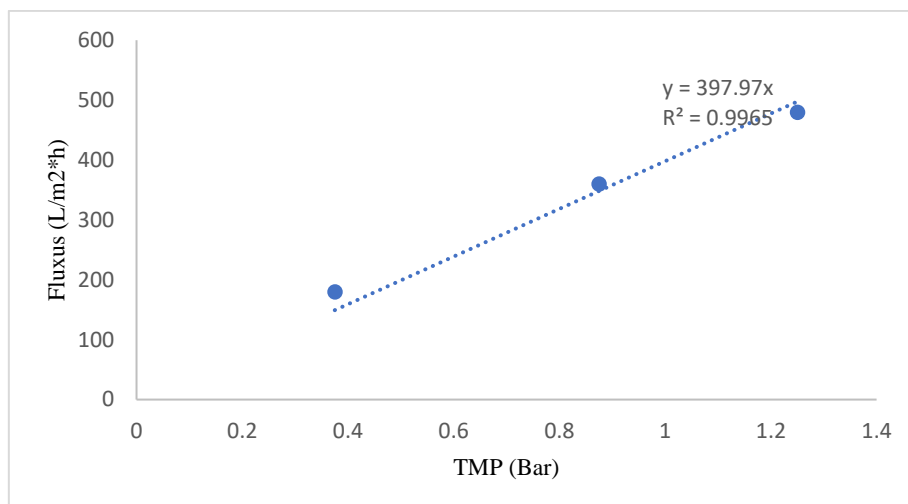


Figure 18: Example of cleaning equation of the membrane.

3.2.2.2. Rotor stator homogenization method (RSH method)

RSH is among the most important continuously operating emulsifying devices. Its principle consists of a rotor of two or more blades and a stator with either vertical or slant slots around the wall of the homogenizer cell. The rotor is incorporated concentrically inside the stator. As the rotor rotates, it generates a vacuum to circulate the liquid in and out of the assembly. One of the two major forces which can reduce the size of the dispersed droplets is mechanical impingement against the wall due to high fluid acceleration. Another force is the shear force created due to the gap between the rotor and the stator. At high rotational speeds, the flow in this region is highly turbulent and contains eddies of different scales (Maa & Hsu, 1996). Figure 19 presents a schematic presentation of this device.

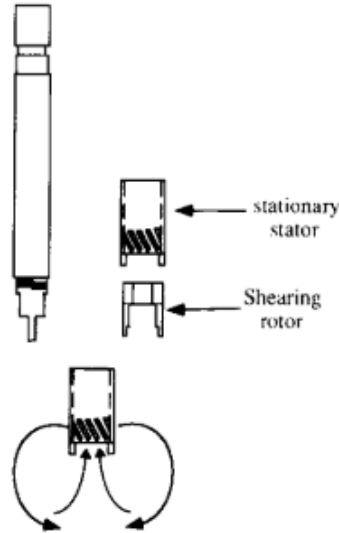


Figure 19: Schematic presentation of RSH (Maa & Hsu, 1996).

Olive oil is added dropwise to the wall material solutions and mixed under the rotor-stator homogenizer (DLAB D-160, LAB-EX Laborkereskedelmi Kft., Hungary), equipped with SS 316L stainless steel dispersing shaft, at 10,000 rpm for 5 min (Appendix-Figure 1).

3.2.3. Emulsion characterisation

3.2.3.1. Emulsion stability

Immediately after the emulsion preparation, 25 ml aliquots of each sample were transferred to graduated cylinders, sealed, stored at room temperature for one day, and the volume of the upper phase was measured after 24 h. Three replicates were performed per sample. The stability was measured by the percentage of separation and expressed as (Tonon et al., 2012):

$$\% \text{ Separation} = \left(\frac{H_1}{H_0} \right) \times 100 \quad (4)$$

Where H_0 represents the emulsion initial height and H_1 is the upper phase height.

3.2.3.2. Emulsion viscosity

Emulsion viscosity was measured at 25°C in the Department of Livestock Products and Food Preservation Technology of MATE and through the determination of steady shear flow curves (Shear stress×Shear rate) using a controlled-stress Physica MCR92 rheometer (Anton Paar, Hungary) rotation viscometer (Appendix-Figure 2), by a measurement system comprising CC 27 (cylinder with 27 mm) measuring body and ST 24 2V-2V-2D measuring head. Viscosity of sample solutions was tested from 10 s⁻¹ to 300 s⁻¹ shear rate at 20°C. Trials were performed in triplicate, using a new sample for each repetition. Rheograms were analyzed according to empirical models and viscosity was calculated as the relationship between shear stress and shear rate.

3.2.3.3 Emulsion droplet size and span

Droplet size was measured immediately after emulsion preparation. Two measuring methods were used. In the first part of my study, I used FRITSCH Laser Particle Sizer and in the second part I used a laser particle size analyser. In both cases, three parallel measurements were performed per sample.

FRITSCH method

The laser particle size analyzer Fritsch Analysette 22 wet dispersing unit was used (in the department of food process engineering of MATE) to determine the particle size and distribution for emulsion and powder samples (Appendix-Figure 6). The particle size analyzer is operating by the laser diffraction principle and is suitable for determining the particle size of emulsions, suspensions, and aerosols. The measuring range of this apparatus is 10 μm to 2000 μm .

The emulsion is first diluted with distilled water. The dispersion unit of the device is a transparent glass container with a volume of 100 ml, which enables the observation of the sample during measurement. The measuring and flushing phases can be regulated with a single-lever valve (4/2-way ball valve). The device is emptied by a centrifugal pump, which gently transports the tested sample or the rinsing water into a container placed for this purpose. During the test, I circulated a small amount of distilled water in the dispersion unit and calibrated the equipment. I then added a sufficient amount of the prepared emulsion to the dosing opening with a pipette until the absorbance reached 7-8. After each sample, I rinsed the equipment with a dilute degreasing solution, and included a methanol wash every 4-5 samples. For the emulsion samples, I determined the diameter of the average droplet size in μm (GMD, geometric mean diameter) and the span value. The value of the span gives information about the size distribution (equation (5)).

Bettersize method

The droplet size distributions of the feed emulsions were determined using a laser particle size analyser instrument (Bettersize ST, LAB-EX, Laborkereskedelmi Kft., Hungary). A small amount of emulsion was suspended in water under agitation and the droplet size distribution was monitored during each measurement until successive readings became constant. After each measurement, a washing cycle with methanol is done.

The droplet mean diameter was expressed as the Sauter and volume mean diameter (D_{32} and D_{43} , respectively).

The width distribution of droplet sizes was determined by the span value, calculated from the following equation:

$$span = \frac{D_{90} - D_{10}}{D_{50}} \quad (5)$$

Where D_{10} , D_{50} , D_{90} correspond to the value of particle diameter that are below of 10%, 50%, 90%, respectively, of the particle diameter of the whole sample. The larger the span value, the wider the size distribution of the particles, the more polydisperse the system.

3.2.3.4. Size and morphology

The size, shape and morphology of emulsion droplets were analyzed by optical microscope (DELTA OPTICAL, USA), oil immersion objectives with the $\times 100$ lenses and associated microscope image reader. The oil droplets of emulsions, immediately after preparation, were poured onto microscopes slides, covered with glass cover slips and their images were taken using an attached digital camera.

The emulsions droplet size is an important aspect to characterize. The size distribution of each type of emulsion was characterized based on a size measurement of multiple random individual droplets using the microscope measurement software.

3.2.3.5. Zeta potential

Zeta potential was measured by Malvern Zetasizer apparatus (Appendix-Figure 8). The zeta potential is a key indicator of the stability of colloidal dispersions. It refers to the ability of aggregation of the dispersed particles. As a rule of thumb, suspensions with zeta-potential above 30 mV and below -30 mV are physically stable (Albert et al., 2016). A disposable bent capillary tube cuvette (DTS1060) was used for the zeta potential measurement. I added the tested solution to the special polystyrene-based cuvette containing two electrodes, taking care not to get moisture on the electrodes. I filled the cells up to the upper part of the electrode without the formation of air bubbles and then plugged them. The laser light can illuminate the sample through small openings carved into the thermocouple plates, and here the electrophoretic mobility between the two electrodes is measured. The measurements were carried out at 25 °C, the time to reach equilibrium was 120 seconds. Trials were performed in triplicate, using a new sample for each repetition.

3.2.4. Emulsion dehydration (ED)

3.2.4.1. ED by Spray drying method

The spray dryer used in this work is a laboratory-scale spray dryer (LabPlant SD-05, Hungary) equipped with a 0.5 mm diameter nozzle (Appendix-Figure 4). The pressure of the compressed air was adjusted to 3.6 bars. The inlet and outlet air temperatures were maintained at $190 \pm 2^\circ\text{C}$, $100 \pm 4^\circ\text{C}$ respectively. The air flow rate was adjusted to $74 \text{ m}^3/\text{h}$. Emulsions were prepared during the spray drying process and were continuously stirred by a magnetic stirrer throughout.

The microcapsules were collected from the collecting chamber and stored in darkness until analyzed. A schematic representation of spray drying process was presented in Figure 11 in the Literature part section 2.7.1. The percentage yield (PY) is a measure of the ability of the elaboration process to produce the bioactive oil loaded units. It is calculated from the following equation.

$$PY (\%) = \frac{M_{\text{microcapsules}}}{M_{\text{dry matter}}} \times 100 \quad (6)$$

Where $M_{\text{microcapsules}}$ is the mass of the powder obtained after drying (g) and $M_{\text{dry matter}}$ is the mass of the total solids present initially in the emulsion (g).

3.2.4.2 ED by Freeze drying method

The emulsions were kept in the freezer for 24 hours at -40 °C and then lyophilized in a freeze-dryer (ScanVac, coolsafe, 110-4 apparatus, Labogene, Lillerod, Denmark) set in the Department of Food Chemistry and Analytics of MATE (Appendix-Figure 3). The percentage yield of this drying method is calculated as in the spray drying method (equation (3)). FD of emulsion was performed at a temperature of -109 °C and a vacuum pressure 12 Pa for 24 hours. After FD, samples were manually ground to obtain a fine powder (Li et al., 2021)

3.2.5. Powder characterization

3.2.5.1. Encapsulation efficiency

Encapsulation efficiency (EE) was determined according to the method described by Bae and Lee 2008. Fifteen milliliters of hexane were added to 1.5 g of powder in a glass jar with a lid, which was shaken by hand for the extraction of free oil, for 2 min, at room temperature. The solvent mixture was filtered through a Whatman filter paper n° 1 and the powder collected on the filter was rinsed three times with 20 ml of hexane. Then, the solvent was left to evaporate at room temperature and after 60 °C, until constant weight. The non-encapsulated oil (surface oil) was determined by mass difference between the initial clean flask and that containing the extracted oil residue (Jafari et al., 2008). Total oil was assumed to be equal to the initial oil, since preliminary tests revealed that all the initial oil was retained, which was expected, since olive oil is not volatile. Microencapsulation efficiency (ME) was calculated from equation (7).

$$EE = \frac{(T_0 - S_0)}{T_0} \times 100 \quad (7)$$

Where T_0 is the total oil in g and S_0 is the surface oil in g.

3.2.5.2. Moisture content

Moisture content of microencapsulated olive oil powders was measured gravimetrically using a moisture analyzer (KERN MLS; KERN & SOHN GmbH, Germany) Heating temperature was maintained at 70 °C until reaching constant weight (Koç et al., 2015).

3.2.5.3. Particle size distribution

Particle mean diameter D32 was measured using a laser particle size analyser instrument (Bettersize ST, LAB-EX, Laborkereskedelmi Kft., Hungary). A small amount of emulsion was suspended in anhydrous ethanol under agitation and the droplet size distribution was monitored during each measurement until successive readings became constant. The droplet mean diameter was expressed as the Sauter and volume mean diameter (D32 and D43, respectively), and the width distribution of droplet sizes was determined by the span value, as described in the section on emulsion droplet size analysis.

3.2.5.4. Solubility

Solubility was evaluated by solving one gram of microcapsules in 25 ml distilled water. The resulting solutions were filtered using Whatman paper No. 42. The filter papers and residues were dried in oven at 105°C for three hours and then were cooled down and weighed. The solubility percentage then was calculated using equations (5) and (6) (Cahyani et al., 2018).

$$\text{Solubility percentage} = 100\% - \text{Residue \%} \quad (8)$$

$$\text{Residue (\%)} = \frac{W_{\text{filter paper and residue}}}{W_{\text{filter paper}}} \times 100 \quad (9)$$

Where W is the weight in g.

3.2.5.5. Bulk density and tapped density

Bulk density and trapped density were performed in triplicate following the method of Zhu et al. (2022).

For bulk density, 2.5 g of microcapsules were poured into a 10 ml graduated measuring cylinder and the volume was measured. The bulk density was calculated according to the following equation.

$$\text{Bulk density (g} \cdot \text{cm}^{-3}\text{)} = \frac{\text{Sample weight in g}}{\text{Sample volume in ml}} \quad (10)$$

Similarly, for tapped density, 2.5 g of microcapsules were transferred into a 10 ml graduated measuring cylinder, and it was gently dropped 100 times onto a rubber mat from a height of 15 cm to determine the tapped volume. Tapped density was calculated according to the following equation:

$$\text{Tapped density (g} \cdot \text{cm}^{-3}) = \frac{\text{Sample weight in g}}{\text{Total volume in ml}} \quad (11)$$

The value of bulk density OOM prepared by FD technology was not measured because after FD, flakes were grounded manually. Therefore, sample volume was inconsistent in every experiment.

3.2.5.6. Flowability and cohesiveness

The flowability and cohesiveness of the microcapsules were determined from the bulk density and tapped density based on the Carr index and the Hausner ratio. Following correlations were adopted for those purposes (Zhu et al., 2022).

$$\text{Carr index (\%)} = \frac{\text{Tapped density} - \text{Bulk density}}{\text{Tapped density}} \times 100 \quad (12)$$

$$\text{Hausner ratio (-)} = \frac{\text{Tapped density}}{\text{Bulk density}} \quad (13)$$

Carr index and Hausner ratio of microcapsules prepared by FD technology were not measured because of the unavailability of freeze-dried products. The reason is mentioned earlier.

3.2.5.7. Scanning electron microscopy SEM

The surface morphology of microcapsule was studied by a field emission scanning electron microscope (FESEM) (Model: JSM 5500 LV, Jeol Ltd., Japan) set in Department of Inorganic and Analytical Chemistry of Budapest University of Technology & Economics Szent Gellert ter 4, 1111 Budapest (Hungary). Microcapsules were coated with a combination of gold and platinum (60:40) for 10 min with a 10-mA plasma current. Coated samples were placed in SEM for analyzing its surface morphology. In FESEM, a working distance was 35 mm and backscattered secondary electron (BSE) electron flow was used (Naz et al., 2020).

3.2.5.8. Oxidative stability of MEVOO by Rancimat method

Accelerated Rancimat test is widely used due to its ease of use and reproducibility. This method is used to estimate olive oil stability before and after microencapsulation. To determine samples' oxidative stability, an automated Metrohm Rancimat (model 743; Herisau, Switzerland) was used (in the Department of Grain and Industrial Plant Processing, MATE) according to the method used by Gallardo et al. (2013). An aliquot (3 g) was weighed into each glass reaction vessel. The conductometric cells were filled with deionized water up to a volume of 50 ml. The heating temperature was set at 110 °C, and filtered, dried air was allowed to bubble through the hot oil at a flow rate of 10L h⁻¹. Each test was performed in duplicate. Peroxides are formed as primary oxidation products via oxidation of fatty acids in the sample.

After some time, the fatty acids are destroyed and low-molecular weight organic acids (especially formic and acetic acid) are formed as secondary oxidation products, in addition to other volatile organic compounds. Figure 20 shows the principle of the Rancimat measurement.

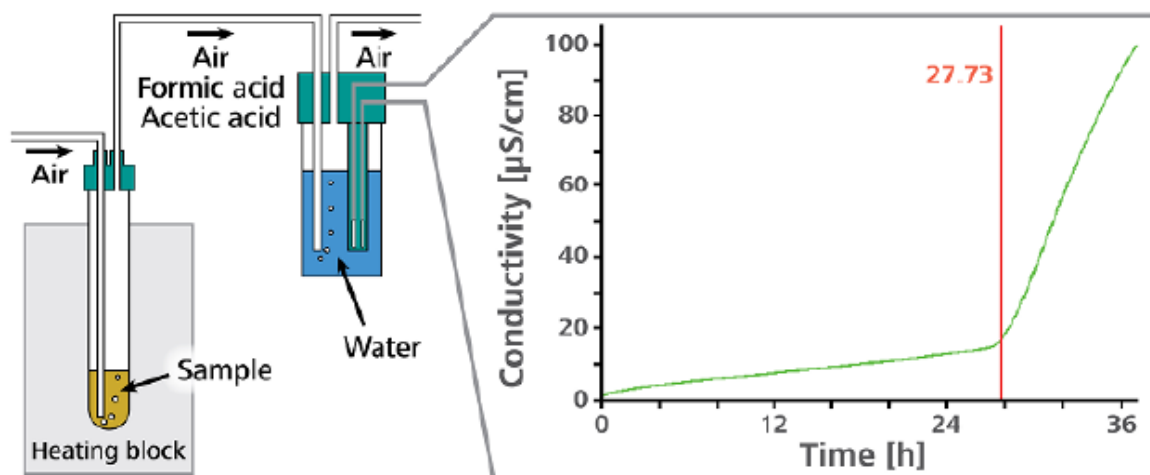


Figure 20: Schematic representation of the Rancimat measurement technique.

3.2.5.9. Statistical analysis by SPSS method

All experiments were performed in triplicate and the mean value with standard deviation (S.D.) was calculated using IBM SPSS (v27, Armok, NY: IBM Corp., 2020). Significant differences between different groups in emulsion were determined by the one-way multivariate analysis of variance (MANOVA) method in case of variables, such as stability (% separation), D43 (µm), span (-) and viscosity (mPa.s). Two-way MANOVA models were used for microcapsules in case of EE (%) and moisture content (%). Furthermore, one-way multivariate analysis of variance (MANOVA) method was performed in case of variables D43 (µm) and span (-) for microcapsules. Having significant MANOVA results, univariate ANOVA models were run with Bonferroni's correction in all cases. Finally, the Tukey's Games-Howell's post hoc tests were performed to separate the significant groups. The differences were considered significant when $P < 0.05$. Stability data was previously transformed by sqrt function to ensure the normality of the residuals that was tested by Kolmogorov-Smirnov test ($P > 0.05$). The homogeneity of variances was checked by Levene's test ($P > 0.05$). Slight heteroscedasticity of EE was managed using Games-Howell's post hoc test.

3.2.6. Preparation of olive oil beads by gelation of sodium alginate or emulsification - external gelation method

This process is based on the chemical reaction between the water-soluble sodium alginate and polyvalent cation, calcium, to form water-insoluble olive oil loaded with alginate beads or capsules. First, for the emulsion characterization study, emulsions of sodium alginate solutions

with olive oil were prepared by using the rotor-stator homogenizer (DLAB D-160, LAB-EX Laborkereskedelmi Kft., Hungary) at a fixed homogenization rate of 15,000 rpm for 5 min (Appendix-Figure 1).

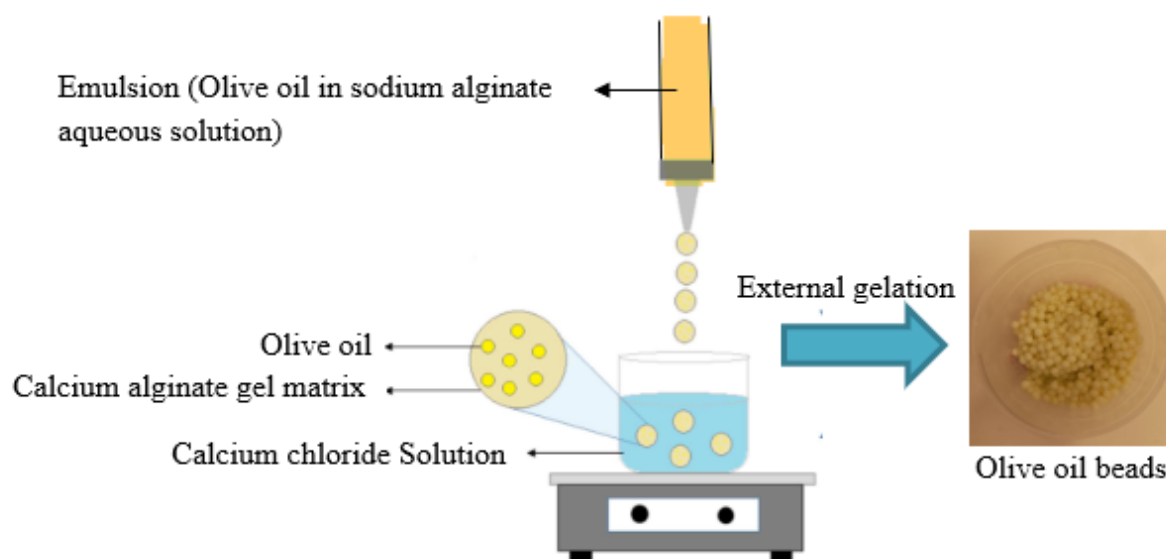


Figure 21: Schematic representation of the process of emulsification/external gelation (Self-developed the concept was adopted from Morales et al. (2017)).

Second, for the optimization study, the emulsion prepared with the corresponding concentrations of alginate and olive oil was homogenized at the corresponding rate and dripped from a specified height into a 2% CaCl_2 solution using a graduated burette like it was shown by the appendix-figure 7. The gelling solution was stirred using a magnetic stirrer during the whole period of encapsulation. After that the gel beads were held for a further 30 min in the gelling solution for hardening to achieve the required mechanical stability. Figure 21 shows the process of emulsification/external gelation. The beads obtained were further dried at room temperature for 24 hours. To screen the effect of various formulation and process variables on formulation of beads, various formulations of sodium alginate/olive oil beads were prepared employing the Box-Behnken design (BBD) as depicted in Table 19.

3.2.6.1. Emulsion stability

Immediately after the emulsion preparation, the emulsions were poured in measuring cylinders with a volume of 100 cm^3 and were held at RT for 24 h. After that the emulsified phase volume and the separated phase volume were recorded. The stability of the emulsions was calculated according to the equation (4) from section 3.2.3.1.

3.2.6.2. Microscopic Test

The characteristics of the oil droplets were determined using microscopic pictures obtained by optical microscope (DELTA OPTICAL, USA). The OOE droplets, immediately after preparation, were viewed under the microscope, and their images were taken using an attached digital camera. The emulsion droplet size is an important aspect to characterize. The size distribution of each type of emulsion was characterized based on a size measurement of multiple random individual droplets using the microscope measurement software.

3.2.6.3. Retention capacity (RC) of the wet olive oil beads

The retention capacity of the capsules was evaluated by determining the amount of oil phase in the gelling solution after the washing of the capsules with distilled water (Poirieux et al., 2017). In a cylinder with a volume of 250 cm³, the gelling solution was poured and after a brief retention the quantity of the oil phase separated in it was determined. After that, 100 cm³ of distilled water were used to wash out the surface oil phase of the capsules separated from the gelling solution by a metal sieve. The washing water was also put into a measuring cylinder and after retention the oil phase amount was recorded. The retention capacity of the capsules was determined according to Poirieux et al. (2017) by following this equation:

$$RC (\%) = \frac{(V_{oil} - V_{oil, CaCl_2} - V_{oil, Water})}{V_{oil}} \times 100 \quad (14)$$

3.2.6.3. Statistical analysis by RSM method

Data were analyzed statistically with Design Expert software (Version 13, USA). Then, all the measurements were evaluated by the analysis of variance (ANOVA) with a significant level of $\alpha = 0.05$ to determine statistical differences among the independent variables.

4. RESULTS AND DISCUSSION

4.1. Characterization of olive oil

Characteristics of olive oil depend on the genetic variety of olive fruit, the degree of olive ripening, the crop season, the geographical area and the climate (Condelli et al., 2015; Manai-Djebali et al., 2012). In the present experiment, 6-12 months old extra virgin olive oil (according to mentioned manufacturing time in bottle), procured from local supermarket in Budapest, Hungary was used. Extinction coefficients, such as K232 and K270 were found 1.45 ± 0.001 and 0.17 ± 0.001 , respectively. The peroxide value of our experimental olive oil was 8.02 ± 0.74 meq O₂/kg of oil. It may realize that studied extra virgin olive oils exhibited the values of some quality indices (K232 ≤ 2.5 ; K270 ≤ 0.22 and peroxide value ≤ 20 meq O₂/kg of oil) within the limits, established by EU regulation for extra virgin olive oil (Demirag & Konuskan, 2021). The total phenolic content of experimental olive oils was around 480 ± 02 mg GA/kg oil. Different types of tocopherols, such as α -, β - and γ - tocopherol were determined and those values are 270 ± 0.4 mg.kg⁻¹, 2.5 ± 0.01 mg.kg⁻¹ and 0.4 ± 0.001 , respectively; however, δ -tocopherol was not found in the experimental olive oil. The acidity value of extra virgin olive oil was 0.35 % C18:1. Fatty acid profiles in the experimental olive oil is mentioned in Table 6. It is noted that oleic acid C18:1, palmitic acid and linoleic acid are abundant in the experimental olive oil. The composition of fatty acids in that olive oil was exhibited within the guideline of International Olive Council (IOC), 2008 (Wiesman, 2009). Furthermore, composition of sterol in extra virgin olive oil is presented in Table 6. It is noted that β -sitosterol, Δ -5-avenasterol, campesterol, stigmasterol and clerosterol are abundant phytosterol in our experimental olive oil.

Table 6 : Composition of fatty acids and sterols in the experimental olive oil sample

Fatty acids (g·100 g of oil ⁻¹)		Sterols (g·100 g of oil ⁻¹)	
Myristic C14:0	0.03 ± 0.001	Cholesterol	0.32 ± 0.008
Palmitic C16:0	13.59 ± 0.01	Brassicasterol	0.03 ± 0.004
<i>t</i> -Palmitoleic C16:1	0.31 ± 0.01	24-methylene cholesterol	0.15 ± 0.002
Palmitoleic C16:1n-7	1.15 ± 0.01	Campesterol	2.55 ± 0.02
Stearic C18:0	2.73 ± 0.02	Campestanol	0.17 ± 0.0203
Oleic C18:1 n-9	72.5 ± 0.03	Stigmasterol	1.44 ± 0.023
<i>c</i> -Vaccenic C18:1 n-7	0.2 ± 0.01	Δ -7-Campesterol	0.11 ± 0.001

<i>c-t</i> Linoleic C18:2	0.25±0.03	Clerosterol	1.03±0.04
Linoleic C18:2 n-6	7.8±0.04	β-sitosterol	84.51±0.06
Arachidic C20:0	0.45±0.02	Sitostanol	0.65±0.003
Eicosenoic C20:1 n-9	0.25±0.02	Δ-5-avenasterol	6.45±0.07
α-Linolenic C18:3 n-3	0.75±0.03	Δ-5,23-stigmastadienol	0.35±0.003
Eicosadienoic C20:2 n-6	0.12±0.01	Δ-5,24-stigmastadienol	0.75±0.0201
Behenic C22:0	0.07±0.008	Δ-7-stigmastenol	0.55±0.004
Eicosatrienoic C20:3 n-3	0.21±0.01	Δ-7-avenasterol	0.65±0.002
Arachidonic C20:4 n-6	0.48±0.01	Apparent β-sitosterol	92.35±0.32
Lignoceric C24:0	0.08±0.005		

4.2. Membrane emulsification of olive oil by different combinations of wall materials:

Preliminary study

This preliminary study aimed at evaluating the potential of maltodextrin combination with different wall materials in emulsification technology process, to achieve better stability and better droplet size distribution. Based on the study conducted by Albert et al.(2018), the emulsification process was selected and the composition of wall materials was studied. In the first step, “membrane emulsification” technology was adopted to encapsulate olive oil using different combinations of gum Arabic (GA), maltodextrin (MD) with whey protein isolate (WPI) and carboxymethylcellulose (CMC). Three formulations were prepared: First, MD-GA contained a binary mixture of 83% maltodextrin and 17 % gum arabic. Second, MD/WPI-GA was a ternary mixture of 59% maltodextrin, 12 % gum arabic and 29% whey protein isolate. Third, MD/CMC-GA contained 53% maltodextrin, 38% gum arabic and 9% carboxymethylcellulose. In the second step, characterization of emulsions from different aspects, morphology, particle sizes, and stability had been discussed.

4.2.1. Formulation and preparation of olive oil emulsion

Wall materials for the emulsification of oil must have high stability, high water solubility, drying properties, a tendency to form a fine and dense network during drying, emulsifying properties and should not permit lipid separation from the emulsion during dehydration (Calvo et al., 2012; Gharsallaoui et al., 2007). The selected wall materials should also protect the core from possible degradation during storage. In our case, the challenge for the selected system is

to protect OOM (obtained by drying the emulsions) from oxidation upon storage. Finally, the costs and availability need to be considered. Almost no wall material can meet all the properties listed; therefore, they are used in combination with each other (Hogan et al., 2001; Jafari et al., 2008). Three formulations were prepared to encapsulate olive oil with different wall materials. Emulsions were formulated according to table 7.

GA was chosen due to its excellent emulsifying capacity having an effective slow dispersion in water at room temperature (Gallardo et al., 2013). The use of GA as an encapsulating matrix is common due to its characteristics of viscosity, solubility and emulsification. It was traditionally used for lipid encapsulation and can produce stable emulsions with most oils (Gharsallaoui et al. 2007). This complex polysaccharide is easily dispersed in water in concentrations of up to 50% due to its highly ramified structure (Samantha et al., 2015). That is why it was used in all of the cases together with Tween 80 which was used as emulsifier for easier emulsification and drop stability. MD, WPI and CMC were used to provide protection from oxidation at emulsion droplet interfaces (Gallardo et al., 2013). Also, maltodextrin with the gum arabic were used in all cases because it has been demonstrated that this combination of wall materials presents a good compromise between cost and effectiveness for the microencapsulation of oils in general (Rubilar et al., 2012). The choice of this formulation was based on the study of (Gallardo et al., 2013) with modifications.

Table 7: Description of formulations for membrane emulsification of olive oil.

	MD-GA	MD/WPI-GA	MD/CMC-GA
Maltodextrin (g)	100	100	30
Gum Arabic (g)	20	20	21.48
Whey protein isolate (g)	-	50	-
Carboxymethylcellulose (g)	-	-	5
Olive oil (g)	60	60	40
Tween 80 (g)	20	20	23.25
Deionized water (g)	500	500	650
Solid % w/v ^a	28.57	33.33	17.69
O/W Ratio (g/g) ^b	0.4	0.5	0.21
Wall material/oil ratio (g/g)	2	2.83	0.94

^a a solid content in emulsion including extra virgin olive oil.

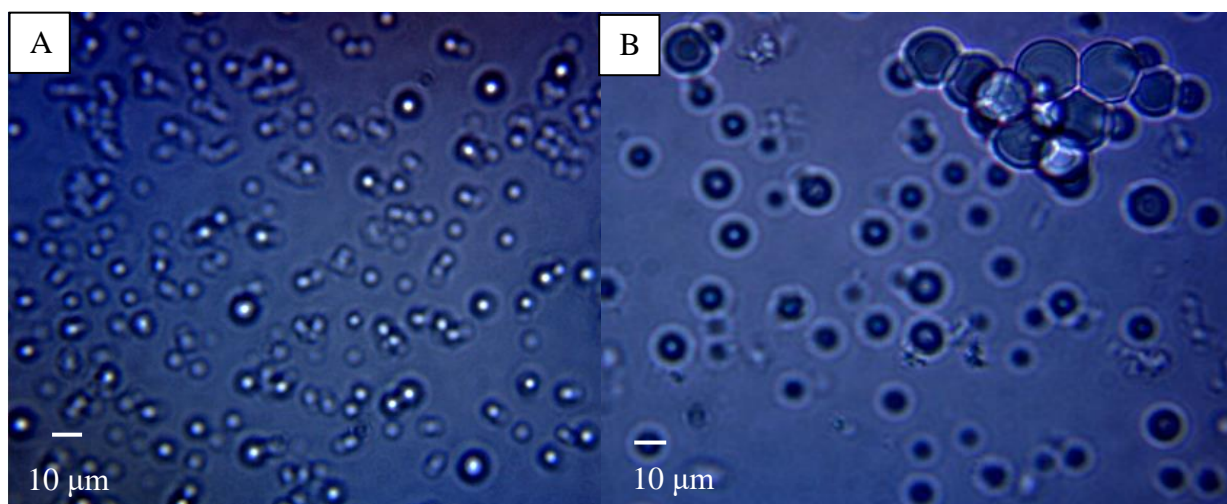
^b Ratio between dispersed (O) and continuous phases (W).

High solid contents result in increasing the viscosity which reduces the migration of oil to the surface and provides a rapid skin formation (Jafari et al., 2008). In this work the solid content

of O/W emulsions was around 30% w/v except for MD/CMC-GA, which was formulated with a solid percentage of around 18 % w/v due to the high viscosity of CMC. Solid contents were fixed because it has been reported that for further step (the spray drying step) it is important to find a compromise between high air temperature and high solid concentration (Gharsallaoui et al., 2007).

4.2.2. Size and morphology

The surface morphologies of the droplets of OOE were studied using optical microscopy. Figure 22 shows size and morphology of the three emulsions formulations. The average droplet size of each type of emulsion was characterized based on a size measurement of multiple random individual droplets. The average droplet diameter of precursor microcapsules was the smallest around 7 μ m in the figure 21 A for emulsions containing only MD and GA, 11 μ m in figure 21 B for emulsions containing WPI beside to MD and GA and 9 μ m in the figure 21 C for emulsions containing CMC beside to MD and GA. Well defined spherical microcapsules were observed in all cases. CMC containing precursor microcapsules presents more homogenous size distribution. The highest droplet mean diameter was observed in the emulsion containing WPI. Nevertheless, this later presented some agglomerates due to the flocculation of the proteins in the solution.



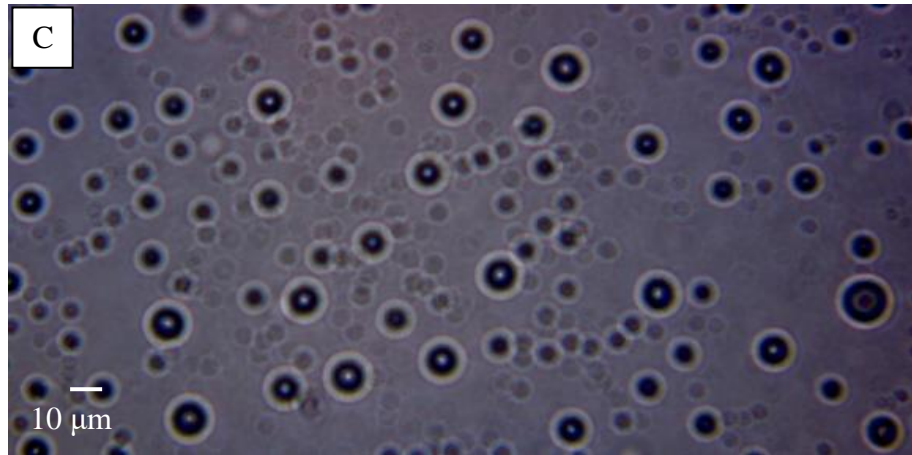


Figure 22: Microstructure of emulsions immediately after their preparation by cross flow membrane emulsification with the $\times 100$ objective lense. A) MD-GA, B) MD/WPI-GA, C) MD/CMC-GA.

In all cases average size of the synthesized microcapsules was in line with the conclusion reached by Joscelyne and Trägårdh (2000) which reported that for membrane emulsification, the size of synthesized emulsion particles might be 2-10 times greater than the pore size of the membrane. In the present work, the membrane pore size is $1.4 \mu\text{m}$. The emulsions droplet sizes detected by the optical microscope were 5 times greater than membrane pore size for MD-GA, 8 times greater than membrane size for MD/WPI-GA and 6.5 times greater than membrane pore size for MD/CMC-GA.

4.2.3. Emulsification results

The dispersed average phase flux is an essential parameter for the membrane emulsification process. Increasing transmembrane pressure increases the flux of dispersed phase through the membrane, according to Darcy's law. At high fluxes, the average droplet size and the size distribution tend to increase because of increased droplet coalescence at the membrane surface (Charcosset 2009). In this section, transmembrane pressure was fixed to 2.5 bars and the dispersed phase calculated average fluxes are $332 \text{ dm}^3 \text{ m}^{-2} \text{ h}^{-1}$, $60.6 \text{ dm}^3 \text{ m}^{-2} \text{ h}^{-1}$ and $40 \text{ dm}^3 \text{ m}^{-2} \text{ h}^{-1}$ for MD-GA, MD/WPI-GA and MD/CMC-GA respectively. In the literature, fluxes ranging from $50\text{--}250 \text{ dm}^3 \text{ m}^{-2} \text{ h}^{-1}$ were obtained with ceramic membranes of $0.2 \mu\text{m}$ α -alumina membrane (Charcosset 2009). An increase in flux is often correlated with droplet increase (Joscelyne & Trägårdh, 2000). According to (Volker et al., 1998), the quality of emulsification process can be described by the mean droplet size and the flux of the disperse phase. Parameters such as pore size of the membrane, pressure of disperse phase and adsorption kinetics of the emulsifier influence the quality of the emulsion. Smaller droplets of emulsion are produced when the emulsifier molecules adsorb rapidly at newly formed interfaces. The flux is also

influenced by the TMP. In our study TMP was adjusted at 2.5 bars because exceeding this TMP lead to a jetting of the dispersed phase leading to coalescence and thus to an uncontrolled droplet size. The fluxes decreased when other materials such as WPI and CMC were added. This could be explained by membrane fouling caused by complex physical, chemical, and even biological interactions between the foulants (including organics, colloids, cells, sludge flocs, and salts) and the membrane surface to decrease flux and increase the operation cost. For example, proteins can stick with their hydrophilic groups to the membrane surface, making the pore hydrophobic which may cause either pore blocking or droplet formation process change (Gijsbertsen-Abrahamse, 2003) besides, the number of active pores (pores at which droplets are formed) in the membrane which is low (section 2.4.1).

The results of the droplet mean diameter are summarized in figure 23. The average mean diameters D_{32} were $12.34 \pm 0.95 \mu\text{m}$, $5.22 \pm 1.03 \mu\text{m}$ and $9.16 \pm 0.26 \mu\text{m}$ for MD/WPI-GA, MD/CMC-GA and MD-GA respectively.

The highest droplet mean diameter corresponds to the emulsion containing MD/WPI-GA which is associated with the disperse phase average flux of $60.6 \text{ dm}^3 \text{ m}^{-2} \text{ h}^{-1}$. In the emulsion containing WPI, the droplet size was greater than emulsion containing only MD-GA and this could be due to the coalescence of the droplets growing on neighboring pores during droplet detachment as explained in section 2.4.2. The increase in droplet diameter may result from the mechanism of droplet formation, which changes with increasing transmembrane fluxes. At higher transmembrane fluxes droplets are formed in a continuous jetting regime (Pawlik & Norton, 2012).

The addition of CMC into maltodextrin and gum arabic resulted in droplet size reducing in the emulsion containing CMC. The emulsion prepared from MD/CMC-GA presented the smallest droplet size. This could be related to the high visible viscosity presented by this mixture which implies a greater resistance to droplets movements, avoiding coalescence and resulting in smaller diameters. This could be explained also by the absence of jetting since the flux was decreasing to $40 \text{ dm}^3 \text{ m}^{-2} \text{ h}^{-1}$. At low transmembrane fluxes, droplets are created via a dripping mechanism where each time the droplet is formed at the pore opening, the hydrodynamic drag force FD of the continuous phase helps the droplet to break away from the membrane (Pawlik & Norton, 2012).

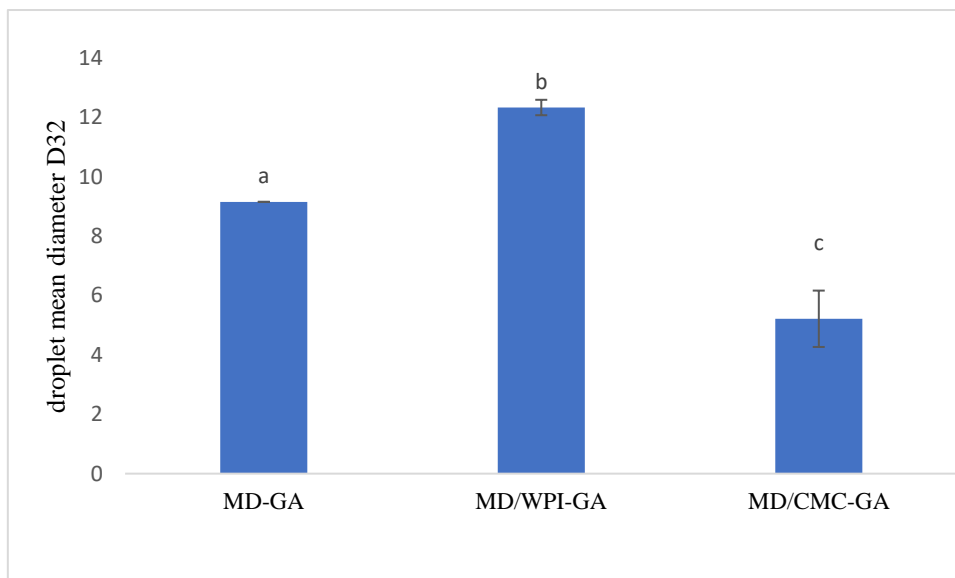


Figure 23: Droplet mean diameter of emulsions with different wall materials. Different letters indicate significant difference at $p < 0.05$.

The span value (figure 24) was considered as an indication of the dispersity of the droplet size. The lower the span value, the more monodisperse the emulsion. In this case MD/CMC-GA is more monodisperse compared to MD/WPI-GA and MD-GA respectively. This fact is also shown by the microscopic imaging. The most monodisperse emulsion is MD/CMC-GA with a span value of 0.39 ± 0.04 .

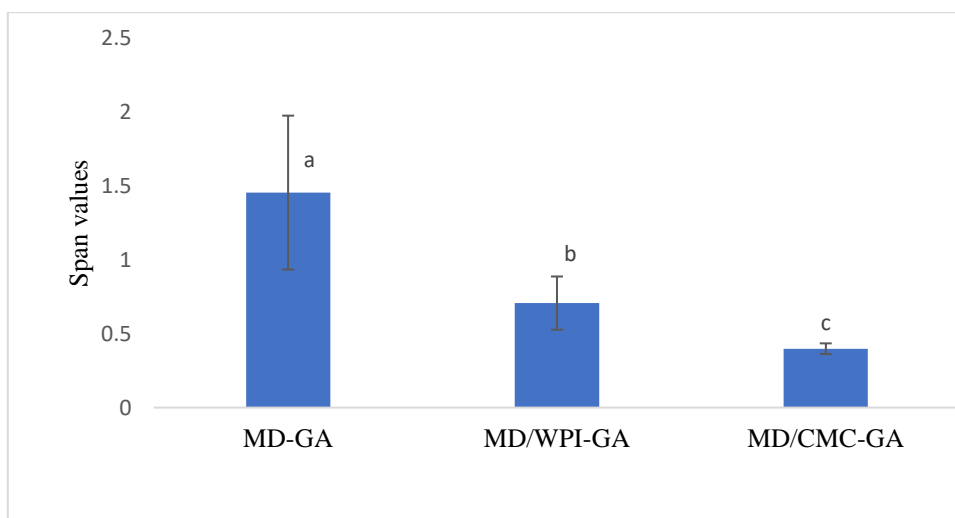


Figure 24: Span values of emulsions with different wall materials. Different letters indicate significant difference at $p < 0.05$.

4.2.4. Emulsions stability

Emulsion stability is expressed as the zeta potential of the emulsions. The results of zeta-potential for the different formulations are summarized in table 8. The zeta-potential of any material depends on its concentration in the solution. The average values of zeta-potential in

three of the emulsions show the instability of the added wall materials in the continuous phase solution. The MD/CMC-GA formulation is closer to being stable compared to the three other formulations and this could be first due to the low concentration of maltodextrin in this emulsion. It has been proved previously by Albert et al. (2016) that low concentration of maltodextrin has a positive impact on the stability of maltodextrin in the solution. Consequently, it is better to use lower concentrations of maltodextrins to achieve better stability (toward -30 mV). Second, the higher stability of CMC containing emulsion could be related to the higher viscosity of the continuous phase. It was previously proved by Tonon et al. (2012), that the increase in viscosity reduces the rate of sedimentation of the particles which results in better emulsion stabilization and thus avoiding droplet coalescence.

Table 8: Zeta-potential results

Sample	Zeta-potential (mV)
MD-GA	-1.97±0.32 ^a
MD/WPI-GA	-0.895±0.23 ^b
MD/CMC-GA	-4.39±1.08 ^c

*Results are represented by mean value with standard deviation (\pm values). Different letters indicate significant difference at $p < 0.05$.

WPI containing emulsion is the most instable. The low stability of such emulsion can be attributed to the unfolding of protein molecules at the droplet surface, which enhances protein-protein interaction resulting in the flocculation phenomena during emulsification. The unfolding of protein molecules of the oil-water interface may result in changes in secondary and tertiary structure, and consequently exposure of their residues which would be linked (S-S- linkages or disulfide linkages) within the native globular structure, leading to the formation of intermolecular interaction at the oil-water interface and flocculation (Carneiro et al., 2013a; Tonon et al., 2011).

4.2.5. Summary

In this chapter it was possible to evaluate the performance of different wall materials combinations in the olive oil emulsification process. The membrane emulsification of OO resulted in microcapsules with spherical shapes in all cases of formulation except the emulsion containing whey protein isolate which presented some agglomerates. This result may be due to the flocculation of WPI during the emulsification and consequently reducing the emulsion stability which was demonstrated by the zeta potential measurement. The addition of CMC to

MD and GA mixture resulted in better stability of the emulsion and into a narrow droplet size distribution. Limitations of the membrane emulsification process may be associated to the low fluxes associated to monodispersed emulsions, and to fouling phenomena. These disadvantages may be solved by recent processes, such as rotating or vibrating membrane devices. It also appears that special membranes must be developed to fulfill properties required for industrial applications: high fluxes, availability of large membrane area. Membrane emulsification should then appear as a very interesting technique for the food processing industry as well as for the pharmaceutical industry. However further studies are still necessary to evaluate encapsulation efficiency after spray drying and the stability to oxidation of the encapsulated olive oil. An attempt to spray dry the most stable sample containing MD, GA and CMC was performed with a laboratory scale spray dryer and the drying process was unsuccessful due to the high viscosity of the sample. The main problem that occurred was the caking phenomenon, which is associated with crystallization of amorphous rubbery sugars, giving up their water to the surrounding matrix. This phenomenon begin to occur rapidly at temperature above glass-transition temperature (T_g) of 20-30°C (Netto et al. 1998). The glass transitional temperature is specific to each type of material. Based on it the materials change from glassy state to the gummy state (Samantha et al., 2015). This operational problem causes a higher interaction of the powders with water (increase of hygroscopicity), higher cohesion between the particles, and a higher adhesion to the walls of drying chamber of the spray dryer.

4.3. Effect of change of emulsification method and wall material composition on microencapsulation of olive oil

The objective of this part of my work was to investigate the microencapsulation of extra virgin olive oil by freeze drying to increase its stability and application area. The effect of homogenization methods in terms of rotor–stator (RSH) and cross flow membrane emulsification (CFME) and the effect of wall materials composition were examined on the physical properties of OOM. MD, CMC and GA were used as wall materials and microencapsulation was carried out in a laboratory type freeze dryer. Concentrations of CMC and MD (with DE 5) were varied; however, the concentration of GA was constant. CMC and MD (DE 5) are considerable hydrophobic (Lee et al. 2017; Liu et al. 2021) which influence the detachment of oil droplets (hydrophobic nature) from membrane pores due to surface tension (hydrophobic-hydrophobic interaction). The flow diagram of this process is shown in Figure 25.

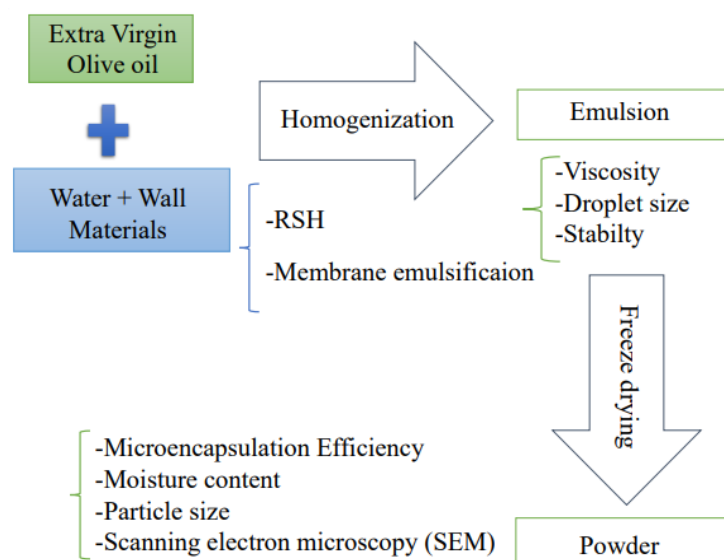


Figure 25: Flow diagram of the microencapsulation process by Freeze-drying.

4.3.1. Formulation of the emulsions

The emulsions were prepared according to Table 9. Different polymeric carbohydrates, such as MD, GA, CMC and emulsifier Tween 80 were dissolved in DI water with constant stirring at temperature 50°C.

Table 9: Description of formulation

	Emulsion 1	Emulsion 2
Maltodextrin (g)	10	15
Gum Arabic (g)	15	15
Carboxymethyl cellulose (g)	10	5
Olive oil (g)	30	30
Tween 80 (g)	5	5
DI water (g)	700	700
wall material/oil ratio (g/g)	1.16	1.16
Total solids % (w/v)	9.09	9.09

The total solids concentration (wall materials and olive oil) was fixed at 9.09 %. This value is below 30 % because CMC viscosity is high. Subsequently, the emulsion was prepared by homogenization with rotor-stator homogenizer (RSH) or crossflow membrane emulsification (CFME). In homogenization process, oil was added dropwise in aqueous polymeric carbohydrate solution and RSH (IKA, T25, Germany) (Koç et al., 2015) was operated with speed 15000 rpm for 5 min at room temperature. Emulsion was also prepared by membrane emulsification technology. A tubular ceramic membrane with pore size 1.4 µm was placed in stainless steel made membrane module. Inside of membrane tube, a stainless steel made

mechanical device, known as static turbulence promoter, was inserted. The detailed geometry of static turbulence promoter was mentioned before (Koris et al., 2011). The detailed description of membrane emulsification method was mentioned in Section 3.2.1.1. Experimental setup of membrane emulsification process and fluid flow within membrane tube are presented in Figure 26 (A). In subsequent step, emulsion was considered for freeze drying.

4.3.2. Emulsions stability

Results of the emulsion stability are presented in table 10. Olive oil emulsions, prepared by RSH provided greater stability (no phase separation after 24 h). It might be attributed by the fact that due to high viscosity in presence of CMC, MD and GA, oil droplets cannot move freely inside the emulsion. It was previously proved by Tonon et al. (2011) that the increase in viscosity reduces the rate of sedimentation of the particles which results in better emulsion stabilization and thus avoiding droplet coalescence and creaming. Similar justification was reported by Carneiro et al. (2013b) in case of emulsion, made by flaxseed oil, MD and GA by RSH. On the other hand, olive oil emulsions, prepared by CFME had faster droplet coalescence and phase separation after 24 h. These results might be influenced by droplet size of emulsion. The overall MANOVA test was significant for both factors emulsification method and composition of emulsions (Wilk's lambda values are below 0.001, $p < 0.001$) as well as for the interaction (Wilk's lambda=0.01; $p < 0.001$).

Table 10: Stability (% of separation), droplet size (D_{32} (μm)) and span of emulsions prepared with different emulsification methods and different wall material composition.

	CFME-1	CFME-2	RSH-1	RSH-2
% of separation	20 \pm 0.20 ^{Ba}	24 \pm 0.15 ^{Bb}	-	-
D_{32} (μm)	41.68 \pm 2.85 ^{Ab}	20.05 \pm 0.49 ^{Ba}	5.83 \pm 0.60 ^{Ba}	5.61 \pm 0.37 ^{Aa}
Span (-)	0.81 \pm 0.16 ^{Bb}	0.40 \pm 0.09 ^{Aa}	1.05 \pm 0.16 ^{Ab}	0.33 \pm 0.10 ^{Aa}

*Results are represented by mean value with standard deviation (\pm values). In superscript, dissimilar alphabet represents the significant difference ($P < 0.05$) between results. Upper case letters are for the comparison of emulsification methods within fixed composition and lower-case letters are for comparison of compositions within fixed emulsification method.

4.3.3. Emulsion droplet size and span

Results of droplet mean diameter (D_{32}) and span of emulsion are reported in table 10. D_{32} values of CFME-1 and CFME-2 were significantly higher compared to RSH-1 and RSH-2. It was proven that emulsion can be the most stable when droplet size and span values are lower

(Carneiro et al., 2013a). The values of D_{32} for CFME-1 and CFME-2 were determined to be $41.68 \pm 2.85 \mu\text{m}$ and $20.05 \pm 0.49 \mu\text{m}$, respectively. The higher mean particle size obtained by CFME is explained by the crossflow velocity or the wall shear stress: when small wall shear stress is applied, the detached droplets are bigger in size (Charcosset, 2009).

Joscelyne and Trägårdh (2000) reported that the size of emulsion droplets might be 2-10 times greater than the pore size of the membrane. In the present investigation, the average pore size of membrane was $1.4 \mu\text{m}$. Therefore, our results were not directly reasonable by the mentioned principle. Our results can be justified by the fact that non-homogeneous droplets might be formed due to asymmetric pore size in membrane surface. After detachment of oil droplets from membrane pores, they can coalesce with each other in presence of polymeric carbohydrates, such as GA, MD and CMC in continuous phase (Figure 26 (B)). It is noted that the size of droplet and span values in case of CFME-1 were higher than CFME-2. Due to the higher amount of CMC in case of CFME-1 preparation, it was more viscous, which promoted coalescence among droplets.

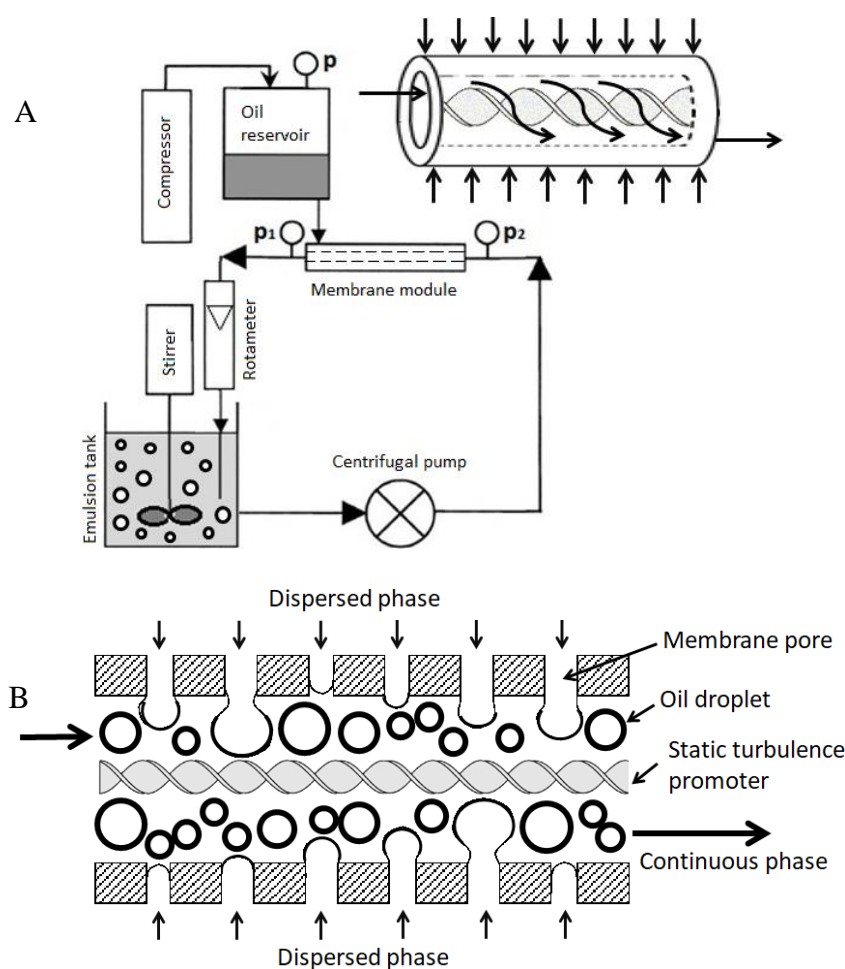


Figure 26 : Membrane emulsification process; inset fluid flow within membrane tube (A), droplet formation in membrane tube (B).

The larger diameter of droplets in CFME-1 may be related to the higher instability of this emulsion. The smaller droplet size in emulsion, produced by RSH is related to higher stability of emulsion. Carneiro et al. (2013b) reported that emulsion, made by flaxseed oil, MD and GA by RSH were highly stable with droplet size $\sim 2 \mu\text{m}$. It was noted that span values are significantly influenced by viscosity of emulsion. Small droplet size in emulsion represents the monodisperse nature of droplets

4.3.4. Encapsulation Efficiency

EE is the most important parameter for determining the success of microencapsulation of oils which is an indicator of coated and surface oil content. The results of EE of microcapsules are presented in Figure 27. Total oil content of emulsions prepared with different wall material compositions was 42.85 % in dry matter and kept constants for all emulsions fed to freeze dryer. The EE% varied from $33.69 \pm 0.95\%$ to $68.96 \pm 2.60\%$. EE% was significantly higher for microcapsules produced by CFME than by RSH with $54.88 \pm 1.18\%$ and $68.96 \pm 2.60\%$ for CFME 1 and CFME 2 respectively.

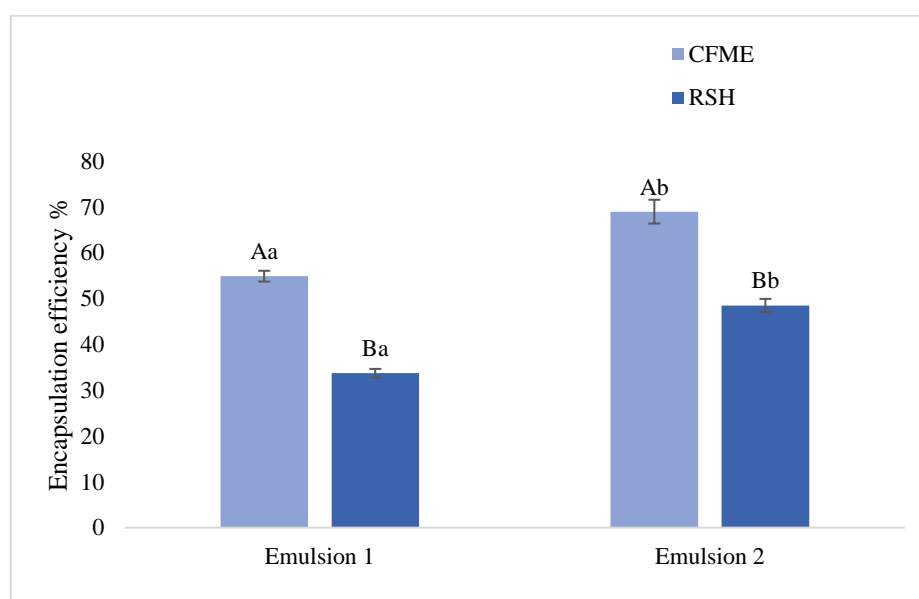


Figure 27 : Encapsulation efficiency of microcapsules, produced by different emulsification methods with different compositions of emulsion.

* Results are represented by mean value with standard deviation (\pm values). In superscript, dissimilar alphabet represents the significant difference ($P < 0.05$) between results. Capital letters for emulsification method and lower letters for emulsion composition.

It can be justified by the fact that when oil droplets were detached from the membrane pores by interfacial force at the droplet base, shear force by continuous fluid crossflow and the Young–Laplace force to continuous phase, it is surrounded by polymeric carbohydrates (Figure 26 (B)).

The detailed mechanism is described in elsewhere (De Luca et al., 2008). On the other hand, oil droplets were agglomerated with polymeric carbohydrates when emulsion was prepared by RSH. In that case, concentration of surface oil was quite higher rather oil droplets were encapsulated. Furthermore, it is noted that EE for CFME-2 and RSH-2 are significantly higher than CFME-1 and RSH-1, respectively. It was reported that EE of vegetable oil within polymeric carbohydrate is significantly influenced by the ratio of oil and wall materials and composition of wall materials (Gallardo et al., 2013). They proposed that if this ratio is lower than 2, surface oil increases, which may negatively affect the EE. In this investigation, the ratio of wall material to oil was 1.16 (Table 9), which may be the reason for EE less than 80%.

In this study, the effect of the composition of polymeric carbohydrate on EE is quite difficult to explain. The degree of the substitute (D.S.) in CMC influences the viscosity of emulsion and it is directly correlated with the concentration of CMC. Furthermore, it has been reported that MD with higher DE-value, such as 5 contains lower amount of oligo-saccharide, which provides higher viscosity (Siemons et al., 2020). FD process also influences the EE. Ice crystals are formed during the freezing stage prior to encapsulation. This fact ruptures the emulsion droplets, disintegrates the capsule wall and subsequently, oil is released to the surface (Ogrodowska et al., 2020).

4.3.5. Particle size and span

Particle size or distribution is also an important parameter for powder- like products. It is associated with the stability of the particles. It was reported that oxidation level of powdered foods decreased when the powder is characterized by smaller particles (Koç et al., 2015) . The particle size of OOM, D_{32} , ranged from $17.76 \pm 0.92 \mu\text{m}$ to $80.36 \pm 0.60 \mu\text{m}$ for the volume mean diameter depending on wall material composition and emulsification method (Table 11). The particle size of microcapsules was high in comparison to size reported by other studies subjecting microencapsulation of oils by spray drying (Pedro et al., 2011). This was possibly caused by the FD method that demands further crushing of the powder which gives different sizes.

The span values of microcapsules ranged from 0.46 ± 0.05 to 0.64 ± 0.05 (table 9). Span value describes the width of the size distribution. Elevation of span value represents an increase of void between the particles. The highest span values were 0.64 ± 0.05 and 0.56 ± 0.03 for powders obtained by CFME2 and RSH2 respectively.

Table 11 : Moisture content, particle size and span of powders obtained by different emulsification methods and different wall material compositions.

	CFME-1	CFME-2	RSH-1	RSH-2
Moisture (%)	4.13±0.18 ^{Aab}	4.12±0.36 ^{Aab}	1.02±0.08 ^{Bab}	1.09±0.37 ^{Bab}
D ₃₂ (μm)	80.36±0.60 ^{Aa}	55.69±0.82 ^{Ab}	37.55±0.58 ^{Ba}	17.76±0.92 ^{Bb}
Span (-)	0.48±0.09 ^{ABab}	0.64±0.05 ^{ABab}	0.46±0.10 ^{ABab}	0.56±0.03 ^{ABab}

*Results are represented by mean value with standard deviation (±values). In superscript, dissimilar alphabet represents the significant difference (P<0.05) between results. Capital letters for emulsification method and lower letters for emulsion composition.

4.3.6. Moisture content

Results obtained for moisture content of freeze-dried microcapsules obtained by two different homogenization methods are shown in Table 11.

The moisture contents of the freeze-dried microcapsules were in the range of 1– 4%. The moisture affects the microcapsule shelf life since the higher moisture causes microbial spoilage (Koç et al., 2015). However, the highest moisture contents were observed in the samples prepared with CFME method. The minimum specification for most dried powders used in the food industry (3–4%). It has been observed that low water contents are usually associated with low water activities, which might prevent lipid oxidation (Gallardo et al., 2013).

4.3.7. Morphology of OOM

Surface of olive oil microcapsule is presented in Figure 28. Here, flat surface with porous and irregular structure of freeze-dried flakes is observed. Dehydration by freeze-drying affects the microstructure and integrity of the capsule wall. Similar observation was observed by Ogrodowska et al. (2020). During FD, a reduction of the surrounding pressure, crystallization of water in the emulsion and sublimation of the frozen water at a minimal temperature take place (Ogrodowska et al., 2020). Therefore, flakes having porous skin are produced. CMC is a hydrophobic derivative from cellulose having high Tg (weak plasticising effect of water) (Liu et al. 2021). MD having DE 5 contains lower molecular weight of saccharides and it is considerable hydrophobic with high Tg (Lee et al., 2017). Their presence reduces the water activity and agglomeration of microcapsules. Furthermore, due to porous surface of flakes, some oil may permeate to the surface layer of flakes, which offer hydrophobicity and reduces

the adsorption of moisture from environment and subsequently, agglomeration (Fioramonti et al., 2017). Similar observation was reported by Ogrodowska et al. (2020).

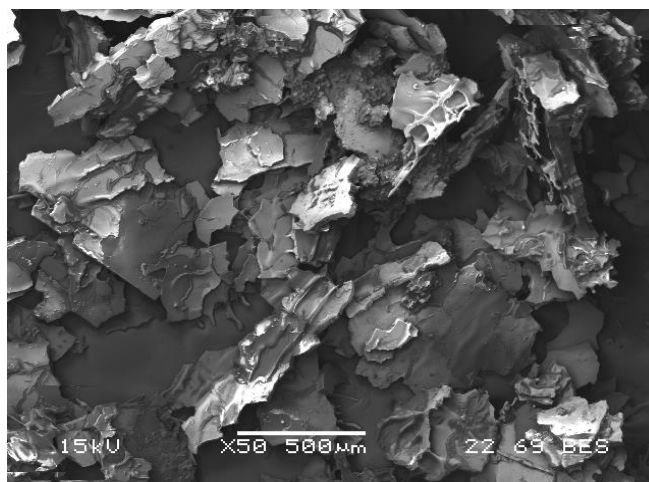


Figure 28: FE-SEM image of olive oil microcapsule (50×magnification) prepared by CFME with matrix composition: 15 g MD, 15 g GA and 5 g CMC.

4.3.8. Summary: Comparison of Emulsification Methods for OOM Properties

In this part, an attempt has been considered to prepare OOM by FD method. The effects of emulsification technologies and the composition of wall materials were studied with judicious way. Two different formulations by changing MD and CMC proportions were considered for emulsion preparation; however, the amount of emulsifiers, such as GA and Tween 80 were fixed. The stability of emulsion was higher when emulsion was prepared by RSH. The value of D_{32} was lowered in case of RSH compared to other one. The higher EE was found by CFME. The most effective wall material composition to produce olive oil microcapsules is MD 15 g, CMC 5 g and GA 15 g. Considering higher EE, CFME may be considered suitable for industrial production of olive oil microcapsule.

4.4. Effect of change of the drying method and wall material composition on the microencapsulation of extra virgin olive oil

The objective of this part of my work was to understand the effects of wall material and method of drying for the encapsulation of extra virgin olive oil. MD and WPI were considered as matrix for the microencapsulation of olive oil. In the first stage, emulsions were prepared with aqueous solutions of MD DE 19 and WPI with olive oil. Different ratios of MD and WPI were considered to prepare emulsion. Tween 20 were used as an emulsifier. Five wall systems were tested consisting of WPI alone, MD alone and three different combinations of them. In later exercise, emulsion was considered to prepare olive oil microcapsule by drying technology. Two different drying technologies, SD and FD were adopted. Emulsion was characterized by

stability, viscosity, and liquid droplet size. Furthermore, OOM was characterized by EE, particle size, moisture content and surface morphology. The flow diagram of this process is shown in Figure 29.

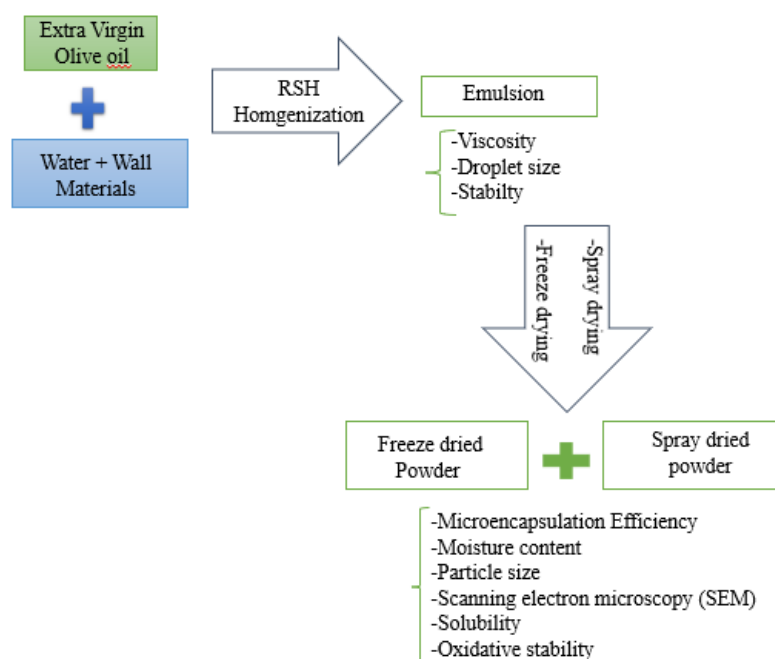


Figure 29: Flow diagram of the microencapsulation process to compare Freeze drying and spray drying.

4.4.1. Description of the formulation of the feeding emulsions

A total of five different microcapsules models have been studied in this research work. The information regarding the microcapsule wall composition and the ratio of oil-wall material is summarized in Table 12.

Table 12: Composition of emulsions, prepared by olive oil with different proportion of matrixes (MD and WPI).

	100 WPI	100 MD	50 MD-50 WPI	25 MD-75 WPI	75 MD-25 WPI
MD (g)	0	100	50	25	75
WPI (g)	100	0	50	75	25
olive oil (g)	40	40	40	40	40
Tween 20 (g)	1	1	1	1	1
DI water (g)	300	300	300	300	300
Oil:matrix	1 :2.3	1:2.3	1:2.3	1:2.3	1:2.3

4.4.2. Emulsion characterization

Characteristics of emulsion and types of drying have a significant contribution on the

preparation of olive oil microcapsule. Therefore, characteristics of emulsions and their contribution to prepare olive oil microcapsule with high EE are presented in subsequent sections.

4.4.2.1. Emulsion stability

A stable emulsion may produce a microcapsule with appreciable EE (Tonon et al., 2012). An emulsion is characterized by its viscosity and droplet size. The percentage of phase separation in emulsion represents the stability of emulsion. In Table 13, it is shown that WPI offers poor stability (higher phase separation) of emulsion. The separation percentages were ranging from 14 to 46 %. Phase separation increased in the model 25 MD :75 WPI. In industry, WPI is produced by de-watering of liquid whey and subsequently, dehydration by spray drying. Heating causes unfolding of protein structure and subsequently, creates aggregation in protein structure (Alting et al., 2003). It has been reported that heat-induced whey protein aggregates lead to higher intrinsic viscosity than native whey protein in solution (Purwanti et al., 2011). High speed homogenization may cause unfolding of protein molecules. Unfolded protein molecules at the oil–water interface may enhance the protein–protein interaction and promote agglomeration due to changes in the secondary and tertiary structures and, consequently, exposure of their residues, which would be linked (-S-S- linkages or disulfide linkages) within the native globular structure, leading to the formation of intermolecular interaction at the oil–water interface and flocculation (Tonon et al., 2012).

Table 13: Characterization of emulsions prepared by olive oil with different proportions of matrices (MD and WPI) expressed by separation (%), droplet diameter (D₄₃, μm), droplet size (span) and viscosity (mPA.s)

	Separation (%)	D ₄₃ (μm)	Span (-)	Viscosity (mPA.s)
100 WPI	24.33±0.58 ^b	4.44±0.04 ^b	3.12±0.02 ^e	50.54±0.02 ^e
100 MD	14.33±0.58 ^a	2.35±0.03 ^a	1.52±0.04 ^a	8.31±0.02 ^a
25 MD-75 WPI	45.67±0.58 ^e	5.26±0.04 ^e	3.04±0.02 ^d	40.91±0.03 ^d
50 MD-50 WPI	37.67±0.58 ^d	5.00±0.01 ^d	2.69±0.01 ^c	33.24±0.02 ^c
75 MD-25 WPI	29.67±0.58 ^c	4.65±0.01 ^c	2.53±0.01 ^b	25.58±0.02 ^b

*Results are represented by mean value with standard deviation (±values). In superscript, a dissimilar alphabet represents the significant difference (Tukey's post hoc test, P<0.05) between results. According to one-way MANOVA, stability, droplet diameter (D₄₃), span and the viscosity of emulsion are significantly affected by the proportions of MD and WPI (Wilk's lambda<0.001, P < 0.001). The follow-up one-way ANOVA with Bonferroni's correction

resulted in the significant effect on all four variables (stability, D_{43} , span and viscosity of emulsion) individually, too ($F(4;10) > 1219.61$; $P < 0.001$).

Therefore, droplet size in emulsion is increased and consequently stability of emulsion is reduced in presence of WPI in emulsion formulation (Carneiro et al., 2013b). Emulsion instability is expressed by flocculation, coalescence, or phase separation phenomena. It has been reported to have an influence on microencapsulation efficiency and on the physical properties of the dried oil powders (Tan et al., 2005).

4.4.2.2. Emulsion viscosity

As stated before, emulsion viscosity was determined through steady-shear flow curves. The viscosity of emulsions produced by olive oil and different proportions of wall materials in water are shown in Figure 30. The viscosity of emulsion influences the size of droplets within emulsion and consequently influences the stability of emulsion. A common concept is a stable emulsion containing droplets with lower diameter and high viscosity (Souza et al., 2015). However, 100 MD emulsion is characterized as a Newtonian fluid, others are characterized as non-Newtonian fluids. Emulsion having high viscosity is more stable because of the free movement of droplets within emulsion and subsequently, their agglomeration is restricted (Tonon et al., 2012). The lowest viscosity is noted for 100 MD emulsion; however, stability of 100 MD emulsion is appreciable. It has been proven that MD with higher DE value, such as 19 contains mostly low-molecular weight of saccharides, which produces emulsion with lower viscosity (Siemons et al., 2020). MD is highly water soluble and may form a local hydrophobic region in an emulsion. Therefore, hydrophobic interaction between oil droplets and MD produces small oil droplets and creates stable emulsion (Lee et al., 2017). The viscosity of 100 WPI emulsion is considerably high compared to 100 MD emulsion. It is worth noting that viscosity is improved when proportion of WPI was increased in emulsion formulation, such as 75 MD-25 WPI, 50 MD-50 WPI and 25 MD-75 WPI.

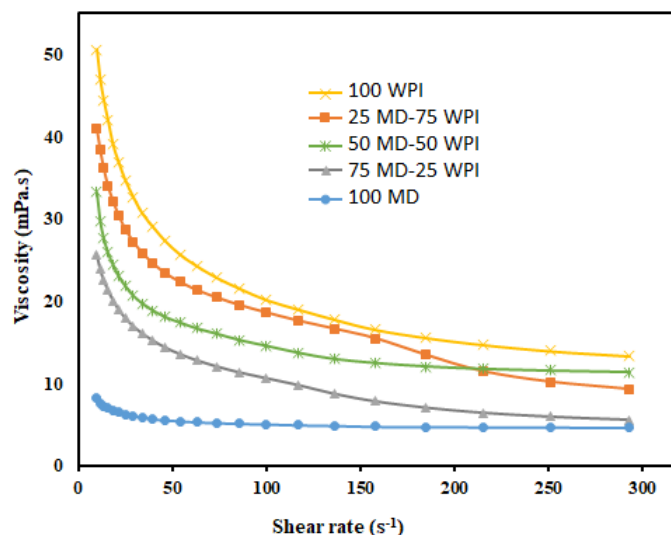


Figure 30: Viscosity as a function of shear rate, obtained from olive oil emulsions prepared with different wall materials proportions (MD and WPI).

4.4.2.3. Emulsion droplet size and span

OOE was prepared at a given oil concentration using five different formulations consisting of either WPI alone, MD alone or WPI/MD mixtures at three different ratios. The droplet mean diameters of the emulsions are presented in Table 13. Droplet mean diameters (D_{43}) were affected by the type and ratio of wall materials. It is noted that the droplet size of 100 MD emulsion is the lowest than other emulsions, such as 100 WPI, 25 MD-75 WPI, 50 MD-50 WPI and 75 MD-25 WPI, having higher viscosity compared to 100 MD emulsion. It may be justified by the fact that movements of droplets inside the emulsion are difficult when emulsion has higher viscosity. In that case, droplet coalescence is reduced (Tonon et al., 2012). 100 MD emulsion has the lowest droplet size because MD is highly soluble in water and soluble MD may form a local hydrophobic region in the emulsion. Well soluble MD is able to capture hydrophobic oil droplets via hydrophobic interactions and produce smaller emulsion droplets (Lee et al., 2017). Figure 28 shows the size distributions of the five formulated emulsions given by the better size machine. The span value was considered as an indication of the dispersity of the droplet size. Lower span value signifies the monodisperse nature of droplets in emulsion (Koç et al., 2015). 100 MD emulsion has lower span value, and it may be considered as more monodispersed compared to other emulsions, such as 100 WPI, 25 MD-75 WPI, 50 MD-50 WPI and 75 MD-25 WPI. This result might be related to the viscosity of emulsion. As previously mentioned, droplet movements within emulsion may be restricted when emulsion has higher viscosity (Jafari et al., 2008; Tonon et al., 2011). It is noted that concentration of WPI in emulsion leads to aggregation of droplets and influences the dispersity of droplets.

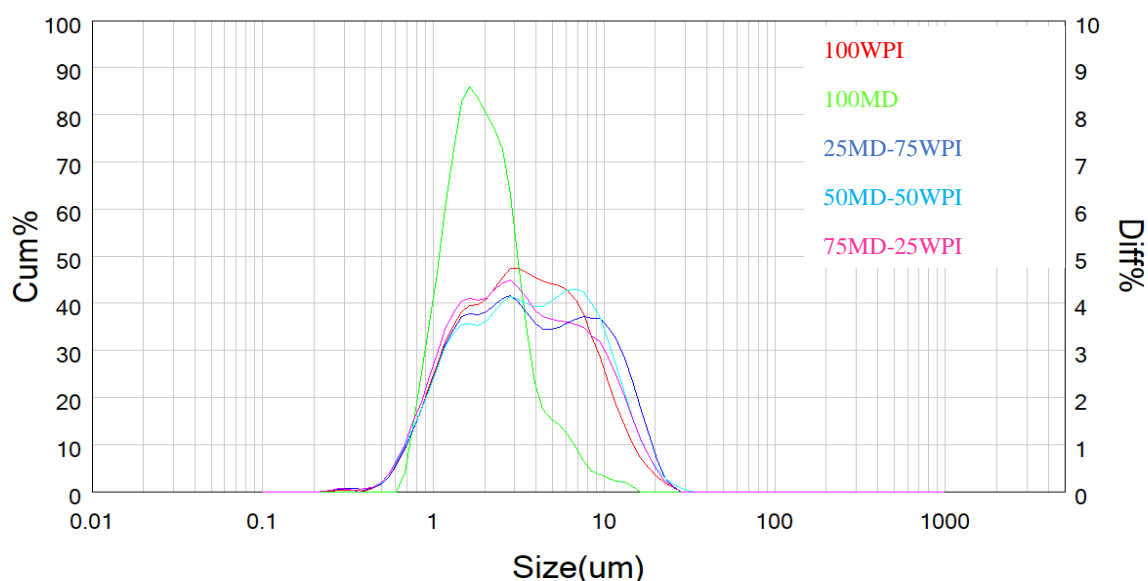


Figure 31: Size distribution of the prepared emulsions.

4.4.3. Powder analysis

The obtained powders which are presented in Appendix-Figure 1, were checked for encapsulation efficiency, moisture content, particle size and solubility.

4.4.3.1. Encapsulation efficiency

As previously described, encapsulation efficiency (EE) was calculated from the surface oil determined for each sample using SD and FD methods. EE is the major parameter to investigate the success of olive oil microencapsulation. Total oil content of emulsions prepared with different wall material compositions was 30.34% in dry matter and kept constant for all emulsions fed to the spray dryer and freeze dryer machines. Also, the core to wall material ratio was kept constant at 1:2.3. The results are presented in Figure 32. EE varied from 9.92 ± 0.08 to 88.61 ± 1.64 % and was influenced by both the type of wall material and the drying method. It has been reported by many researchers that the EE depends from the nature of the core material, the type and composition of the wall materials, the ratio of core to wall materials and a the droplet size distribution in the feed emulsions (Fioramonti et al., 2017). It is noted that microcapsules from 100 WPI emulsion have higher EE than microcapsules from 100 MD emulsion. In an investigation, it has been proven that encapsulation of fatty acids by WPI was appreciable due to higher proportion of proteins in WPI, which promotes hydrophilic-hydrophobic interaction. Lack of hydrophobic regions in MD may provide lower EE of fatty acids (Choi et al., 2010).

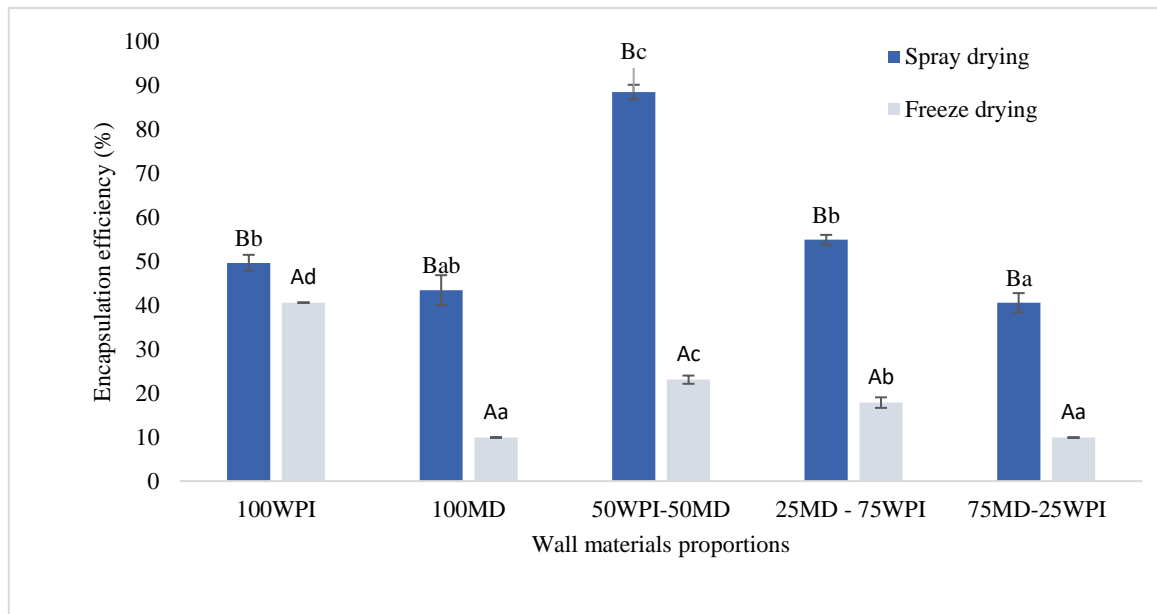


Figure 32: Encapsulation efficiency of microcapsules produced with different wall material proportions and different drying methods.

*Results are represented by mean value with standard deviation (\pm values). In superscript, a dissimilar alphabet represents the significant difference ($P < 0.05$) between results. Upper case superscripts represent the comparison of drying methods within fixed emulsion compositions and lower-case superscripts represent the comparison of emulsion compositions within fixed drying method. According to two-way MANOVA, the proportions of matrices (MD and WPI) and the drying types, and their interactions have an overall significant contribution on EE (Wilk's lambda < 0.001 , $P < 0.001$). The follow-up two-way ANOVA with Bonferroni's correction resulted in significant effect of matrices, drying types and interactions of both two variables ($F_{\text{matrix}(4;20)} > 381.22$; $F_{\text{drying}(1;20)} > 3562.37$; $F_{\text{interaction}(4;20)} > 177.12$; all with $P < 0.001$).

EE of microcapsules from 100 WPI emulsion was $49.67 \pm 1.86\%$ and it was increased significantly due to incorporation of MD in emulsion formulation, such as 50 MD-50 WPI. WPI has been considered as an appreciable emulsifier with film forming capacity; however, it is hygroscopic (high water activity) with low T_g (Zhou & Labuza, 2007). The use of MD with WPI provides a unique advantage to prepare stable emulsion as well as microencapsulation of oil. Appreciable emulsifying property of protein due to amphiphilic nature, together with the hydrophobic nature and film-forming property of MD offer higher EE of microcapsule (Frascareli et al., 2012). It has been reported that combination of WPI and MD with higher DE provides better stability to oil-in-water emulsion under light acidic (pH 6), neutral (pH ~ 7) and alkaline (pH 8-9) conditions (Wangsakan et al., 2003). MD contains linear amylose regions that

have internal helical structure with hydrophobic nature and branched amylopectin region. Highly aqueous soluble MD may produce a stable emulsion because MD may form a local hydrophobic region within the emulsion and facilitates hydrophobic interaction with oil droplets (Lee et al., 2017). Hydrophobic areas of MD with DE 19 are more exposed for the interaction with oil droplets, which can minimize the loss of oil content during SD and thus effectively improve EE (Hogan et al., 2001). According to Figure 31, EEs of microcapsules from 75 MD-25 WPI emulsion and 100 MD emulsion are significantly lower than microcapsules from 50 MD-50 WPI emulsion. It can be justified by the fact that retro-degradation or aggregation of hydrophobic regions in helical structure of MD due to increase of MD in emulsion formulation (Lee et al., 2017). In contrast, EEs of microcapsules produced by the FD process are significantly lower than SD process (Figure 31). This result could be attributed to the destabilization of emulsion during freezing for 24 h. FD significantly affects the microstructure and integrity of matrix of oil droplets. Therefore, a matrix with a porous and irregular surface is produced, which promotes oil leakage and lower EE (Silva et al., 2013). Olive oil microcapsules containing MD alone had higher EE than the microcapsules containing WPI alone in the case of spray drying. The opposite behavior was observed when using freeze drying method. Thus, the emulsions containing MD were more stable than those containing WPI during the spray drying process (Figure 32). The same result was shown by Koç et al. (2015) that used the spray drying method.

Barbosa et al. (2005) who used the spray drying method, reported that the EE depended also on the emulsion stability. In their study, the more stable emulsions resulted in a lower amount of non-encapsulated material and thus on higher EE. However, in the present study, the results obtained for the encapsulation efficiency were also affected by the emulsion stability. All emulsions were instable over the 24-h storage at room temperature, showing different phase separations. From Table 13 and Figure 31, the most stable sample with the lower phase separation is 100 MD with an efficiency of 54.97 % in the case of SD method. In contrast, by using FD method, the EE is the lowest (9.92 %). This result could be related to the emulsion destabilization during freezing. The highest EE ($40.65 \pm 0.0.3\%$) obtained by FD method was when only whey protein isolate is used as wall material.

According to Jafari et al. (2008), the lower EE could be related to the fact that during atomization when spray drying, the shearing effect disrupts the larger droplets allowing them to evaporate and loose there core materials which increases the surface oil content of the powder. This oil which remains in the surface of the dry particles is subject to oxidation and

off-flavor formation. That is why, producing finer emulsions is required to keep the oil inside the wall material (Silva et al., 2013).

4.4.3.2. Moisture content

Results obtained for moisture content of spray- and freeze-dried microcapsules are shown in Table 14. The moisture contents of the powders were in the range of 1– 3 %. The results are in adequacy with the maximum limits specified for dry powders in the food industry which are between 3 and 4% (Karina et al., 2014). Moisture content of microcapsule is associated with water activity, prevention of lipid oxidation in capsules from oxidative agents during storage (Klaypradit & Huang, 2008), shelf life and microbial spoilage (Karina et al., 2014). It is noted that moisture content of microcapsules is greater when the proportion of MD is higher (Table 14). MD with DE 19 exhibits some ramifications with hydrophilic groups due to presence of low molecular weight of saccharides (Siemons et al., 2020), contributing to absorption of water from the environment. The values of Tg of MD-WPI mixtures are reduced with increase of the proportion of MD (Fongin et al., 2017). Higher water activities and lower Tg (high plasticising effect of water) may be attributed by MD having DE 19 (Frascareli et al., 2012). WPI contains a low number of hydrophilic groups due to less contaminant lactose by membrane processing (Frascareli et al., 2012) offers lower hygroscopicity. The moisture contents are lower for microcapsules produced by FD than SD. It may be justified by the fact that microcapsules, produced by FD contain high amounts of oil in the surface of the matrix. Hydrophobic nature of oil resists the diffusion of moisture within microcapsule and water activity (Charles et al., 2021).

Table 14: Moisture content (%) and particle diameter (D_{43} , μm) and span of microcapsules, produced with olive oil, different proportions of matrices (MD and WPI) and drying methods.

Emulsion composition	Moisture content %		D_{43} (μm)		Span (-)	
	SD	FD	SD	FD	SD	FD
100 WPI	1.70±0.06 ^{Ba}	1.03±0.04 ^{Aa}	9.14± 0.06 ^d	ND	4.30± 0.03 ^d	ND
100 MD	3.07±0.05 ^{Bd}	2.04±0.03 ^{Ac}	4.94± 0.09 ^b	ND	2.88± 0.02 ^c	ND
25 MD-75 WPI	2.04±0.04 ^{Bb}	1.01±0.02 ^{Aa}	7.41± 0.08 ^c	ND	4.32± 0.02 ^d	ND
50 MD-50 WPI	2.45±0.03 ^{Bc}	1.02±0.04 ^{Aa}	4.81± 0.02 ^b	ND	2.69± 0.01 ^b	ND
75 MD-25 WPI	3.06±0.03 ^{Bd}	1.31±0.03 ^{Ab}	4.22± 0.02 ^a	ND	2.27± 0.03 ^a	ND

*ND: Not determined. Results are represented by mean value with standard deviation (\pm values). In superscript, a dissimilar alphabet represents the significant difference ($P<0.05$) between

results. Upper case superscripts represent the comparison of drying methods within fixed emulsion compositions and lower-case superscripts represent the comparison of emulsion compositions within fixed drying method. According to two-way MANOVA, the proportions of matrices (MD and WPI) and the drying types, and their interactions have an overall significant contribution on moisture content of olive oil microcapsule (Wilk's lambda < 0.001, $P < 0.001$). The follow-up two-way ANOVA with Bonferroni's correction resulted in significant effect of matrices, drying types and interactions of both two variables ($F_{\text{matrix}(4;20)} > 381.22$; $F_{\text{drying}(1;20)} > 3562.37$; $F_{\text{interaction}(4;20)} > 177.12$; all with $P < 0.001$). Meanwhile, one-way MANOVA revealed that the proportions of matrices have also an overall significant effect on D43 and the distribution of particle (span) of olive oil microcapsule if SD is used (Wilk's lambda < 0.001, $P < 0.001$). That significant effect was also detected for D43 and span value of particle individually (one-way univariate ANOVA: $F(4;10) > 3644.66$; $P < 0.001$).

4.4.3.3. Particle characterization

Particle size constitutes an important parameter for powders characterization. According to Table 14, the particle size of microencapsulated olive oil ranged from 4.22 to 9.14 μm for the volume mean diameter depending on wall material composition. Compared to other studies, the particle size of microcapsules was low. This could be attributed to the ultrasonic dispersion of the particles during the measurement which lasts for 3 minutes. Tontul and Topuz (2014) found similar results of powder particle size which ranged 5.47-7.09 μm using spray drying method and a combination of maltodextrin and whey protein concentrate. In their study the method of emulsification was based on ultrasonication. Other researchers found particle mean diameter varying from 7.88 to 13.13 μm for encapsulation of coffee oil by spray drying (Frascareli et al., 2012). The diameter of microcapsules depends on the composition of the matrix and drying method. The size of microcapsules is higher with a higher proportion of WPI in emulsion formulation. Microcapsules with higher proportion of WPI having low T_g may easily agglomerate during SD (Koç et al., 2015; Netto et al., 1998). It is also noted that the size of emulsion droplets is higher when the proportion of WPI was greater in formulation.

The span values of microencapsulated extra virgin olive oil powders ranged from 2.27 to 4.32. Span value describes the width of the size distribution. Elevation of span value represents an increase of void between the particles. The highest span value was obtained with 25MD-75WPI. The span value of microcapsules is greater with a higher proportion of WPI. Agglomeration due to the presence of a higher proportion of WPI is responsible for the higher values of span.

The monodispersed nature of microcapsules is noted when proportion of MD is higher in formulation, and it is associated with lower span value.

The particle size distribution of the spray-dried powders is presented in figure 33.

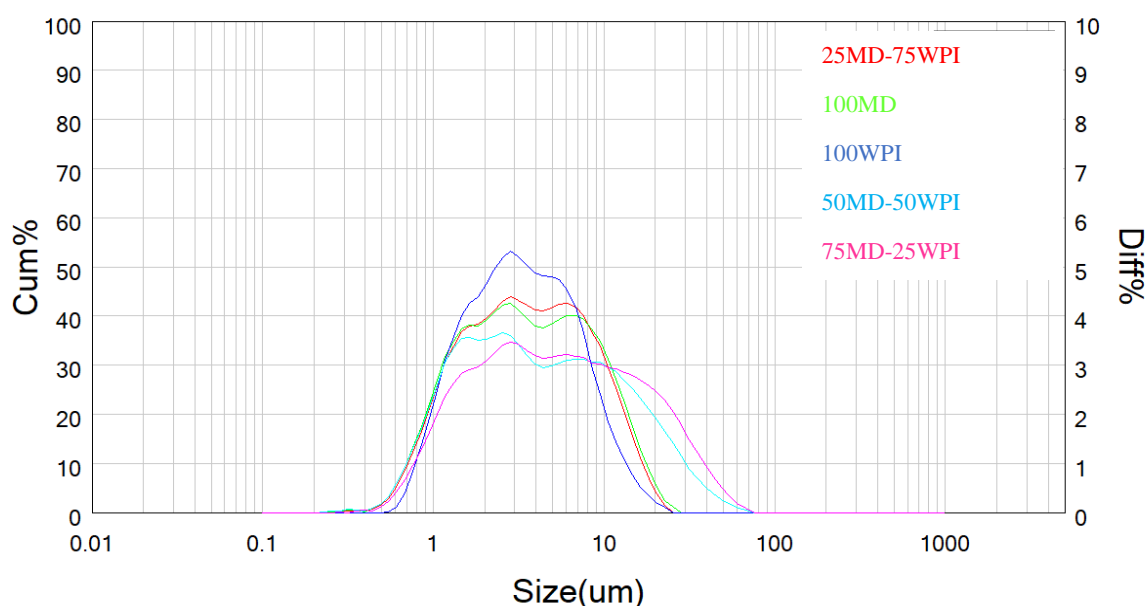


Figure 33: Size distribution of the spray-dried samples.

4.4.3.4. Powder solubility

Results obtained for solubility of spray- and freeze-dried microcapsules are shown in Table 15. The particles produced using the different formulation in this study displayed several variations in their solubility. The powders produced with higher EE showed an average solubility (35 ± 2 %) caused by the hydrophobic nature of the core material.

Table 15: Solubility of powders produced with different wall material composition and different drying methods.

Wall materials	Solubility %	
	SD	FD
100WPI	36.17 ± 1.11^{acB}	28.31 ± 0.63^{aA}
100MD	18.05 ± 0.17^{bB}	13.82 ± 0.21^{bA}
50WPI-50MD	35 ± 2^{acB}	47.36 ± 0.35^{cA}
25MD-75WPI	24.30 ± 0.59^{dB}	42.23 ± 0.32^{deA}
75MD-25WPI	28.92 ± 0.31^{eB}	42.38 ± 0.44^{deA}

*a,b,c,d,e means in the same column with different superscript are significantly different regarding the sample composition; A,B means in the same row with different superscript are significantly different regarding the drying method ($P < 0.05$).

The studied variable is also strongly affected by the nature of the carrier material. Carbohydrates and proteins are known to exhibit high solubility in water at various concentrations (Botrel et al., 2014). The calculated solubility was low by both drying methods. This could be due to the surface oil present in the samples which enhance hydrophobicity because of the nature of the core material (oil). The highest solubility was for the sample 100 WPI when SD was used. The statistical analysis verifies that in terms of solubility, spray drying method is significantly different ($p < 0.05$) from freeze drying method.

4.4.3.5. Process yields

According to the results shown in Figure 34, the highest process yields were obtained when freeze drying method is adopted as drying method. Therefore, in freeze drying method, there is no material loss since the feeding emulsions are freeze dried in the same containers and no air is used.

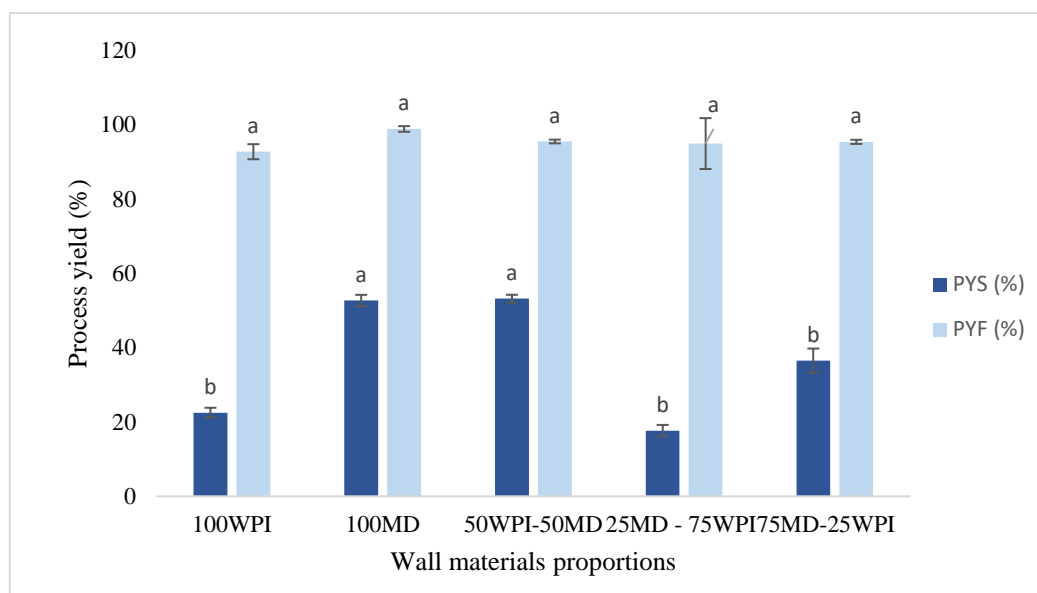


Figure 34: Process yield of microcapsules produced with different wall materials proportions and different drying methods.

For spray drying process, the best results were obtained when the proportion of wall materials is 50MD-50WPI. It means that carbohydrates and proteins, when associated together, led to the highest process yield ($53.18 \pm 1.03\%$). Whereas, when using WPI alone as wall material, spray drying yield dropped considerably to $22.5 \pm 1.32\%$. Calvo et al. (2010) have obtained the highest encapsulation yields when gelatin, GA and MD ($51.20 \pm 5.9\%$) and sodium caseinate and MD ($51.21 \pm 2.38\%$) were used as encapsulation agents and the ratio of wall solid-to-oil was 1:4 and 1:2, respectively. This fact is due to the initial viscosities of the feeding emulsions. Indeed, the recovery mode of powder was manual (the powder is recovered by scraping the

walls of the cyclone and the drying chamber). Losses of microparticles are due to the stickiness of powders containing a high proportion of protein.

4.4.3.6. Bulk density and tapped density

The bulk density and tapped density of OOM with different proportions of MD and WPI, and dehydration methods are reported in Table 16. Bulk density reflects the gap size between microcapsules in a static condition; whereas, tapped density reflects the space between microcapsules, influenced by external force. Higher bulk density indicates a lower amount of air in the powder void, which can prevent the oxidation of microcapsules. It is noted that both are reduced with increasing the particle size due to presence of WPI in formulation. Similar results were reported by other investigators (Li et al. 2020).

Table 16: Bulk density, tapped density, flowability and cohesiveness of microcapsules, produced by olive oil with different proportions of MD and WPI, and dehydration methods.

	Bulk density (g·ml ⁻¹)		Tapped density (g·ml ⁻¹)		Carr index (%)		Hausner ratio (-)	
	SD	FD	SD	FD	SD	FD	SD	FD
100 WPI	0.242±0.002 ^d	ND	0.305±0.002 ^d	ND	28.861±0.02 ^a	ND	1.389±0.002 ^a	ND
100 MD	0.233±0.001 ^{ab}	ND	0.295±0.002 ^{bc}	ND	31.252±0.01 ^e	ND	1.435±0.001 ^e	ND
25 MD-75 WPI	0.238±0.002 ^{cd}	ND	0.298±0.001 ^c	ND	29.452±0.0 ^b	ND	1.406±0.00 ^b	ND
50 MD-50 WPI	0.235±0.001 ^{bc}	ND	0.293±0.001 ^{ab}	ND	29.751±0.02 ^c	ND	1.415±0.002 ^c	ND
75 MD-25 WPI	0.229±0.002 ^a	ND	0.289±0.002 ^a	ND	30.512±0.0 ^d	ND	1.427±0.00 ^d	ND

*SD: Spray drying, FD: Freeze drying, EE: Encapsulation efficiency, MD: Maltodextrin, WPI: Whey protein isolate, ND: Not determined. Results are represented by mean value with standard deviation. In superscript, a dissimilar alphabet represents the significant difference (Tukey's, $P < 0.05$) between results. According to one-way MANOVA, the proportions of matrices (MD and WPI) have an overall significant effect on bulk density (g·ml⁻¹), tapped density(g·ml⁻¹), Carr index (%) and Hausner ratio (-) if SD was used (Wilk's lambda < 0.001 , $P < 0.001$). The significant effect was also detected for all the dependent variables individually (one-way univariate ANOVA with Bonferroni's correction: $F(4;10) > 30.78$; $P < 0.001$).

Furthermore, it has been reported that along with proportion of MD and WPI, DE of MD influences the bulk density of microcapsules (Bae and Lee 2008; Li et al. 2020). The free-flowing characteristics of each microcapsules was evaluated by the Carr index, whereas the cohesiveness was evaluated using the Hausner ratio (Zhu et al., 2022). It is noted that developed microcapsules exhibited poor flowability and high cohesiveness (Lebrun et al., 2012), which

indicates high friction among microcapsules (Mahdi et al., 2020). Higher proportion of MD in formulation led to higher values of the Carr index and the Hausner ratio, which signifies reduced flowability of microcapsules. It may be because the hydrophilic nature of low molecular weight of carbohydrates in MD having DE 19 might be responsible for higher interparticle cohesiveness and lower flowability of microcapsules. The low molecular weight of saccharides could adsorb moisture from environment, contributing to the agglomeration of microcapsules. Zhu with co-authors reported that the Carr index and the Hausner ratio of soybean oil microcapsules were improved due to increasing DE of MD (Zhu et al., 2022).

4.4.3.7. Powder morphology

The morphology of microcapsules may be influenced by the characteristics of emulsion and dehydration process of emulsion. Microcapsules produced by different compositions of wall materials and drying processes are presented in Figure 35.

In general, microcapsules produced by SD are spherical in shape and have smooth surfaces without visible pores or cracks. The spherical shape of microcapsules by SD are formed by melting the matrix of a stable emulsion due to high inlet temperature and nozzle of spray dryer (Reineccius, 2004). Microcapsules, produced by FD are flat flakes, have porous and irregular surfaces. A reduction of the surrounding pressure, crystallization of water in the emulsion and sublimation of the frozen water at a minimal temperature take place during FD (Ogrodowska et al., 2020). Therefore, dehydration by FD affects the microstructure and integrity of the capsule wall (Fioramonti et al., 2017).

WPI having a lower value of Tg may change its form during SD (Koç et al., 2015). Therefore, the dent structure of microcapsules with smooth surface was produced from 100 WPI emulsion by SD (Fig. 35A). On the other hand, flakes with encapsulated oil were produced from 100 WPI emulsion and FD. They have a porous irregular surface (Fig. 35B). Microcapsules from 100 MD emulsion and SD or FD have smooth surfaces (Fig. 35C and Fig. 35D). MD with a high concentration of lower molecular weight of saccharides has low Tg. They make a high contribution to water activity and agglomeration of microcapsules (Fig. 35C). Low molecular weight of saccharides in MD acts as a plasticizer during microcapsule formation by SD.

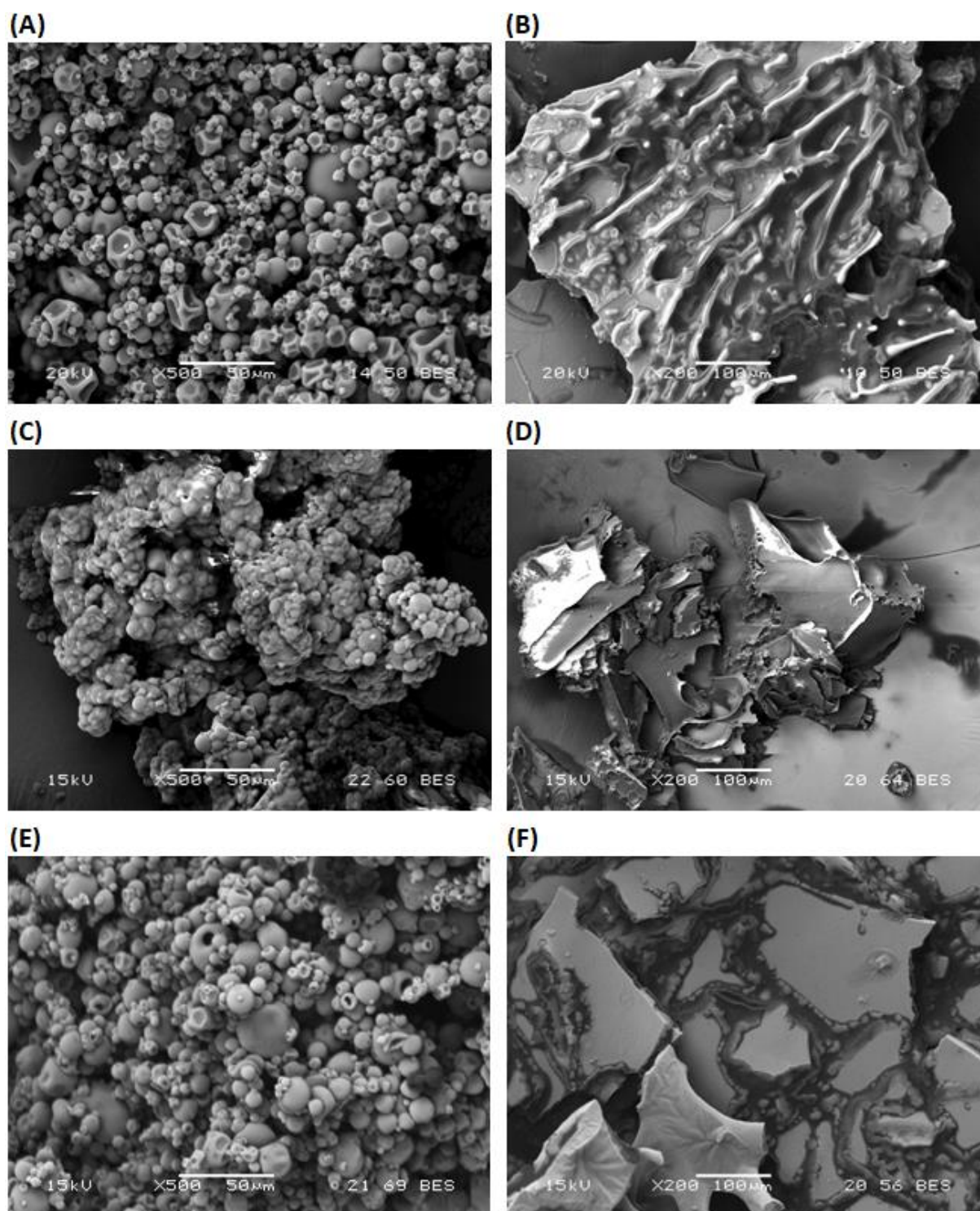


Figure 35: Scanning electron microscopy images of olive oil microcapsule prepared by different proportions of matrices (MD, WPI) and drying methods (SD, FD); (A) 100 WPI SD, (B) 100 WPI FD, (C) 100 MD SD, (D) 100 MD FD, (E) 50 MD-50 WPI SD and (F) 50 MD-50 WPI FD.

Surface morphology was also studied for microcapsules from 50 MD-50 WPI emulsion and SD, because maximum EE was obtained. Microcapsules with spherical smooth surfaces were

produced by SD (Fig. 35E). For the comparison purpose, microcapsules from 50 MD-50 WPI emulsion and FD were considered. It is noted that flat flakes with some irregularity in surface were produced by FD (Fig. 35F).

4.4.4. Process intensification by using CFME coupled with SD to the optimum sample

Bearing in mind the result from the section 4.3.8 that CFME was more effective for the microencapsulation of olive oil with different formulations of wall materials, I realized a powder by coupling the CFME and the spray drying for the formulation containing 50WPI-50MD.

4.4.4.1. Emulsion morphology and droplet size

The obtained emulsion contained well defined spherical microcapsules. The average droplet size was deduced from the mean of 30 measurements and corresponds to $4.89 \mu\text{m}$ (Figure 36). The membrane pore size was $1.4 \mu\text{m}$ and the average droplet size was 3.5 times greater. This result is in line with the conclusion obtained by Joscelyne and Trägårdh. (2000) who reported that the emulsion droplet size obtained by membrane emulsification should be 2 to ten times greater that the membrane pore size.

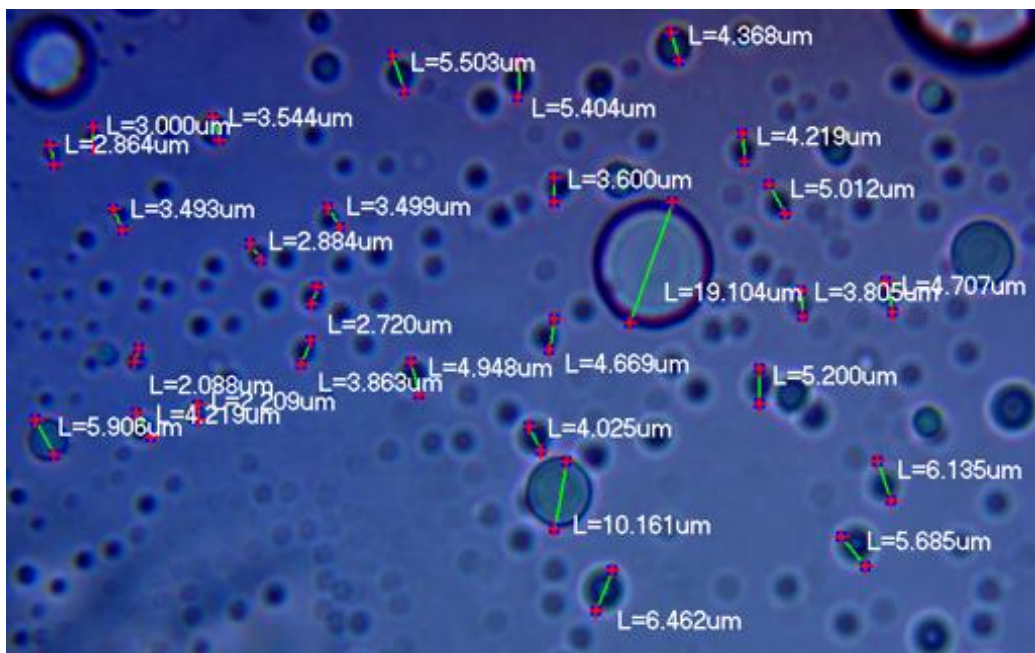


Figure 36: Microscopic image of the emulsion obtained by CFME containing 50WPI-50MD.

4.4.4.2. Comparison of powders obtained by RSH and CFME

The powder comparison results are set in Figure 37. After spray drying, the obtained powder had the best EE which is $91.16 \% \pm 0.84$. The moisture content was higher and reached $3.99 \% \pm 0.08$. The percentage yield of this process was $62.82 \pm 1.9 \%$. The higher yield is associated with the higher EE.

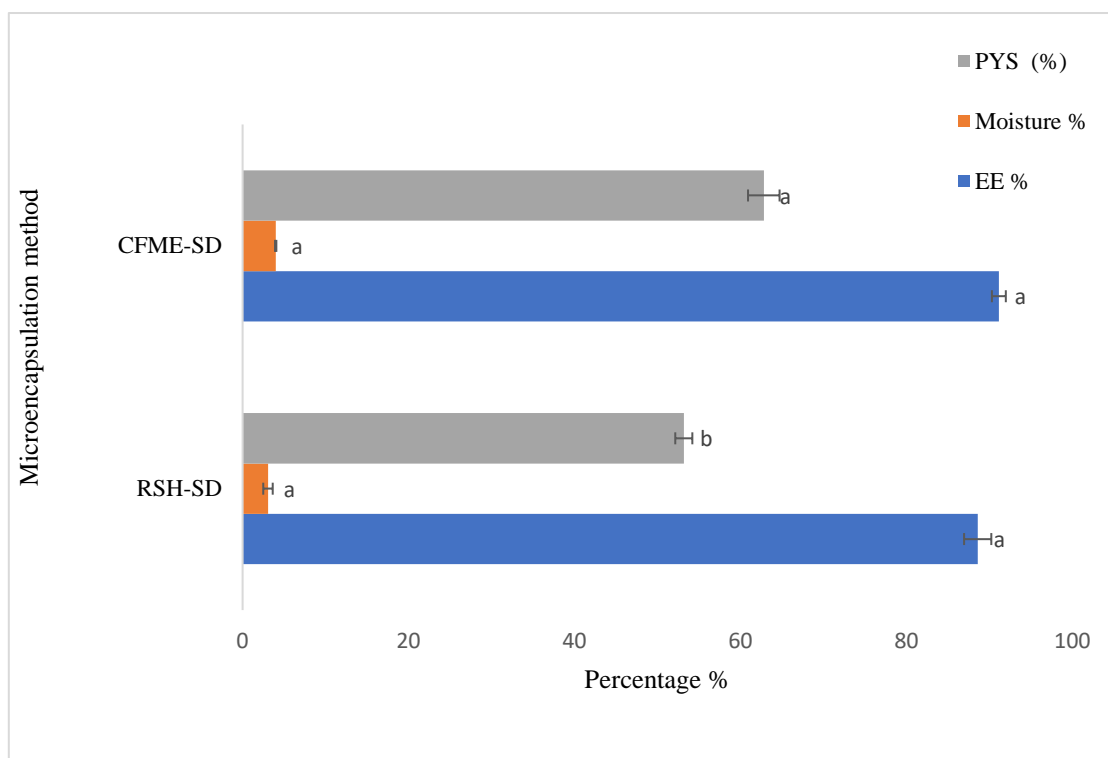


Figure 37: Comparison of the EE, process yield, and moisture contents of the powders obtained by CFME and RSH.

4.4.4.3. Stability to oxidation of microencapsules

The accelerated Rancimat test was chosen due to its ease of use and reproducibility. Its basis is an accelerated oxidation test since the sample is heated under atmospheric pressure at the selected temperature and bubbled with oxygen at a constant flow. Under these controlled conditions, the lipoperoxidative process reaches its final steps and lipids are oxidized to short-chain volatile acids which are collected in distilled water increasing its conductivity. The IP (induction period) is the time required to produce a sudden increase of conductivity, which can be defined as an indirect measure of oil stability: the higher the IP, the more stable the sample (Gallardo et al., 2013). The oxidation test was carried to the samples CFME-SD and RSH-SD by the rancimat method. Figure 38 shows the oxidation curves obtained for microencapsulated olive oil samples compared to bulk olive oil where the two samples exhibited a significant difference comparing to bulk olive oil ($P < 0.05$). IP values were easily determined due to the detectable increase in conductivity. Bulk olive oil presented an IP of 1.2 h which is comparable to the value reported for sunflower oil (1.3 h) in similar conditions (Velasco et al. 2000). Linseed oil was also analyzed in the same conditions and an IP of 2.04 ± 0.01 h was obtained according to (Gallardo et al., 2013). For the two samples of microcapsules, the conductivity curves showed a protective effect of the wall materials composed of 50% MD and 50% WPI

against olive oil oxidation. Therefore, both RSH-SD and CFME-SD presents IP values which were 2.75 and 4.15 times respectively greater than the IP of bulk oil (Figure 38). Regarding the emulsification method of the samples, RSH-SD resulted in a lower IP compared to CFME-SD. Thus, it can be concluded the EE affects the IP since CFME-SD samples contain less amount of surface oil which makes the oxidation process slower. This finding are in adequacy with previous results which attributed Rancimat responses to the free oil fractions of microencapsulated powders obtained by freeze drying (Velasco et al., 2009).

In this work, emulsification of the olive oil with the mixture of MD and WPI by CFME could lead to a wall matrix more permeable to oxygen than the emulsion obtained by RSH method. We can notice that the moisture content of CFME-SD is slightly higher than RSH-SD (Figure 37) $3.99\% \pm 0.08$ and $3.06\% \pm 0.57$, respectively. The low water content in OOM minimizes lipid oxidation by interfering with oxygen permeation. This could affect the accessibility of oxygen to the OOM resulting in decreasing the antioxidant activity of the sample. Another parameter to be considered to affect the antioxidant activity of the samples is the glass transition temperature of the biopolymers (Gallardo et al., 2013). Gallardo and coauthors have demonstrated that WPI and MD were in the glassy state between 30 and 270 °C showing no endothermic transitions. That means that they would be in a glassy state throughout Rancimat test (at 110°C).

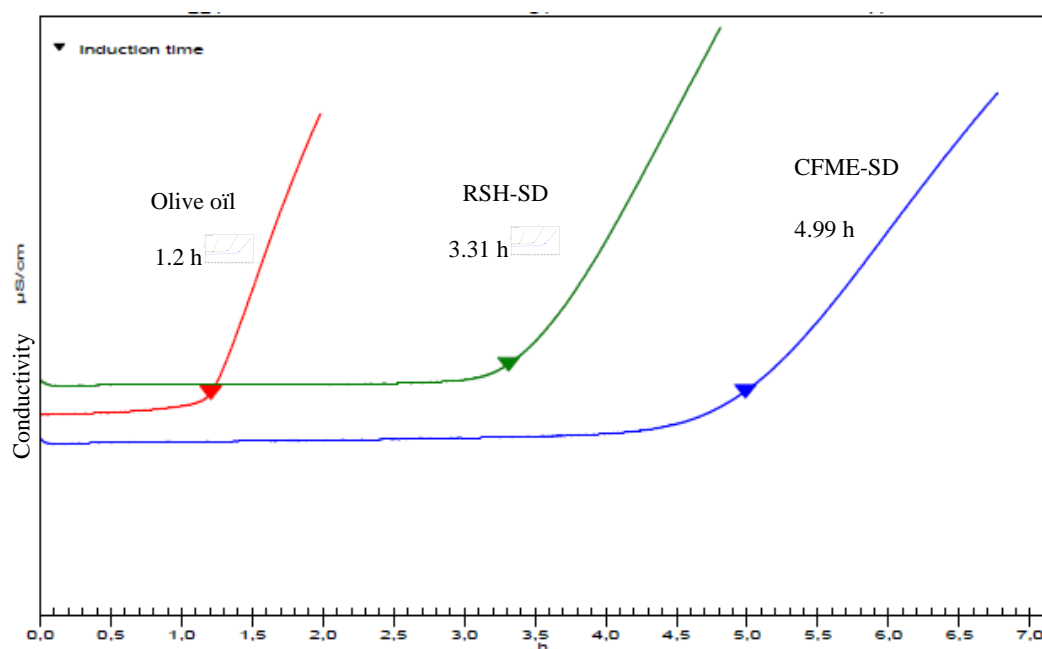


Figure 38: Oxidation curves (conductivity vs time) obtained from Rancimat accelerated test of microencapsulated olive oil. Bulk olive oil was used as control. Inverted arrows point out the mean induction period (IP) for each sample.

4.4.4.4. Comparison of the powder's morphology

Representative FSEM micrograph of the samples CFMR-SD and RSH-SD are shown in Figure 39. Microcapsules with spherical smooth surfaces were produced by SD in both cases. Figure 39 A and Figure 39 B show the microcapsules obtained by CFME which were slightly smaller than the particles observed in Figure 39 C and Figure 39 D which show the powder particles obtained by RSH method.

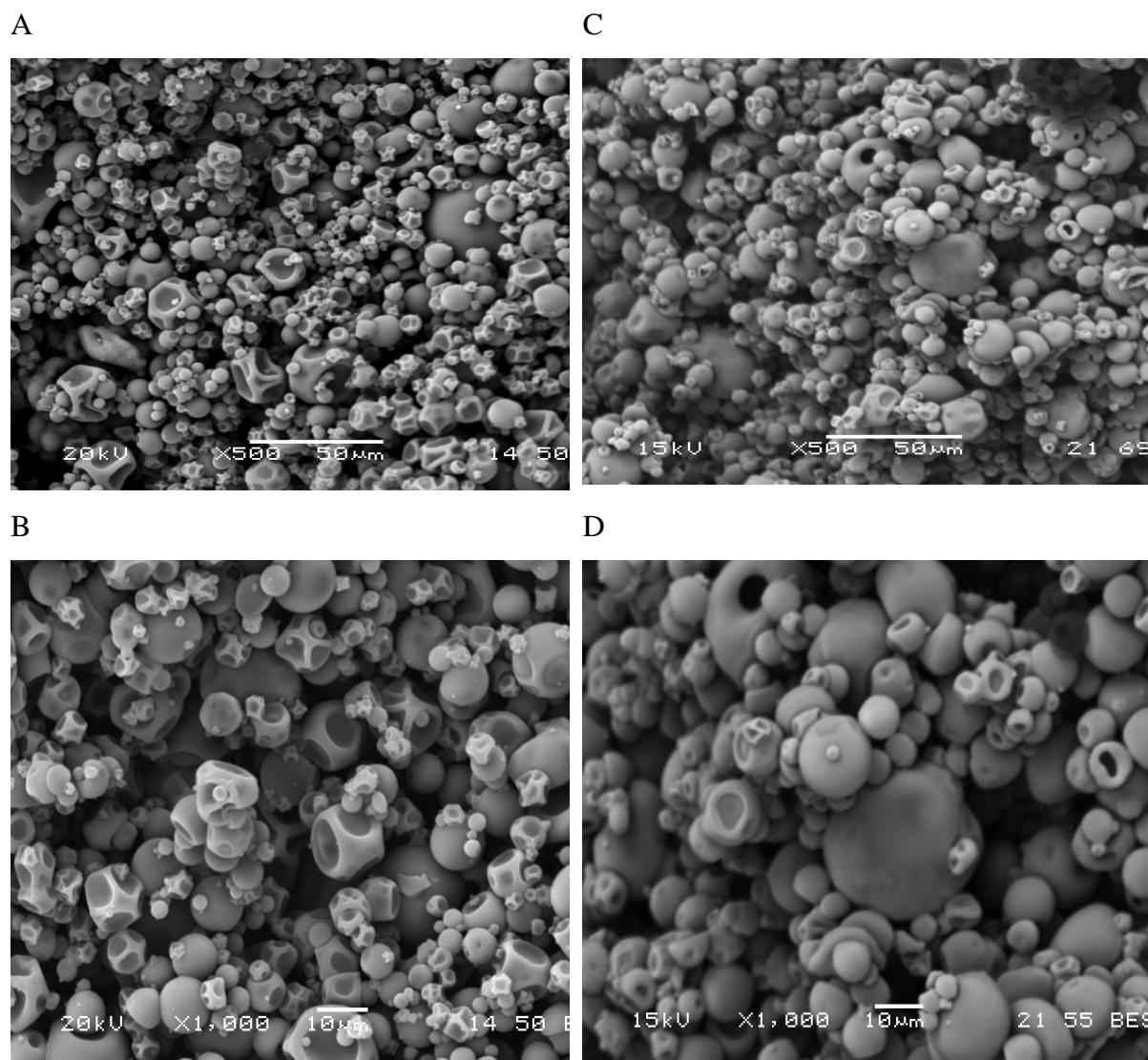


Figure 39: Scanning electron microscopy image of spray dried extra virgin olive oil powder containing 50WPI-50MD obtained by CFME A (at 500 \times magnification), B (at 1000 \times magnification) and RSH C (at 500 \times magnification), D (at 1000 \times magnification).

Similar morphological shapes of MD/WPI based powders were also shown by other studies (Bae & Lee, 2008; Koç et al., 2015).

The spherical shape of microcapsules by SD are formed by melting of matrix of a stable emulsion due to high inlet temperature and nozzle of spray dryer. They were free-flowing due to the lower

concentration of oil on surface of microcapsules. The free oil contents of 11–16% may thus be responsible for this fact (Reineccius, 2004).

The smooth surface of OOM is due to the presence of MD with lower molecular weight of saccharides. These low molecular weight sugars may act as a plasticizer on the particle surface during spray drying. The particles tend to agglomerate due to the presence of WPI, known for its low Tg. The WPI presence in the formulation of the powder could lead to some cracks in their morphology (Koç et al., 2015). At TG, the stickiness of powder particles increase, which leads to inter-particle bridge formations that results on caking and collapse of the particles (Bae & Lee, 2008).

4.4.5. Summary

Olive oil microcapsules were produced using different proportions of MD with DE 19 and WPI, followed by SD or FD. It was noted that the characteristics of microcapsules, such as EE, moisture content, size, and their distribution (span), bulk density, tapped density, flowability, cohesiveness and surface morphology were influenced by the different aspects of emulsion (stability, viscosity, droplet diameter and their distribution) and dehydration methods (SD and FD). The viscosity of emulsions was increased by the higher proportion of WPI in emulsion and the stability of emulsion was reduced. A stable emulsion with lower droplet size was obtained by the higher proportion of MD in emulsion. The use of MD with WPI provides a unique advantage to produce a stable emulsion as well as OOM. The highest EE ($88.61\% \pm 1.64$) was achieved from 50 MD-50 WPI emulsion and SD. Size of microcapsules and span value were greater by the higher proportion of WPI having lower value of Tg, which influence the aggregation during SD. Bulk density and tapped density of microcapsules were reduced with increase of the size of microcapsules. Microcapsules with the higher proportions of MD contained more moisture due to the presence of low molecular weight of saccharides, which are hydrophilic. Furthermore, microcapsules with higher amount of MD exhibited poor flowability and high cohesiveness due to the presence of low molecular weight of carbohydrates. OOM produced by SD were generally spherical with smooth surface; however, some dent shaped microcapsules were produced after SD of 100 WPI emulsion. The smooth surface of microcapsule was produced due to the presence of MD in formation. Microcapsules produced by FD were flat flakes with irregular surface due to the sublimation of water and disintegration of microstructure during FD. In this investigation, limited numbers of matrix (MD and WPI) and emulsion formulations were considered for the microencapsulation of olive oil.

To intensify the process, cross flow membrane emulsification was applied for the optimal sample 50MD-50WPI. The obtained EE was improved from $88.61\% \pm 1.64$ to $91.16\% \pm 0.27$. The microcapsules produced by CFME-SD were spherical in shape and had smooth surface and free-

flowing due to the lower concentration of surface oil on skin of microcapsules. Since OO is enriched with polyphenolic antioxidants, tocopherols, phytosterols and fatty acids, a quality assessment of encapsulated olive oil was performed through Rancimat accelerated test of oxidation. Consequently, the oxidative stability of the CFME-SD sample was higher due to its higher EE and low surface oils content comparing to RSH-SD sample that had a lower protective function against oxidation.

4.5. Investigation of microencapsulation of olive oil by external gelation to obtain alginate/olive oil capsules

The overall aim of this part of my PhD was to encapsulate olive oil in Ca-alginate beads to produce beads containing a higher oil content. One of the most common methods of encapsulation is the ionic gelation with formation of alginate gels by ionic cross-linking with multivalent cations (section 2.7.5). The process of encapsulation is affected by various factors such as sodium alginate and olive oil concentrations and the homogenization rate of the rotor stator homogenizer.

Design of experiments (DOE) are techniques that quantify the effects of various factors on a response and optimize them in well-defined experimental areas. This technique consists in the organization of a series of tests consisting in manipulating the factors to describe the method making it possible to obtain an optimal response. The response surface methodology (RSM) is part of the design of experiments used for optimization. It is an empirical modeling technique devoted to the evaluation of the relationship of a set of controlled and observed experimental factors with the results (Goupy, 2006). RSM is an effective tool for the optimization of the processing condition through the determination of the impacts of the independent values on the dependent values under the range of investigation. The three most used types of RSM are Box-Behnken designs (BBD), Doehlert designs and centered composite designs.

The first step in establishing an RSM is to choose the experimental design. For my case study it was the BBD which applies to problems with three design variables or more. Its main advantage, compared to other designs, for example centered composites, is that it requires fewer experiments to build a quadratic model. According to this DOE, each factor takes a maximum value, a minimum value and an intermediate value (Ba & Boyaci, 2007). BBD was used to verify the effect of variations in sodium alginate concentration, olive oil concentration and homogenization rate on the two responses, the emulsion stability and the retention capacity (RC) of the beads (capsules loaded with oil). This design based on the RSM is the most used in this type of experiment. It consists of modeling the results in the form of second-degree polynomial equation which is a quadratic model. Thus, the observed response Y can be

expressed as a function of the other explanatory variables in addition to the measurement error ϵ (Ba & Boyaci, 2007).

$$Y = f(X_1, X_2, \dots, X_i) + \epsilon \quad (13)$$

In our case, X_1 = % [sodium alginate], X_2 = rpm-homogenization rate, and X_3 = % [oil phase].

To estimate the function f , we consider that it can be written in the form of a second degree polynomial: a_{ii} and a_{ij} are regression coefficients for intercept, linear, quadratic and interaction coefficients respectively and x_i and x_j are coded independent variables.

$$y = a_0 + a_i x_i + a_{ii} x_i^2 + \dots + a_{ij} x_i x_j \quad (14)$$

$$Y_{TL} = a_0 + a_1 X_1 + a_2 X_2 + a_3 X_3 + a_{11} X_1^2 + a_{22} X_2^2 + a_{33} X_3^2 + a_{12} X_1 X_2 + a_{13} X_1 X_3 + a_{23} X_2 X_3 \quad (15)$$

a_i : linear effects regression coefficients; a_{ii} : regression coefficients of quadratic effects.

X_i and X_j : coded experimental variables.

It has been noted from the literature that the best condition for the preparation of capsules of high stability, without a high level of oil phase migration in the liquid phase was medium viscosity alginate- 1.37%; olive oil concentration - 30%; homogenization rate - 20000 rpm (Poirieux et al., 2017). However, a small variation of these factors can probably improve the stability of emulsion and the retention capacity of the capsules. This finding allowed to consider that these values represent the points in the center relative to these three factors. Thus, the aim of this part of my work was to investigate the influence of alginate concentration, homogenization rate and the oil phase amount in the preparation of capsules rich in olive oil. The flow diagram of this process was explained in section 3.2.6.1 and figure 21. To establish the joint influence of the factors, expert design software was used, the optimization features selected being emulsion stability and beads oil retention capacity. The optimal levels of the factors were established from the mathematical model. The obtained capsules showed maximum stability and possibility to be used in food industries.

4.5.1. Optimization of the process parameters for preparation of capsules with high oil phase content

Conditions optimization for obtaining capsules with oil phase content was performed by using Design Expert software with three factors in three levels. Alginate solution concentration, the concentration of the oil phase in the emulsion and the homogenization rate were selected as independent variables. They are shown in Table 17. The independent variables were coded in accordance with the generally accepted methodology. The plan of the experiment is presented

in Table 17. The stability of the resulting emulsions was selected for target functions. Processing of experimental data and obtaining mathematical models were performed using Design Expert version 13.0.

Table 17: Levels of variation of the independent variables in emulsion optimization.

	Lower level	Center level	Upper level
Alginate solution concentration, % (w/v)	0.5	1	1.5
Homogenization rate, rpm	10000	15000	20000
Oil phase concentration, % (v/v)	15	30	45

4.5.1.1. Emulsion characterization

Emulsions containing a mixture of oil and sodium alginate at different concentrations were mixed at 15000 rpm and checked for their stability. In the combination of high alginate concentration with different concentrations of oil phase, OOE had high viscosity which subsequently led to high emulsion stability (90.9 % to 100 %). Data showed that emulsion stability depended to a great extent on alginate concentration and oil concentration. The visual observations made during the study on the stability (Figure 40), showed that the higher the concentrations of the alginate solution, the better the emulsification of the oil phase in the alginate solution was. Whereas, in the combination of low alginate concentration with different oil phase concentrations, the stability of the formed emulsion was linear to the solution viscosity. At low viscosity when oil concentration was only 15%, stability of the emulsion was the lowest (70%) yielding high oil phase globules and areas of pure alginate. Similarly, Morales et al. (2017), found that stability of emulsion progresses when oil concentration is between 30 and 40% and that it decreases at higher oil concentrations. Maximum stability was obtained for emulsions prepared with 1.5 % alginate.

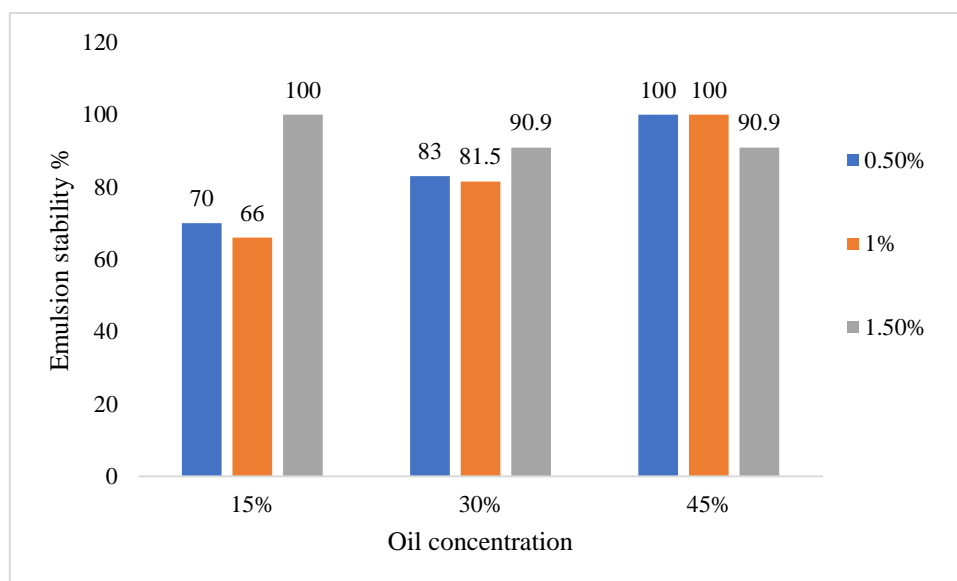
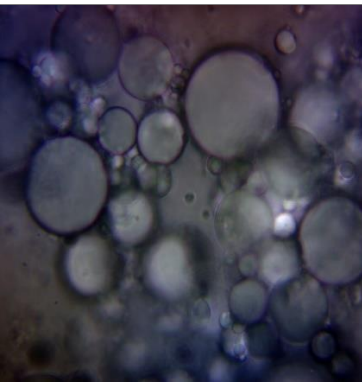
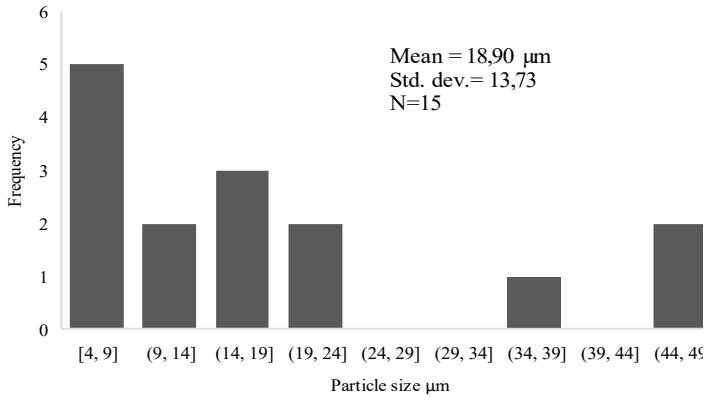
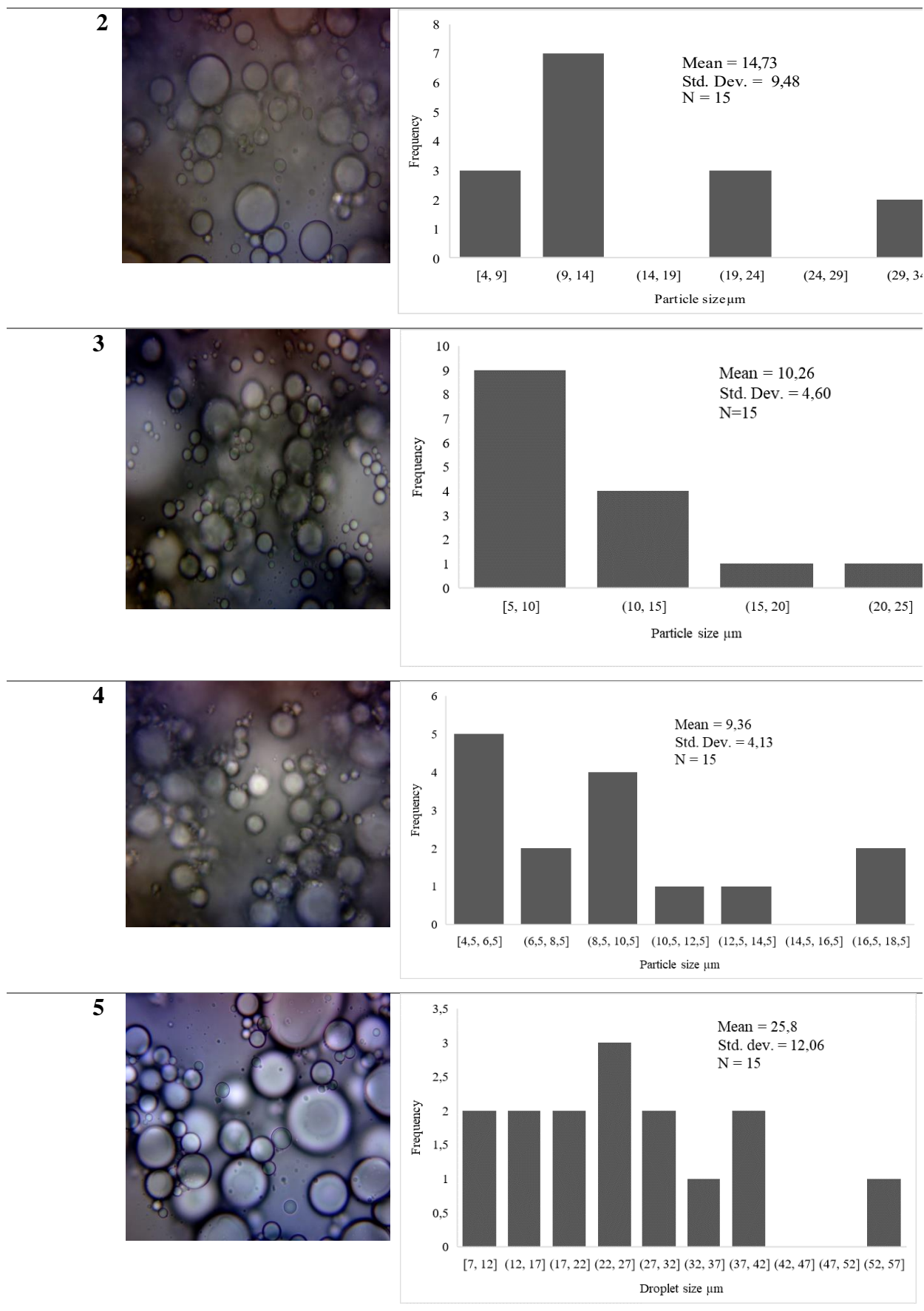


Figure 40: Stability of the emulsions prepared using different alginate concentrations (0.5 %, 1 % and 1.5 %) and different oil concentrations (15%, 30% and 45%).

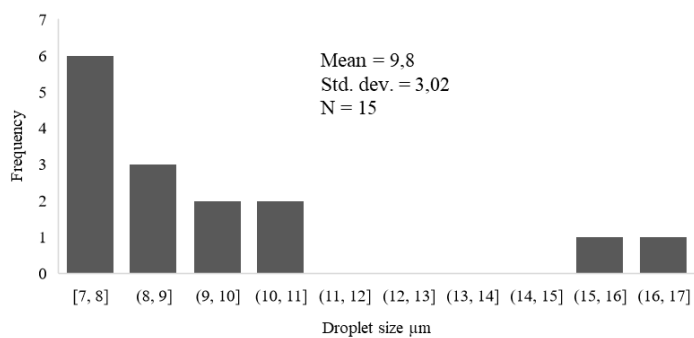
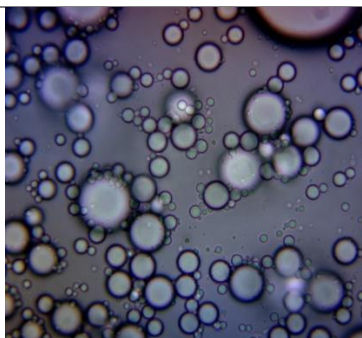
The emulsions suggested by the BBD were prepared. Table 18 includes a picture for each emulsion variant that helped the determination of the oil phase globule size in the composition of the emulsion. Size of the formed globules are important aspects when it comes to incorporating them in and consuming them through probiotic food products. The size distribution of each type of globule was characterized based on a size measurement of multiple random individual globule diameters using microscope software. Size distributions of different emulsion globules, along with the mean and the standard deviation values, are presented in Table 18.

Table 18: Results from the design experiment for modeling the emulsification conditions.

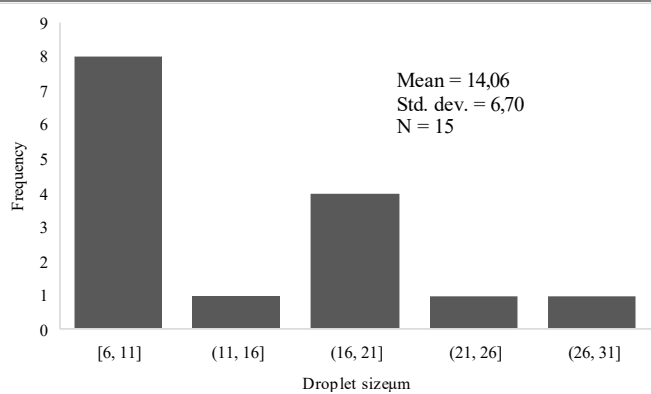
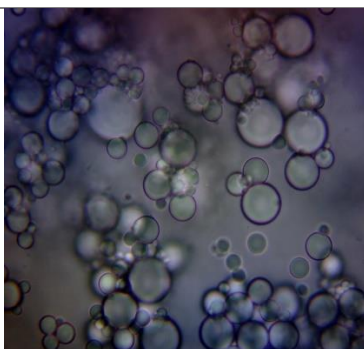
Run	Picture	Particle distribution
1		 <p>Mean = 18,90 μm Std. dev.= 13,73 N=15</p>



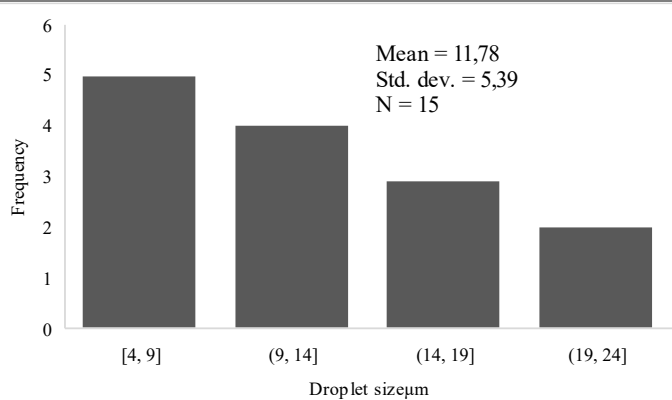
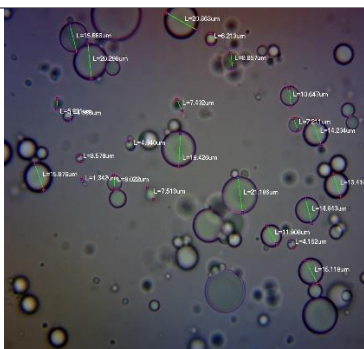
6



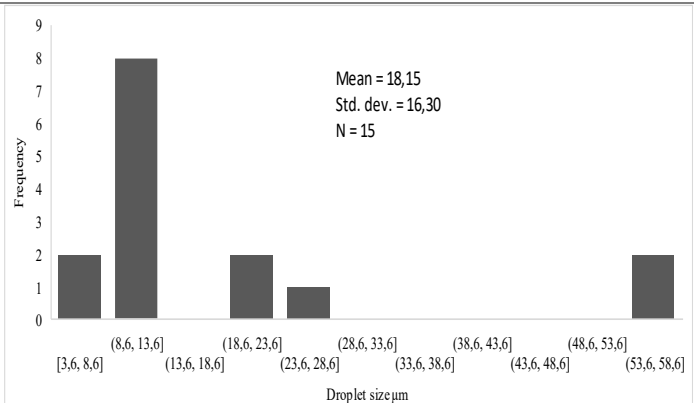
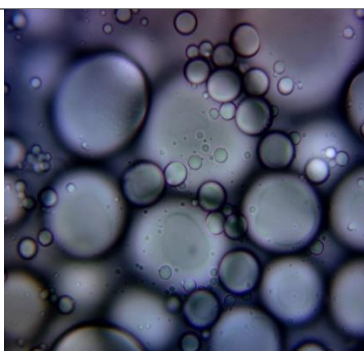
7



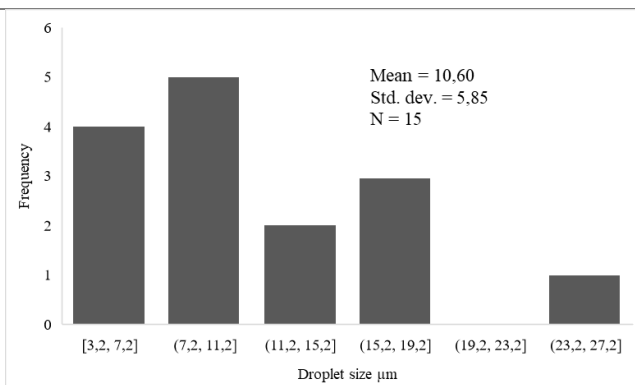
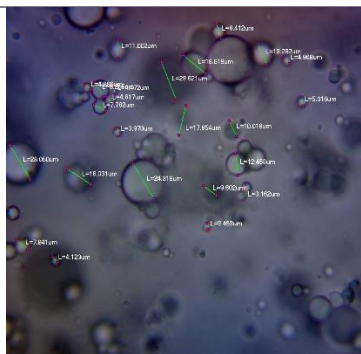
8



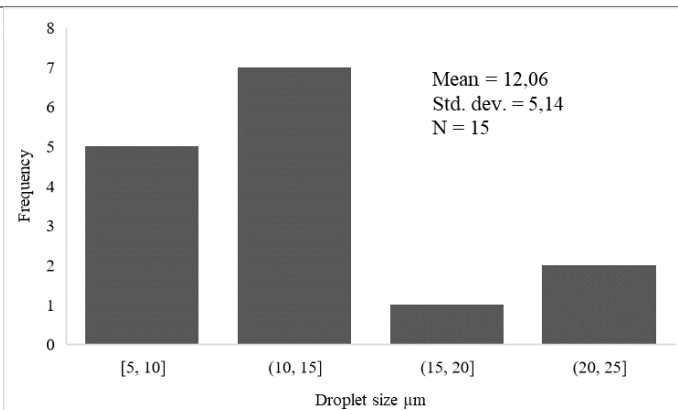
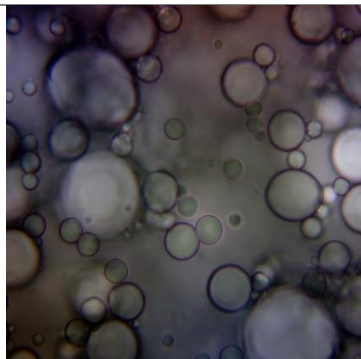
9



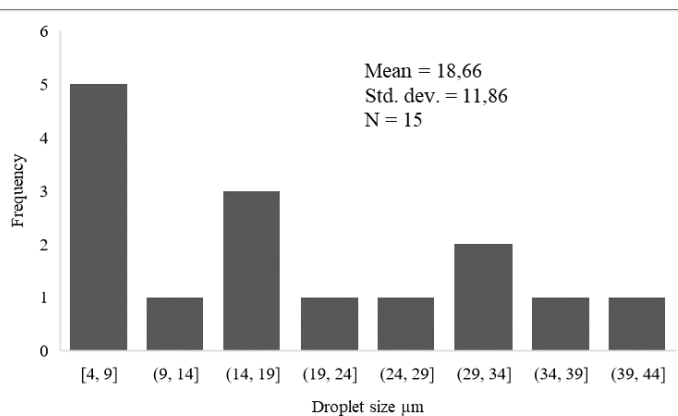
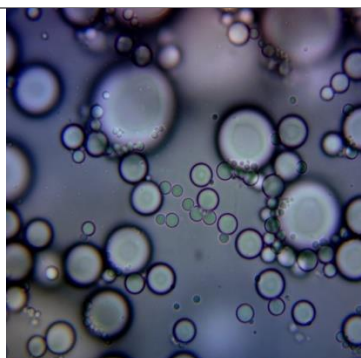
10



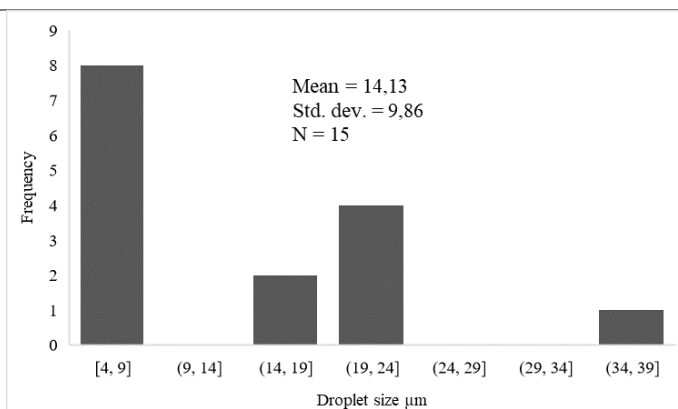
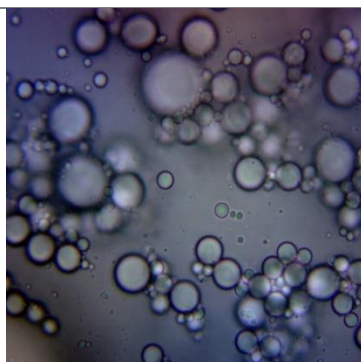
11



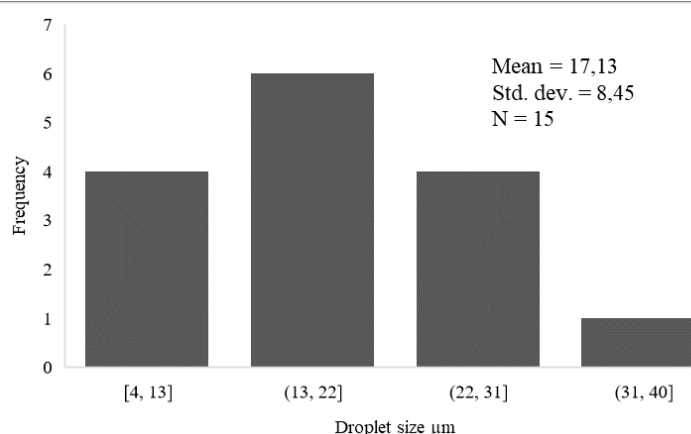
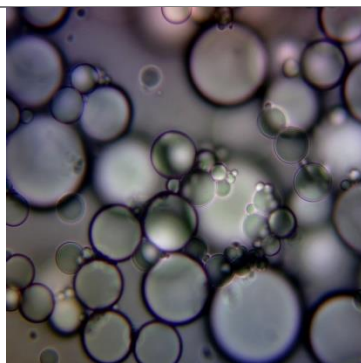
12



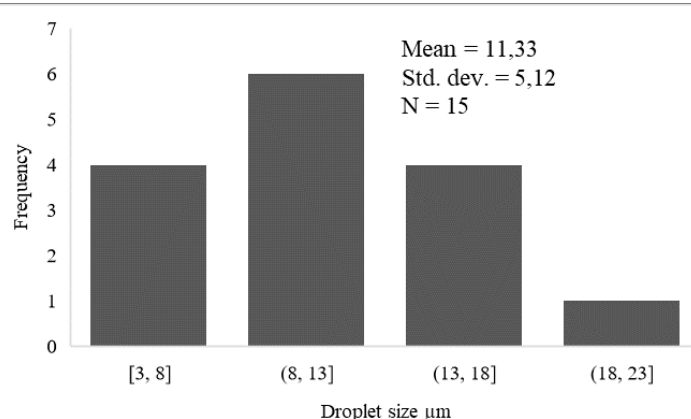
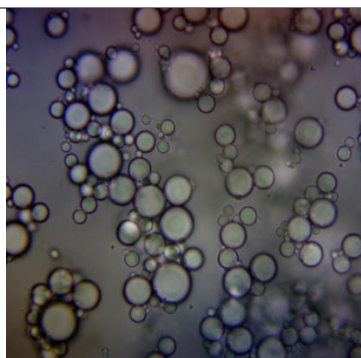
13



14



15



A wide micrometers size range was obtained, and droplets mean diameters ranged from around 9 to 25 μm .

4.5.1.2. Optimization design experiment

The effects of sodium alginate concentration, olive oil concentration and homogenization rate were studied by an optimization plan and the stability and retention capacity were taken as evaluation indexes. To minimize the impact of unexplained variability in the observed responses, the experiments were performed in random order. The responses corresponding to the 3 trials performed in the center of the domain allowed us to estimate the variance of the pure error and thus to determine the variance related to the lack of fit.

A Box–Behnken design (BBD) with three independent variables was applied to optimize the process conditions. The three parameters, including alginate solution concentration, homogenization rate and oil phase concentration were designated as A, B and C, respectively. Stability(Y1) and RC (Y2) were taken as the corresponding values. Table 19 summarized the scope and level of the independent variables.

Table 19: Box-Behnken design and response values.

Run	A %	B %	C rpm	Stability (Y1) %	RC (Y2) %
-----	-----	-----	-------	------------------	-----------

				Experimental value	Predicted value	Experiment al value	Predicted value
1	1,5	30	10000	90,9	88.41	48,21	47.72
2	1	30	15000	100	100	64,32	65.61
3	1	30	15000	100	100	69,54	65.61
4	1	45	20000	100	94.25	81,38	75.94
5	0,5	15	15000	70	70.4	32,5	32.95
6	0,5	30	20000	95	97.49	42,9	43.39
7	1,5	15	15000	100	96.74	33	28.05
8	1	30	15000	100	100	62,98	65.61
9	0,5	30	10000	91	84.51	8	2.12
10	1,5	45	15000	90,9	90.16	71,23	70.78
11	1	45	10000	63	66.24	35,7	36.64
12	0,5	45	15000	100	103.26	23,85	28.80
13	1,5	30	20000	100	106.49	29	34.88
14	1	15	10000	60	65.75	37	42.44
15	1	15	20000	72,04	68.81	32,5	31.56

4.5.1.3. Fitting the mathematical model and statistical analysis

Based on the experiments conducted have been developed mathematical models for the stability and retention capacity of the capsules. Analysis of variance (ANOVA) was conducted for the two responses together with the regression coefficients in Tables 20 and 21. They show that the model is significant at $p < 0,0001$ up to (Goupy, 2006). The model with the larger absolute value of F and the smaller value of p was the more significant. The correlation coefficients ($R^2 = 0.93$ and $R^2 = 0.96$) and adjusted correlation coefficient (adjusted $R^2 = 0.81$ and adjusted $R^2 = 0.90$) in tables 20 and 21 respectively showed the goodness of fitting model.

The predicted values and actual values which can be correlated by the coded and actual equations built by the model were depicted in Figure 41.

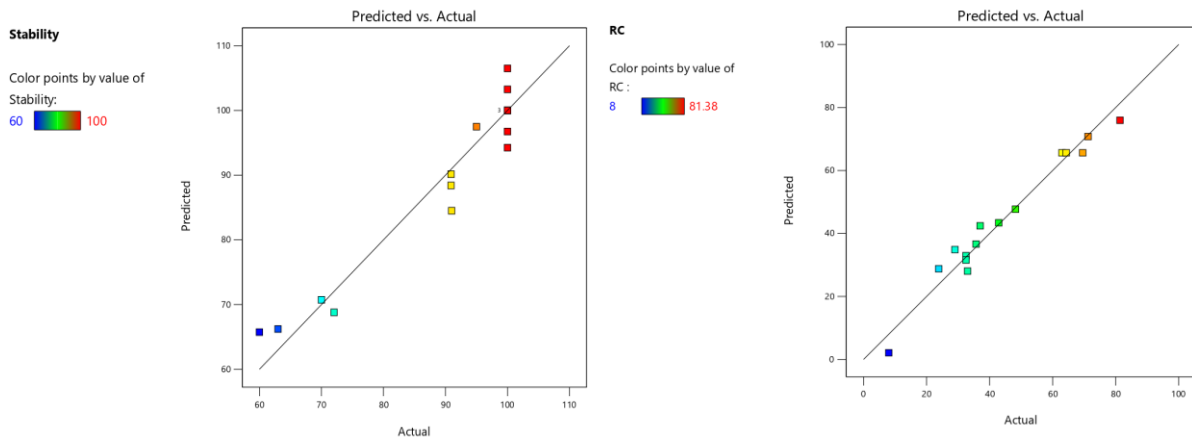


Figure 41: Correlation between the predicted values and actual values calculated by the model according to the regression equations.

The coefficient of variation when less than 10% reflects that the experimental values had a good reliability. From table 20, C.V.% = 7.23. The results obtained show that oil concentration and homogenization rate have a significant influence on stability. Whereas, from table 21, the results obtained show that the three independent factors have a significant influence on the RC ($P < 0.05$). Furthermore, the quadratic effects of all factors were also significant at $p < 0.05$ except for B^2 . These results clearly show the good predictive quality of the adopted model.

Table 20: ANOVA of the quadratic model for emulsion stability.

Source	Sum of Squares	DF ^a	Mean Square	F-value ^b	p-value	Significance ^c
Model	2853,44	9	317,05	7,69	0,0185	significant
A-Alginate	83,20	1	83,20	2,02	0,2146	Not significant
B-Oil	336,18	1	336,18	8,16	0,0356	significant
C-H	482,67	1	482,67	11,71	0,0188	significant
AB	382,20	1	382,20	9,27	0,0286	significant
AC	6,50	1	6,50	0,1577	0,7076	Not significant
BC	155,75	1	155,75	3,78	0,1095	Not significant
A²	105,49	1	105,49	2,56	0,1706	Not significant
B²	844,11	1	844,11	20,48	0,0063	significant
C²	456,57	1	456,57	11,08	0,0208	significant
Residual	206,11	5	41,22			
Lack of Fit	206,11	3	68,70			
Pure Error	0,0000	2	0,0000			

Cor Total	3059,55	14	
Std. Dev.	6,42	R²	0,9326
Mean	88,86	Adjusted R²	0,8114
C.V. %	7,23	Predicted R²	-
			0,0779
Adeq Precision			7,7719

*a,b and c mean degrees of freedom, test for comparing term variance with residual value and $p < 0.05$ significant respectively.

Table 21: ANOVA of the quadratic model for RC.

Source	Sum of Squares	DF^a	Mean Square	F-value^b	p-value	Significance^c
Model	5799,84	9	644,43	15,80	0,0036	significant
A-Alginate	688,02	1	688,02	16,87	0,0093	significant
B-Oil	744,21	1	744,21	18,25	0,0079	significant
C-H	404,27	1	404,27	9,91	0,0254	significant
AB	549,43	1	549,43	13,47	0,0144	significant
AC	731,97	1	731,97	17,95	0,0082	significant
BC	629,51	1	629,51	15,44	0,0111	significant
A²	1483,27	1	1483,27	36,37	0,0018	significant
B²	108,68	1	108,68	2,67	0,1635	Not significant
C²	677,21	1	677,21	16,61	0,0096	significant
Residual	203,90	5	40,78			
Lack of Fit	179,88	3	59,96	4,99	0,1714	not significant
Pure Error	24,03	2	12,01			
Cor Total	6003,74	14				
Std. Dev.	6,39	R²	0,9660			
Mean	44,81	Adjusted R²	0,9049			
C.V. %	14,25	Predicted R²	0,5116			
Adeq Precision			14,1590			

*a,b and c mean degrees of freedom, test for comparing term variance with residual value and $p < 0.05$ significant respectively.

The fitted model equation for emulsion stability (Y1) is given by the following equation:

$$Y1 = -75.90750 - 4.86000A + 4.51950B + 0.011892C - 1.30333AB + 0.000510AC \\ + 0.000083BC + 21.38000A^2 - 0.067200B^2 - 4.44800 \cdot 10^{-7}C^2 \quad (16)$$

The fitted model equation for the retention capacity of capsules (Y2) is given as the following equation:

$$Y2 = -176.32500 + 213.17583A - 1.98189B + 0.018066C + 1.56267AB \\ - 0.005411AC + 0.000167BC - 80.17167A^2 - 0.024113B^2 \\ - 5.41717 \cdot 10^{-7}C^2 \quad (17)$$

4.5.1.4. Analysis of response surface model

The visual interactions for stability were presented in Figures 42. As exhibited by Figure 42 (a), oil concentration and sodium alginate concentration had a significant influence on the emulsion's stability which demonstrated that the suitable alginate and oil concentration were in favor of the emulsion stability. As presented in Figure 42 (b), the emulsion stability was given as a function of homogenization rate and alginate concentration. Increasing homogenization rate until 17000 rpm at a given alginate concentrations leads to a significant increase of stability. After this rate stability tends to decrease. Figure 42(c) shows stability as a function of homogenization rate and oil concentration. At a fixed homogenization rate, the RC initially increased and then declined with increasing oil concentration. Higher oil concentration caused an excessive surface oil content which resulted in a low RC of the beads.

Similarly, the visual interactions for RC were presented in Figure 43. As exhibited in Figure 43(a), oil concentration and sodium alginate concentration had a significant effect on the RC. It demonstrated that RC increased significantly at a fixed olive oil concentration when alginate concentration is increasing until reaching the value of 1.1 % after which the trend of increasing became less significant. As presented in Figure 43(b), the RC was given as a function of homogenization rate and alginate concentration. Therefore, at a fixed alginate concentration, the RC increased significantly with increasing the rate of homogenization. Figure 43(c) also showed that the RC initially increased and then declined with decreasing homogenization rate at a fixed oil concentration of 40.5%. Based on equations (16) and (17), the optimal experimental conditions were as follows: sodium alginate concentration 1.133%, olive oil concentration 40.49% and homogenization rate 17472.903rpm. Considering the actual situation, the experimental conditions were modified slightly as follows: sodium alginate concentration 1.13%, olive oil concentration 40.5% and homogenization rate 18000 rpm. Appendix-Figure 8 shows a picture of the obtained beads using this encapsulation process.

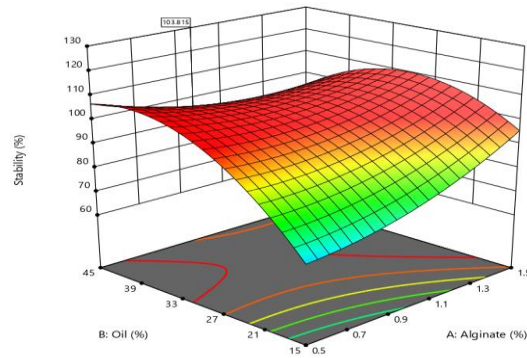
Factor Coding: Actual

Stability (%)
60 100

X1 = A
X2 = B

Actual Factor
C = 17242.6

3D Surface



(a)

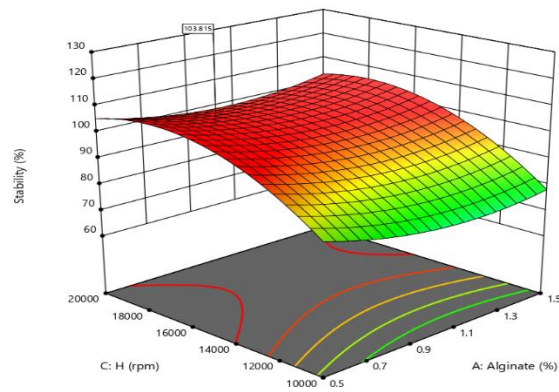
Factor Coding: Actual

Stability (%)
60 100

X1 = A
X2 = C

Actual Factor
B = 38.4502

3D Surface



(b)

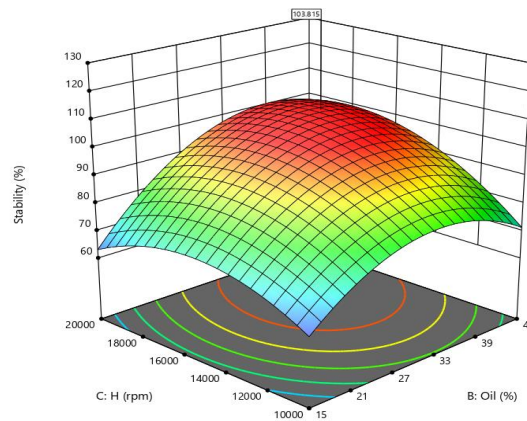
Factor Coding: Actual

Stability (%)
60 100

X1 = B
X2 = C

Actual Factor
A = 0.753798

3D Surface



(c)

Figure 42: The 3D response surface plots for the influence of process parameters on the emulsion stability. (a) Sodium alginate concentration and olive oil concentrations; (b)

Homogenizations rate and sodium alginate; (c) Homogenization rate and olive oil concentration.

4.5.2. Summary: Modeling and optimization of the emulsions for the preparation of capsules with high oil phase content

After a series of experiments and data analysis it can be concluded that the emulsification/external gelation method is suitable for high oil loading retention. The optimal conditions proposed by the models, together with the predicted values of the stability of emulsion and retention capacity, and the value of desirability, are represented in the table

Table 22: The optimal conditions proposed by the quadratic models and the predicted stability and retention capacity.

Factor	Estimation	Optimal predicted Stability (%)	Optimal predicted RC (%)	Desirability
Sodium alginate (%)	1.133			
Olive oil (%)	40.494	100	75.700	0.961
Homogenization rate (rpm)	17472.903			

Based on experimental data, mathematical models were established, and process optimization was carried out to determine crucial operating parameters: sodium alginate concentration 1.13%, olive oil concentration 40.5% and homogenization rate 18000 rpm. It was concluded as well that further studies are needed to investigate the effect of incorporating optimized microcapsules in the composition of some selected food products.

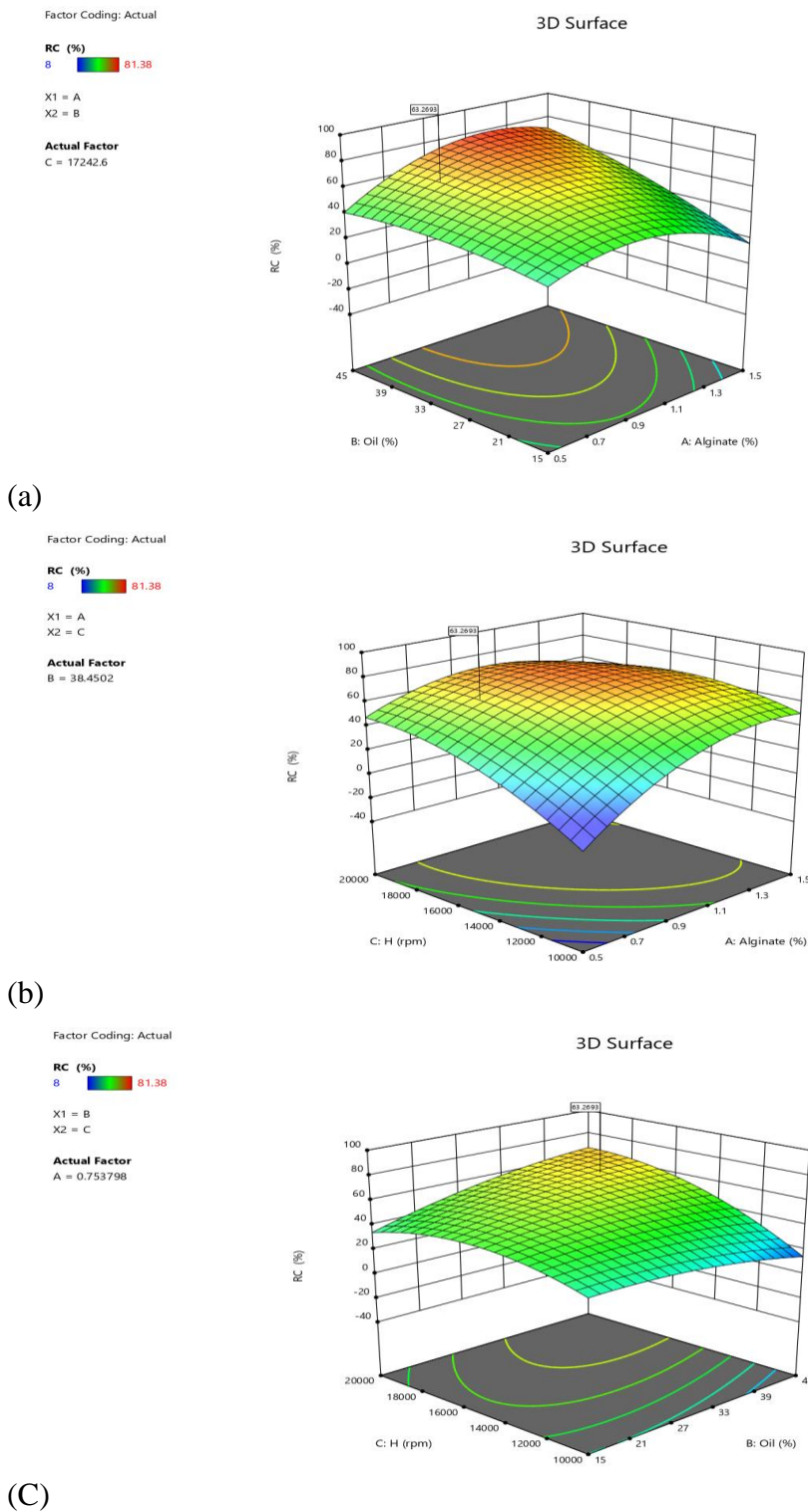


Figure 43: The 3D response surface plots for the influence of process parameters on the retention capacity of microcapsules. (a) Sodium alginate concentration and olive oil concentrations; (b) Homogenization rate and sodium alginate; (c) Homogenization rate and olive oil concentration.

5 CONCLUSIONS AND RECOMMENDATIONS

Microencapsulation of olive oil is as a unique approach to conserve the biochemical properties of bioactive compounds of olive oil, such as polyunsaturated fatty acids (ω -3 and ω -6 fatty acids), vitamins and phenolic antioxidants, from oxidation and change of environmental condition. As a result, the quality and biological activity of olive oil are not deteriorated in the food matrix during processing, cooking, and storage. Therefore, several applications of microencapsulated olive oil in food, pharmaceutical and cosmetic industries have received high status. There are different techniques to prepare olive oil microcapsule and for its characterization. Application of encapsulated olive oil may be in food, pharmaceutical and cosmetic industries. The method selection to prepare microcapsule depends according to the situation and product interest. Furthermore, different process parameters influence the characteristics of olive oil microcapsule. The major purpose of this dissertation was to prepare microcapsules from olive oil loaded with bioactive by a variety of methods. The preliminary study based on the membrane emulsification method using different combinations of wall materials showed that CFME is an effective method to perform stable emulsions with narrow droplet size. Considering that efficiency of encapsulation is the most important parameter to investigate, the effects of emulsification technologies in terms of RSH and CFME and the composition of wall materials were studied in a judicious way. Two different formulations by changing MD with DE5 and CMC were considered for emulsion preparation; however, amount of emulsifiers, such as GA and Tween 80 were fixed. The stability of emulsion was higher when emulsion was prepared by RSH. The value of D_{32} was lowered in case of RSH compared to other one. The higher EE was found by CFME. The most effective wall material composition to produce olive oil microcapsules is MD 15 g, CMC 5 g and GA 15 g. Considering higher EE, CFME may be considered suitable for industrial production of olive oil microcapsule. Further investigation may be performed to understand the effects of the geometry of turbulent promoter, other formulation of emulsion and the quality of encapsulated olive oil during different times of storage.

Olive oil microcapsules were produced using different proportions of MD with DE 19 and WPI, followed by SD or FD. It was noted that the characteristics of microcapsules, such as EE, moisture content, size, and their distribution (span), bulk density, tapped density, flowability, cohesiveness and surface morphology were influenced by the different aspects of emulsion (stability, viscosity, droplet diameter and their distribution) and dehydration methods (SD and FD). The viscosity of emulsions was increased by the higher proportion of WPI in emulsion

and the stability of emulsion was reduced. A stable emulsion with lower droplet size was obtained by the higher proportion of MD in emulsion. The use of MD with WPI provides a unique advantage to produce a stable emulsion as well as OOM. The highest EE ($88.61\% \pm 1.64$) was achieved from 50 MD-50 WPI emulsion and SD. Size of microcapsules and span value were greater by the higher proportion of WPI having lower value of, which influences the aggregation during SD. Bulk density and tapped density of microcapsules were reduced with increase of the size of microcapsules. Microcapsules with the higher proportions of MD contained more moisture due to the presence of low molecular weight of saccharides, which are hydrophilic. Furthermore, microcapsules with higher amount of MD exhibited poor flowability and high cohesiveness due to the presence of low molecular weight of carbohydrates. OOM produced by SD were generally spherical with smooth surface; however, some dent shaped microcapsules were produced after SD of 100 WPI emulsion. The smooth surface of microcapsule was produced due to the presence of MD in formation. Microcapsules produced by FD were flat flakes with irregular surface due to the sublimation of water and disintegration of microstructure during FD. In this investigation, limited numbers of matrix (MD and WPI) and emulsion formulations were considered for the microencapsulation of olive oil. Further investigation will be performed to understand the effects of other formulations of emulsions and MD with different DE on EE, moisture content and Tg. Olive oil is enriched with polyphenolic antioxidants, tocopherols, phytosterols and fatty acids. In future, investigations will be performed to understand the quality of encapsulated olive oil during different storage times. Furthermore, the release of encapsulated olive oil from its matrix and fate of different functional compounds shall be investigated by the in vitro digestion protocol.

In the platform of process intensification, cross flow membrane emulsification was applied for the optimal sample from the previous investigation.: optimum sample (50MD-50WPI) and the obtained EE was improved from $88.61\% \pm 1.64$ to $91.16\% \pm 0.27$. The microcapsules produced by CFME-SD were spherical in shape and had smooth surface and free-flowing due to the lower concentration of oil on skin of microcapsules. The quality assessment of encapsulated olive oil was performed through Rancimat accelerated test of oxidation. Consequently, the oxidative stability of the CFME-SD sample was higher due to its higher EE and low surface oils content compared to RSH-SD sample that had a lower protective function against oxidation.

Emulsification/external gelation method is suitable for high oil loading retention (40.5%). The technology we used looks suitable for pharmaceutical applications such as nutraceuticals. Based on experimental data, mathematical models were established, and process optimization

was carried out to determine crucial operating parameters: sodium alginate concentration 1.13%, olive oil concentration 40.5% and homogenization rate 18000 rpm. It was concluded as well that further studies are needed to investigate the effect of incorporating optimized microcapsules in the composition of some selected food products. It was concluded as well that further studies are needed to investigate the effect of incorporating optimized microcapsules in the composition of some selected food products.

6 NEW SCIENTIFIC RESULTS

From my dissertation, I have found out:

[1] The addition of carboxymethylcellulose to maltodextrin and gum Arabic mixture of wall materials resulted in a better stability of the emulsion and into a narrow droplet size distribution. Therefore, considering that adding CMC to the emulsion resulted in more monodisperse compositions, explains the acceptable viscosity of this mixture towards the crossflow membrane machine which implies resistance to the droplets movements and thus avoiding coalescence and resulting in smaller diameters.

[2] As a result of the comparison of emulsification by cross flow membrane method and rotor stator homogenization method, I found that after drying using the freeze drier, a best efficiency 68.86% was achieved by cross flow membrane emulsification method using emulsion formulation containing 15 g maltodextrin, 5 g carboxymethylcellulose and 15 g gum Arabic. The freeze-dried powder micrographs showed irregularly shaped particles which were due to the drying process.

[3] By comparing different drying methods, I proved that spray drying technique was the most promising process to microencapsulate olive oil. The highest efficiency and the highest yields were observed 88.61 % and 52.25 % respectively when spray drying method was used and when the wall materials composition is 50 g whey protein isolate, 50 g maltodextrin and 1 g tween 20 emulsifier.

[4] By intensifying the process using CFME coupled with spray drying for the optimum sample, the obtained EE was improved from 88.61% \pm 1.64 to 91.16 % \pm 0.27. Microcapsules, produced by CFME-SD were spherical in shape and had smooth surface and free-flowing due to the lower concentration of oil on skin of microcapsules. The oxidative stability of the CFME-SD sample was higher due to the lower surface oil content on the skin of the capsules, while the RSH-SD sample had a lower protective function against oxidation.

[5] In my attempts, to produce microcapsules with high olive oil loading, I opted to the microencapsulation method by emulsification/ external gelation which consists of dripping alginate/ oil emulsion into a calcium chloride solution. That enhances the ionic gelation with formation of alginate gels by ionic cross-linking with multivalent cations. Consequently, the optimum concentration of olive oil by using this process is 40.5 % which is higher than the oil concentration in the previous encapsulation methods (maximum of 30%). Additionally, based on the surface response methodology in this part, the optimal experimental conditions were as follows: sodium alginate concentration 1.13%, olive oil concentration 40.5% and homogenization rate 18000 rpm.

7 SUMMARY

Olive oil has been considered as a culinary for its excellent organoleptic properties due to presence of ketones, alcohols, aldehydes, hydrocarbons, esters, furans, etc. It also has a great importance for biopharmaceutical formulation because it prevents the risks of several chronic and acute metabolic disorders (type 2 diabetes, obesity, cancer, rheumatoid arthritis, 8 Alzheimer's disease and cardiovascular diseases). Olive oil is enriched with monounsaturated fatty acids (ω -6 and ω -3 fatty acids), phenolic antioxidants (hydroxytyrosol and oleuropein), vitamin E and vitamin K. Unfortunately, oxidative deterioration of fatty acids in olive oil provides short shelf-life, responsible for undesirable organoleptic properties and reduced biological activities. It may feel that microencapsulation of olive oil is considered as a promising approach to preserve its quality and biological activities. Microencapsulation is an emerging technology, which has been received interest in food biopharmaceutical and cosmetic industries. It is used to protect bioactive compounds within surrounding layer (coating) and control their release in environment. In this process, a small droplet of liquid or solid particle is surrounded by a thin film, known as a wall material or matrix. For microencapsulation of vegetable oil, several emulsification technologies have been used. Presently, membrane emulsification has come to the forefront, and it is considered as an emerging technology. In the platform of "process intensification", membrane emulsification is a low energy consuming technique with lower equipment footprint.

The major concept of this dissertation is to investigate the encapsulation of extra virgin olive oil by sequential technologies, such as preparation of emulsion (oil in water with polymeric carbohydrate) and subsequently, freeze drying and /or spray drying or external gelation of emulsion. In this investigation, polymeric carbohydrates, such as maltodextrin (MD), carboxymethyl cellulose (CMC) and gum Arabic (GA), WPI (whey protein isolate) and sodium alginate were used as matrix. The preliminary study showed that CFME is an effective method to perform stable emulsions with narrow droplet size using CMC, MD and GA as wall materials.

At the first stage, the effects of emulsification technologies in terms of RSH and CFME and the composition of wall materials were studied in a judicious way. Two different formulations by changing MD with DE5 and CMC were considered for emulsion preparation; however, the amount of emulsifiers, such as GA and Tween 80 were fixed. The stability of emulsion was higher when emulsion was prepared by RSH. The value of D32 was lowered in case of RSH compared to other one. The higher EE was found by CFME. The most effective wall material

composition to produce olive oil microcapsules is MD 15 g, CMC 5 g and GA 15 g. Considering higher EE, CFME may be considered suitable for industrial production of olive oil microcapsule.

At a second stage, olive oil microcapsules were produced using MD with DE 19 and WPI as matrix by SD and FD. Characteristics of emulsion were influenced by proportion of matrix. Emulsion with appreciable stability was achieved by highly viscous emulsion, except 100 MD. Droplet size in stable emulsion was lower and it is influenced by viscosity of emulsion. Stable emulsion was achieved with higher concentration of MD; however, 100 MD emulsion was not viscous. EE of microcapsules were influenced by stability of emulsion, ratio and characteristics of matrix, and dehydration method. The highest EE ($88.61 \pm 1.64\%$) was achieved by 50 MD-50 WPI emulsion and subsequently, SD; whereas, freeze-dried 100 WPI emulsion offer appreciable EE ($40.64 \pm 0.03\%$). The size of microcapsules was higher with high concentration of WPI. The span value of microcapsules was higher with high concentration of WPI having lower value of Tg, which influence the agglomeration. Microcapsules with higher concentration of MD contained higher moisture due to presence of low molecular weight of saccharides. Microcapsules produced by SD were spherical in shape and had smooth surface and free-flowing due to the lower concentration of oil on skin of microcapsules. The microcapsules produced by FD were agglomerated flat flakes with porous surface and irregular edges due to disintegration of microstructure by FD and presence of high level of oil on surface of flat flakes.

At a third stage, in the platform of process intensification, cross flow membrane emulsification was applied for the optimal sample from the previous investigation.: optimum sample (50MD-50WPI), the obtained EE was improved from $88.61\% \pm 1.64$ to $91.16\% \pm 0.27$. Since OO is enriched with polyphenolic antioxidants, tocopherols, phytosterols and fatty acids, a quality assessment of encapsulated olive oil was performed through Rancimat accelerated test of oxidation. Consequently, the oxidative stability of the CFME-SD sample was higher due to its higher EE and low surface oils content compared to RSH-SD sample that had a lower protective function against oxidation.

Finally, emulsification/external gelation method was investigated for high oil loading retention. The technology I used looks suitable for industrial applications. Based on experimental data, mathematical models were established, and process optimization was carried out to determine crucial operating parameters. Based on experimental data, mathematical models were established, and process optimization was carried out to determine crucial operating parameters: sodium alginate concentration 1.13%, olive oil concentration 40.5% and homogenization rate

18000 rpm. It was concluded as well that further studies are needed to investigate the effect of incorporating optimized microcapsules in the composition of some selected food products.

I concluded as well that further studies are needed to investigate the effect of incorporating optimized microcapsules in the composition of some selected food products.

Appendices

Annex 1 References

- Albert, K., Tóth, C., Verasztó, B., Vatai, G., & Koris, A. (2016). Microencapsulation analysis based on membrane technology: Basic research of spherical, solid precursor microcapsule production. *Periodica Polytechnica Chemical Engineering*, 60(1), 49–53. <https://doi.org/10.3311/PPch.8500>
- Albert, K., Vatai, G., & Koris, A. (2018). Microencapsulation of Vegetable Oil: Alternative Approaches Using Membrane Technology and Spray Drying. *Hungarian Journal of Industry and Chemistry*, 45(2), 29–33. <https://doi.org/10.1515/hjic-2017-0017>
- Alting, A. C., Hamer, R. J., De Kruif, C. G., Paques, M., & Visschers, R. W. (2003). Number of thiol groups rather than the size of the aggregates determines the hardness of cold set whey protein gels. *Food Hydrocolloids*, 17(4), 469–479. [https://doi.org/10.1016/S0268-005X\(03\)00023-7](https://doi.org/10.1016/S0268-005X(03)00023-7)
- Anandharamakrishnan, C., & Padma Ishwarya, S. (2015). Spray Drying Techniques for Food Ingredient Encapsulation. In *Spray Drying Techniques for Food Ingredient Encapsulation*. <https://doi.org/10.1002/9781118863985>
- Ansorena, D., Echarte, A., Ollé, R., & Astiasarán, I. (2013). 2012: No trans fatty acids in Spanish bakery products. *Food Chemistry*, 138(1), 422–429. <https://doi.org/10.1016/j.foodchem.2012.10.096>
- Aronson, M. P. (1989). The Role of Free Surfactant in Destabilizing Oil-in-Water Emulsions. *Langmuir*, 5(2), 494–501. <https://doi.org/10.1021/la00086a036>
- Ba, D., & Boyaci, I. H. (2007). Modeling and optimization i: Usability of response surface methodology. *Journal of Food Engineering*, 78(3), 836–845. <https://doi.org/10.1016/j.jfoodeng.2005.11.024>
- Badiu, D., Luque, R., & Rajendram, R. (2010). Effect of Olive Oil on the Skin. In *Olives and Olive Oil in Health and Disease Prevention*. Elsevier Inc. <https://doi.org/10.1016/B978-0-12-374420-3.00123-6>
- Bae, E. K., & Lee, S. J. (2008). Microencapsulation of avocado oil by spray drying using whey protein and maltodextrin. *Journal of Microencapsulation*, 25(8), 549–560. <https://doi.org/10.1080/02652040802075682>
- Bakry, A. M., Abbas, S., Ali, B., Majeed, H., Abouelwafa, M. Y., Mousa, A., & Liang, L. (2016). Microencapsulation of Oils: A Comprehensive Review of Benefits, Techniques, and Applications. *Comprehensive Reviews in Food Science and Food Safety*, 15(1), 143–182. <https://doi.org/10.1111/1541-4337.12179>
- Barbosa, M. I. M. J., Borsarelli, C. D., & Mercadante, A. Z. (2005). Light stability of spray-dried bixin encapsulated with different edible polysaccharide preparations. *Food Research International*, 38(8–9), 989–994. <https://doi.org/10.1016/j.foodres.2005.02.018>
- Barbulova, A., Colucci, G., & Apone, F. (2015). *New Trends in Cosmetics: By-Products of Plant Origin and Their Potential Use as Cosmetic Active Ingredients*. 82–92. <https://doi.org/10.3390/cosmetics2020082>
- Boskou, D. (2007). Olive oil. *World Review of Nutrition and Dietetics*, 97(1999), 180–210. <https://doi.org/10.1159/000097916>

- Botrel, D. A., de Barros Fernandes, R. V., Borges, S. V., & Yoshida, M. I. (2014). Influence of wall matrix systems on the properties of spray-dried microparticles containing fish oil. *Food Research International*, 62, 344–352. <https://doi.org/10.1016/j.foodres.2014.02.003>
- Cahyani, I. M., Anggraeny, E. N., Nugraheni, B., Retnaningsih, C., & Kristina Ananingsih, V. (2018). The optimization of maltodextrin and arabic gum in the microencapsulation of aqueous fraction of *Clinacanthus nutans* using simplex lattice design. *International Journal of Drug Delivery Technology*, 8(2), 110–115. <https://doi.org/10.25258/ijddt.v8i2.13877>
- Calvo, P., Castaño, Á. L., Lozano, M., & González-Gómez, D. (2012). Influence of the microencapsulation on the quality parameters and shelf-life of extra-virgin olive oil encapsulated in the presence of BHT and different capsule wall components. *Food Research International*, 45(1), 256–261. <https://doi.org/10.1016/j.foodres.2011.10.036>
- Calvo, P., Hernández, T., Lozano, M., & González-Gómez, D. (2010). Microencapsulation of extra-virgin olive oil by spray-drying: Influence of wall material and olive quality. *European Journal of Lipid Science and Technology*, 112(8), 852–858. <https://doi.org/10.1002/ejlt.201000059>
- Carneiro, H. C. F., Tonon, R. V., Grosso, C. R. F., & Hubinger, M. D. (2013a). Effect of different combination of wall materials on the encapsulation efficiency of flaxseed oil microencapsulated by spray drying. *Journal of Food Engineering*, 115, 443–451.
- Carneiro, H. C. F., Tonon, R. V., Grosso, C. R. F., & Hubinger, M. D. (2013b). Encapsulation efficiency and oxidative stability of flaxseed oil microencapsulated by spray drying using different combinations of wall materials. *Journal of Food Engineering*, 115(4), 443–451. <https://doi.org/10.1016/j.jfoodeng.2012.03.033>
- Carvalho da Silva L., Castelo R.M., Cheng H.N., Biswas A., Furtado R.F., A. C. R. (2022). Methods of Microencapsulation of Vegetable Oil: Principles, Stability and Applications – A Minireview. *Food Technology and Biotechnology*, 60(3), 308–320. <https://doi.org/10.17113/ftb.60.03.22.7329>
- Chan, L. W., Lim, L. T., & Heng, P. W. S. (2000). Microencapsulation of oils using sodium alginate. *Journal of Microencapsulation*, 17(6), 757–766. <https://doi.org/10.1080/02652040050161747>
- Charcosset, C. (2009). Preparation of emulsions and particles by membrane emulsification for the food processing industry. In *Journal of Food Engineering*. <https://doi.org/10.1016/j.jfoodeng.2008.11.017>
- Charcosset, C., Limayem, I., & Fessi, H. (2004). The membrane emulsification process - A review. *Journal of Chemical Technology and Biotechnology*, 79(3), 209–218. <https://doi.org/10.1002/jctb.969>
- Charles, A. L., Abdillah, A. A., Saraswati, Y. R., Sridhar, K., Balderamos, C., Masithah, E. D., & Alamsjah, M. A. (2021). Characterization of freeze-dried microencapsulation tuna fish oil with arrowroot starch and maltodextrin. *Food Hydrocolloids*, 112(August 2020), 106281. <https://doi.org/10.1016/j.foodhyd.2020.106281>
- Choi, K. O., Ryu, J., Kwak, H. S., & Ko, S. (2010). Spray-dried conjugated linoleic acid encapsulated with Maillard reaction products of whey proteins and maltodextrin. *Food Science and Biotechnology*, 19(4), 957–965. <https://doi.org/10.1007/s10068-010-0134-7>

- Condelli, N., Caruso, M. C., Galgano, F., Russo, D., Milella, L., & Favati, F. (2015). Prediction of the antioxidant activity of extra virgin olive oils produced in the Mediterranean area. *Food Chemistry*, 177, 233–239. <https://doi.org/10.1016/j.foodchem.2015.01.001>
- Czaplicki, S., Ogrodowska, D., Derewiaka, D., Tańska, M., & Zadernowski, R. (2011). Bioactive compounds in unsaponifiable fraction of oils from unconventional sources. *European Journal of Lipid Science and Technology*, 113(12), 1456–1464. <https://doi.org/10.1002/ejlt.201000410>
- Dahl, W. J., Tandlich, M. A., & England, J. (2016). *Health Benefits of Olive Oil and Olive Extracts 1*. 1–5. <http://edis.ifas.ufl.edu>
- Danby, S. G., Ph, D., Alenezi, T., Sultan, A., Lavender, T., Ph, D., Chittock, J., Sc, B., Brown, K., Sc, B., Cork, M. J., & Ph, D. (2013). *Effect of Olive and Sunflower Seed Oil on the Adult Skin Barrier: Implications for Neonatal Skin Care*. 30(1), 42–50. <https://doi.org/10.1111/j.1525-1470.2012.01865.x>
- De Luca, G., Di Maio, F. P., Di Renzo, A., & Drioli, E. (2008). Droplet detachment in cross-flow membrane emulsification: Comparison among torque- and force-based models. *Chemical Engineering and Processing: Process Intensification*, 47(7), 1150–1158. <https://doi.org/10.1016/j.cep.2007.03.010>
- Demirag, O., & Konuskan, D. B. (2021). Quality properties, fatty acid and sterol compositions of east mediterranean region olive oils. *Journal of Oleo Science*, 70(1), 51–58. <https://doi.org/10.5650/jos.ess20179>
- Desai, K. G. H., & Jin Park, H. (2005). Recent Developments in Microencapsulation of Food Ingredients. *Drying Technology*. <https://doi.org/10.1081/DRT-200063478>
- Devi, N., Hazarika, D., Deka, C., & Kakati, D. K. (2012). Study of complex coacervation of gelatin a and sodium alginate for microencapsulation of olive oil. *Journal of Macromolecular Science, Part A: Pure and Applied Chemistry*, 49(11), 936–945. <https://doi.org/10.1080/10601325.2012.722854>
- Dias, M.I., Ferreira, I.C. & Barreiro, M.F. (2015). Microencapsulation of bioactives for food applications. *Food and Function*, 6(4), 1035–1052. <https://doi.org/10.1039/c4fo01175a>
- Dickinson, E. (2009). Hydrocolloids as emulsifiers and emulsion stabilizers. *Food Hydrocolloids*, 23(6), 1473–1482. <https://doi.org/10.1016/j.foodhyd.2008.08.005>
- Dimitrios, B. (2006). Sources of natural phenolic antioxidants. *Trends in Food Science and Technology*, 17(9), 505–512. <https://doi.org/10.1016/j.tifs.2006.04.004>
- Dini, I., Seccia, S., Senatore, A., Coppola, D., & Morelli, E. (2020). Development and Validation of an Analytical Method for Total Polyphenols Quantification in Extra Virgin Olive Oils. *Food Analytical Methods*, 13(2), 457–464. <https://doi.org/10.1007/s12161-019-01657-7>
- Espí, F., Vidal, A. M., Espí, J. M., & Moya, M. (2021). *Processing Effect and Characterization of Olive Oils from Spanish Wild Olive Trees (Olea europaea var . sylvestris)*. 1–14.
- Fang, Z., & Bhandari, B. (2010). Encapsulation of polyphenols - A review. In *Trends in Food Science and Technology* (Vol. 21, Issue 10, pp. 510–523). <https://doi.org/10.1016/j.tifs.2010.08.003>
- Fang, Z., & Bhandari, B. (2012). Spray drying, freeze drying and related processes for food

- ingredient and nutraceutical encapsulation. In *Encapsulation Technologies and Delivery Systems for Food Ingredients and Nutraceuticals*. Elsevier Masson SAS. <https://doi.org/10.1533/9780857095909.2.73>
- Fioramonti, S. A., Rubiolo, A. C., & Santiago, L. G. (2017). Characterisation of freeze-dried flaxseed oil microcapsules obtained by multilayer emulsions. *Powder Technology*, 319, 238–244. <https://doi.org/10.1016/j.powtec.2017.06.052>
- Fongin, S., Kawai, K., Harnkarnsujarit, N., & Hagura, Y. (2017). Effects of water and maltodextrin on the glass transition temperature of freeze-dried mango pulp and an empirical model to predict plasticizing effect of water on dried fruits. *Journal of Food Engineering*, 210, 91–97. <https://doi.org/10.1016/j.jfoodeng.2017.04.025>
- Frankel, E. N. (1984). Lipid oxidation: Mechanisms, products and biological significance. In *Journal of the American Oil Chemists' Society* (Vol. 61, Issue 12, pp. 1908–1917). <https://doi.org/10.1007/BF02540830>
- Frascareli, E. C., Silva, V. M., Tonon, R. V., & Hubinger, M. D. (2012). Effect of process conditions on the microencapsulation of coffee oil by spray drying. *Food and Bioprocess Technology*, 90(3), 413–424. <https://doi.org/10.1016/j.fbp.2011.12.002>
- Friberg, S. E., Corkery, R. W., & Blute, I. A. (2011). Phase inversion temperature (PIT) emulsification process. *Journal of Chemical and Engineering Data*. <https://doi.org/10.1021/je101179s>
- Gaforio, J. J., Visioli, F., Alarcón-De-la-lastra, C., Castañer, O., Delgado-Rodríguez, M., Fitó, M., Hernández, A. F., Huertas, J. R., Martínez-González, M. A., Menendez, J. A., de la Osada, J., Papadaki, A., Parrón, T., Pereira, J. E., Rosillo, M. A., Sánchez-Quesada, C., Schwingshackl, L., Toledo, E., & Tsatsakis, A. M. (2019). Virgin olive oil and health: Summary of the iii international conference on virgin olive oil and health consensus report, JAEN (Spain) 2018. *Nutrients*, 11(9). <https://doi.org/10.3390/nu11092039>
- Gaikwad, S. G., & Pandit, A. B. (2008). Ultrasound emulsification: Effect of ultrasonic and physicochemical properties on dispersed phase volume and droplet size. *Ultrasonics Sonochemistry*. <https://doi.org/10.1016/j.ultsonch.2007.06.011>
- Gallardo, G., Guida, L., Martinez, V., López, M. C., Bernhardt, D., Blasco, R., Pedroza-Islas, R., & Hermida, L. G. (2013). Microencapsulation of linseed oil by spray drying for functional food application. *Food Research International*, 52(2), 473–482. <https://doi.org/10.1016/j.foodres.2013.01.020>
- Ghanbari Shendi, E., Sivri Ozay, D., Ozkaya, M. T., & Ustunel, N. F. (2018). Changes occurring in chemical composition and oxidative stability of virgin olive oil during storage. *OCL - Oilseeds and Fats, Crops and Lipids*, 25(6), 4–11. <https://doi.org/10.1051/ocl/2018052>
- Gharsallaoui, A., Roudaut, G., Chambin, O., Voilley, A., & Saurel, R. (2007). Applications of spray-drying in microencapsulation of food ingredients: An overview. In *Food Research International*. <https://doi.org/10.1016/j.foodres.2007.07.004>
- Gijsbertsen-Abrahamse, A. (2003). *Membrane emulsification: process principles* [Wageningen University]. ISBN 90-5808-845-6
- Gorini, I., Iorio, S., Armocida, G., Ciliberti, R., & Marta, M. L. (2019). Olive oil in pharmacological and cosmetic traditions. *September 2018*, 1575–1579.

<https://doi.org/10.1111/jocd.12838>

- Goupy, J. (2006). Les plans d'expériences. *Revue Modulad*, 34, 74–116.
- Gunstone, F. D. (2011). Production and Trade of Vegetable Oils. In *Vegetable Oils in Food Technology*. <https://doi.org/10.1002/9781444339925.ch1>
- Hogan, S. A., McNamee, B. F., O'Riordan, E. D., & O'Sullivan, M. (2001). Emulsification and microencapsulation properties of sodium caseinate/carbohydrate blends. *International Dairy Journal*, 11(3), 137–144. [https://doi.org/10.1016/S0958-6946\(01\)00091-7](https://doi.org/10.1016/S0958-6946(01)00091-7)
- Jafari, S. M., Assadpoor, E., He, Y., & Bhandari, B. (2008). *Encapsulation Efficiency of Food Flavours and Oils during Spray Drying*. 3937. <https://doi.org/10.1080/07373930802135972>
- Japir, A. A. W., Salimon, J., Derawi, D., Bahadi, M., Al-Shuja'A, S., & Yusop, M. R. (2017). Physicochemical characteristics of high free fatty acid crude palm oil. *OCL - Oilseeds and Fats, Crops and Lipids*, 24(5). <https://doi.org/10.1051/ocl/2017033>
- Jos, F. (2018). *The Use of Plants in Skin-Care Products, Cosmetics and Fragrances: Past and Present*. 1–9. <https://doi.org/10.3390/cosmetics5030050>
- Joscelyne, S. M., & Trägårdh, G. (2000). Membrane emulsification-a literature review. In *Journal of Membrane Science* (Vol. 169).
- Jyothi, N. V. N., Prasanna, P. M., Sakarkar, S. N., Prabha, K. S., Ramaiah, P. S., & Srawan, G. Y. (2010). Microencapsulation techniques, factors influencing encapsulation efficiency. *Journal of Microencapsulation*, 27(3), 187–197. <https://doi.org/10.3109/02652040903131301>
- Karaca, A. C., Nickerson, M., & Low, N. H. (2013). Microcapsule production employing chickpea or lentil protein isolates and maltodextrin: Physicochemical properties and oxidative protection of encapsulated flaxseed oil. *Food Chemistry*, 139(1–4), 448–457. <https://doi.org/10.1016/j.foodchem.2013.01.040>
- Karina, A., Barroso, M., Paola, A., Rocha, T., Freitas, P., Torres, A. G., & Helena, M. (2014). Oxidative stability and sensory evaluation of microencapsulated flaxseed oil. *Journal of Microencapsulation*, 31(2), 193–201. <https://doi.org/10.3109/02652048.2013.824514>
- Karoui, I. J., Ayari, J., Ghazouani, N., & Abderrabba, M. (2020). Physicochemical and biochemical characterizations of some Tunisian seed oils. *OCL - Oilseeds and Fats, Crops and Lipids*, 27. <https://doi.org/10.1051/ocl/2019035>
- Kashaninejad, M., Sanz, M. T., Blanco, B., Beltrán, S., & Niknam, S. M. (2017). Food and Bioproducts Processing Freeze dried extract from olive leaves: Valorisation, extraction kinetics and extract characterization. *Food and Bioproducts Processing*, 124, 196–207. <https://doi.org/10.1016/j.fbp.2020.08.015>
- Kaushik, P., Dowling, K., Barrow, C. J., & Adhikari, B. (2015). Microencapsulation of omega-3 fatty acids: A review of microencapsulation and characterization methods. In *Journal of Functional Foods* (Vol. 19, pp. 868–881). Elsevier Ltd. <https://doi.org/10.1016/j.jff.2014.06.029>
- Kinyanjui, T., Artz, W. E., & Mahungu, S. (2003). EMULSIFIERS | Organic Emulsifiers. *Encyclopedia of Food Sciences and Nutrition*, 2070–2077. <https://doi.org/10.1016/b0-12-227055-x/00401-6>

- Klaypradit, W., & Huang, Y. W. (2008). Fish oil encapsulation with chitosan using ultrasonic atomizer. *LWT - Food Science and Technology*, 41(6), 1133–1139. <https://doi.org/10.1016/j.lwt.2007.06.014>
- Koç, M., Güngör, Ö., Zungur, A., Yalçın, B., Selek, İ., Ertekin, F. K., & Ötles, S. (2015). Microencapsulation of Extra Virgin Olive Oil by Spray Drying: Effect of Wall Materials Composition, Process Conditions, and Emulsification Method. *Food and Bioprocess Technology*, 8(2), 301–318. <https://doi.org/10.1007/s11947-014-1404-9>
- Koidis, A., & Boskou, D. (2014). Virgin Olive Oil: Losses of Antioxidant Polar Phenolic Compounds due to Storage, Packaging, and Culinary Uses. In *Processing and Impact on Active Components in Food*. Elsevier Inc. <https://doi.org/10.1016/B978-0-12-404699-3.00032-9>
- Koris, A., Piacentini, E., Vatai, G., Bekassy-Molnar, E., Drioli, E., & Giorno, L. (2011). Investigation on the effects of a mechanical shear-stress modification method during cross-flow membrane emulsification. *Journal of Membrane Science*, 371(1–2), 28–36. <https://doi.org/10.1016/j.memsci.2011.01.005>
- Kurozawa, L. E., & Hubinger, M. D. (2017). Hydrophilic food compounds encapsulation by ionic gelation. *Current Opinion in Food Science*, 15, 50–55. <https://doi.org/10.1016/J.COFS.2017.06.004>
- la Lastra, C., Barranco, M., Motilva, V., & Herrerias, J. (2005). Mediterranean Diet and Health Biological Importance of Olive Oil. *Current Pharmaceutical Design*, 7(10), 933–950. <https://doi.org/10.2174/1381612013397654>
- Lambrich, U., & Schubert, H. (2005). Emulsification using microporous systems. *Journal of Membrane Science*, 257(1–2), 76–84. <https://doi.org/10.1016/j.memsci.2004.12.040>
- Lapez-Montilla, J. C., Herrera-Morales, P. E., Pandey, S., & Shah, D. O. (2002). Spontaneous emulsification: Mechanisms, physicochemical aspects, modeling, and applications. *Journal of Dispersion Science and Technology*. <https://doi.org/10.1081/DIS-120003317>
- Lebrun, P., Krier, F., Mantanus, J., Grohgan, H., Yang, M., Rozet, E., Boulanger, B., Evrard, B., Rantanen, J., & Hubert, P. (2012). Design space approach in the optimization of the spray-drying process. *European Journal of Pharmaceutics and Biopharmaceutics*, 80(1), 226–234. <https://doi.org/10.1016/j.ejpb.2011.09.014>
- Lee, S. M., Cho, A. R. ., Yoo, S.-H. ., & Kim, Y.-S. (2017). *Effects of maltodextrins with different dextrose - equivalent values*. 33, 153–159. <https://doi.org/10.1002/ffj.3410>
- Lei, M., Jiang, F.-C., Cai, J., Hu, S., Zhou, R., Liu, G., Wang, Y.-H., Wang, H.-B., He, J.-R., & Xiong, X.-G. (2018). Facile microencapsulation of olive oil in porous starch granules: Fabrication, characterization, and oxidative stability. *International Journal of Biological Macromolecules*. <https://doi.org/10.1016/j.ijbiomac.2018.01.051>
- Li, K., Pan, B., Ma, L., Miao, S., & Ji, J. (2020). Effect of Dextrose Equivalent on Maltodextrin/Whey Protein Spray-Dried Powder Microcapsules and Dynamic Release of Loaded Flavor during Storage and Powder Rehydration. *Foods*, 12(9), 1878. <https://doi.org/10.3390/foods9121878>
- Li, Y., Zhang, Y., Dai, W., & Zhang, Q. (2021). Enhanced oral absorption and anti-inflammatory activity of ellagic acid via a novel type of case in nanosheets constructed by simple coacervation. *International Journal of Pharmaceutics*, 594(July 2020), 120131.

<https://doi.org/10.1016/j.ijpharm.2020.120131>

- Liu, C., Qin, S., Xie, J., Lin, X., Zheng, Y., Yang, J., & Kan, H. (2021). *Using Carboxymethyl Cellulose as the Additive With Enzyme-Catalyzed Carboxylated Starch to Prepare the Film With Enhanced Mechanical and Hydrophobic Properties*. 9(February), 1–11. <https://doi.org/10.3389/fbioe.2021.638546>
- Liu, T. T., & Yang, T. S. (2011). Optimization of Emulsification and Microencapsulation of Evening Primrose Oil and Its Oxidative Stability During Storage By Response Surface Methodology. *Journal of Food Quality*, 34(1), 64–73. <https://doi.org/10.1111/j.1745-4557.2010.00358.x>
- Lloyd, D. M., Norton, I. T., & Spyropoulos, F. (2015). Process optimisation of rotating membrane emulsification through the study of surfactant dispersions. *Journal of Food Engineering*, 166, 316–324. <https://doi.org/10.1016/j.jfoodeng.2015.06.028>
- López, A., Castro, S., Andina, M. J., Ures, X., Munguía, B., Llabot, J. M., Elder, H., Dellacassa, E., Palma, S., & Domínguez, L. (2014). Insecticidal activity of microencapsulated Schinus molle essential oil. *Industrial Crops and Products*, 53, 209–216. <https://doi.org/10.1016/j.indcrop.2013.12.038>
- Ludwig, D. S. (2020). The Ketogenic Diet: Evidence for Optimism but High-Quality Research Needed. *Journal of Nutrition*, 150(6), 1354–1359. <https://doi.org/10.1093/jn/nxz308>
- Luz, C., Pinto, D., Delerue-matos, C., & Rodrigues, F. (2021). *Olive Fruit and Leaf Wastes as Bioactive Ingredients for Cosmetics — A Preliminary Study*.
- Maa, Y. F., & Hsu, C. (1996). Liquid-liquid emulsification by rotor/stator homogenization. *Journal of Controlled Release*, 38(2–3), 219–228. [https://doi.org/10.1016/0168-3659\(95\)00123-9](https://doi.org/10.1016/0168-3659(95)00123-9)
- Mahdi, A. A., Mohammed, J. K., Al-Ansi, W., Ghaleb, A. D. S., Al-Maqtari, Q. A., Ma, M., Ahmed, M. I., & Wang, H. (2020). Microencapsulation of fingered citron extract with gum arabic, modified starch, whey protein, and maltodextrin using spray drying. *International Journal of Biological Macromolecules*, 152, 1125–1134. <https://doi.org/10.1016/j.ijbiomac.2019.10.201>
- Mailer, R., & Beckingham, C. (2006). Testing olive oil quality : chemical and sensory methods. *Profitable & Sustainable Primary Industries, PRIMEFACT*, 231, 1–5.
- Manai-Djebali, H., Krichène, D., Ouni, Y., Gallardo, L., Sánchez, J., Osorio, E., Daoud, D., Guido, F., & Zarrouk, M. (2012). Chemical profiles of five minor olive oil varieties grown in central Tunisia. *Journal of Food Composition and Analysis*, 27(2), 109–119. <https://doi.org/10.1016/j.jfca.2012.04.010>
- Maria T. Morales and Roman Przybylski. (2013). Olive oil oxidation. In *Handbook of Olive Oil: Analysis and Properties* (pp. 1–772). <https://doi.org/10.1007/978-1-4614-7777-8>
- Martins, E., Poncelet, D., Rodrigues, R. C., Martins, E., Poncelet, D., Rodrigues, R. C., & Renard, D. (2017). Oil encapsulation techniques using alginate as encapsulating agent : applications and drawbacks. *Journal of Microencapsulation*, 0(0), 754–771. <https://doi.org/10.1080/02652048.2017.1403495>
- Martins, I. M. D. (2012). *Microencapsulation of Thyme Oil by Coacervation: Production, Characterization and Release Evaluation*. University of Porto.

- McClements, D. J., & Jafari, S. M. (2018). Improving emulsion formation, stability and performance using mixed emulsifiers: A review. *Advances in Colloid and Interface Science*, 251, 55–79. <https://doi.org/10.1016/j.cis.2017.12.001>
- Mishra, M. (2015). Overview of Encapsulation and Controlled Release. In *Handbook of Encapsulation and Controlled Release* (pp. 3–19). CRC Press. <https://doi.org/10.1201/b19038-3>
- Moldão-Martins, M., Beirão-da-Costa, S., Neves, C., Cavaleiro, C., Salgueiro, L., & Luísa Beirão-da-Costa, M. (2004). Olive oil flavoured by the essential oils of *Mentha × piperita* and *Thymus mastichina* L. *Food Quality and Preference*, 15(5), 447–452. <https://doi.org/10.1016/j.foodqual.2003.08.001>
- Morales, E., Rubilar, M., Burgos-Díaz, C., Acevedo, F., Penning, M., & Shene, C. (2017). Alginate/Shellac beads developed by external gelation as a highly efficient model system for oil encapsulation with intestinal delivery. *Food Hydrocolloids*, 70, 321–328. <https://doi.org/10.1016/j.foodhyd.2017.04.012>
- Mousavi, S., Mariotti, R., Stanzione, V., Pandolfi, S., Mastio, V., Baldoni, L., & Cultrera, N. G. M. (2021). Evolution of extra virgin olive oil quality under different storage conditions. *Foods*, 10(8), 1–19. <https://doi.org/10.3390/foods10081945>
- Nabilah, A., Handayani, S., Setiasih, S., Rahayu, D. U. C., & Hudiyono, S. (2020). Emulsifier and antimicrobial activity against *Propionibacterium acnes* and *Staphylococcus epidermidis* of oxidized fatty acid esters from hydrolyzed castor oil. *IOP Conference Series: Materials Science and Engineering*, 833(1). <https://doi.org/10.1088/1757-899X/833/1/012025>
- Nakashima, T., Shimizu, M., & Kukizaki, M. (2000). Particle control of emulsion by membrane emulsification and its applications. *Advanced Drug Delivery Reviews*, 45(1), 47–56. [https://doi.org/10.1016/S0169-409X\(00\)00099-5](https://doi.org/10.1016/S0169-409X(00)00099-5)
- Naz, S., Shabbir, M. A., Aadil, R. M., Khan, M. R., Ciftci, O. N., Sameen, A., Yasmin, I., Hayee, A., & Maqsood, M. (2020). Effect of polymer and polymer blends on encapsulation efficiency of spray-dried microencapsulated flaxseed oil. *International Food Research Journal*, 27(1), 78–87. <http://www.ifrj.upm.edu.my>
- Nazari, M., Mehrnia, M. A., Jooyandeh, H., & Barzegar, H. (2019). Preparation and characterization of water in sesame oil microemulsion by spontaneous method. *Journal of Food Process Engineering*, 42(4), 1–8. <https://doi.org/10.1111/jfpe.13032>
- Netto, F. M., Desobry, S. A., & Labuza, T. P. (1998). Effect of water content on the glass transition, caking and stickiness of protein hydrolysates. *International Journal of Food Properties*, 1(2), 141–161. <https://doi.org/10.1080/10942919809524573>
- Ogrodowska, D., Tanska, M., Brandt, W., & Czaplicki, S. (2020). Impact of the encapsulation process by spray- And freeze-drying on the properties and composition of powders obtained from cold-pressed seed oils with various unsaturated fatty acids. *Polish Journal of Food and Nutrition Sciences*, 70(3), 241–252. <https://doi.org/10.31883/pjfn/120314>
- Onsaard, E., & Onsaard, W. (2019). Microencapsulated Vegetable Oil Powder. *Microencapsulation - Processes, Technologies and Industrial Applications*, 1–19. <https://doi.org/10.5772/intechopen.85351>
- Otles, S., & Cagindi, O. (2007). *Food Chemistry Determination of vitamin K 1 content in olive*

- oil , chard and human plasma by RP-HPLC method with UV – Vis detection. 100, 1220–1222. <https://doi.org/10.1016/j.foodchem.2005.12.003>
- Ozkan, G., Franco, P., De Marco, I., Xiao, J., & Capanoglu, E. (2019). A review of microencapsulation methods for food antioxidants: Principles, advantages, drawbacks and applications. *Food Chemistry*, 272(July 2018), 494–506. <https://doi.org/10.1016/j.foodchem.2018.07.205>
- Paulo, F., & Santos, L. (2020). Deriving valorization of phenolic compounds from olive oil by-products for food applications through microencapsulation approaches: a comprehensive review. *Critical Reviews in Food Science and Nutrition*, 0(0), 1–26. <https://doi.org/10.1080/10408398.2020.1748563>
- Pawlik, A. K., & Norton, I. T. (2012). Encapsulation stability of duplex emulsions prepared with SPG cross-flow membrane, SPG rotating membrane and rotor-stator techniques-A comparison. *Journal of Membrane Science*, 415–416, 459–468. <https://doi.org/10.1016/j.memsci.2012.05.032>
- Pedro, R. B., Tonon, R. V., & Hubinger, M. D. (2011). Effect of Oil Concentration on the Microencapsulation of Flaxseed Oil By Spray Drying. *III Jornadas Internacionais Sobre Avances En La Tecnología de Filmes y Coberturas Funcionales En Alimentos*, 5.
- Piacentini, E., Drioli, E., & Giorno, L. (2014). Membrane emulsification technology: Twenty-five years of inventions and research through patent survey. In *Journal of Membrane Science* (Vol. 468, pp. 410–422). Elsevier. <https://doi.org/10.1016/j.memsci.2014.05.059>
- Poirieux, M., Kostov, G., Denkova, R., Shopska, V., Ivanova, M., Balabanova, T., & Vlasseva, R. (2017). Optimization of Conditions for Obtaining Alginate/Olive Oil Capsules for Application in Dairy Industry. *Acta Universitatis Cibiniensis. Series E: Food Technology*, 21(1), 11–22. <https://doi.org/10.1515/auaft-2017-0002>
- Poshadri, A., & Kuna, A. (2010). MICROENCAPSULATION TECHNOLOGY: A REVIEW. *The Journal of Research ANGRAU*, 38(1), 86–102.
- Psomiadou, E., Tsimidou, M., & Boskou, D. (2000). alpha-tocopherol content of Greek virgin olive oils. *Journal of Agricultural and Food Chemistry*, 48(5), 1770–1775.
- Purwanti, N., Smiddy, M., Jan van der Goot, A., de Vries, R., Alting, A., & Boom, R. (2011). Modulation of rheological properties by heat-induced aggregation of whey protein solution. *Food Hydrocolloids*, 25(6), 1482–1489. <https://doi.org/10.1016/j.foodhyd.2011.02.027>
- Reineccius, G. A. (2004). The spray drying of food flavors. *Drying Technology*, 22(6), 1289–1324. <https://doi.org/10.1081/DRT-120038731>
- Reis, C. P., Neufeld, R. J., Vilela, S., Ribeiro, N. I. O. J., & Veiga, F. (2006). Review and current status of emulsion / dispersion technology using an internal gelation process for the design of alginate particles. 23(May), 245–257. <https://doi.org/10.1080/02652040500286086>
- Risch, S. J. (1988). Encapsulation of Flavors by Extrusion. In Risch Sara J. and Reineccius Gary A. (Ed.), *Flavor Encapsulation* (ACS Sympos, Vol. 370, pp. 103–109). American Chemical Society. <https://doi.org/10.1021/bk-1988-0370.ch011>
- Rodríguez, J., Martín, M. J., Ruiz, M. A., & Clares, B. (2016). Current encapsulation strategies for bioactive oils: From alimentary to pharmaceutical perspectives. In *Food Research*

International (Vol. 83, pp. 41–59). Elsevier Ltd.
<https://doi.org/10.1016/j.foodres.2016.01.032>

- Roszkowska, B., Tańska, M., Czaplicki, S., & Konopka, I. (2015). Variation in the composition and oxidative stability of commercial rapeseed oils during their shelf life. *European Journal of Lipid Science and Technology*, 117(5), 673–683. <https://doi.org/10.1002/ejlt.201400271>
- Rubilar, M., Morales, E., Contreras, K., Ceballos, C., Acevedo, F., Villarroel, M., & Shene, C. (2012). Development of a soup powder enriched with microencapsulated linseed oil as a source of omega-3 fatty acids. *European Journal of Lipid Science and Technology*, 114(4), 423–433. <https://doi.org/10.1002/ejlt.201100378>
- Rutz, J. K., Borges, C. D., Zambiasi, R. C., Crizel-Cardozo, M. M., Kuck, L. S., & Noreña, C. P. Z. (2017). Microencapsulation of palm oil by complex coacervation for application in food systems. *Food Chemistry*, 220, 59–66. <https://doi.org/10.1016/j.foodchem.2016.09.194>
- Samantha, S. C., Bruna, A. S. M., Adriana, R. M., Fabio, B., Sandro, A. R., & Aline, R. C. A. (2015). Drying by spray drying in the food industry: Micro-encapsulation, process parameters and main carriers used. *African Journal of Food Science*, 9(9), 462–470. <https://doi.org/10.5897/ajfs2015.1279>
- Šarolić, M., Gugić, M., Marijanović, Z., & Šuste, M. (2014). Virgin olive oil and nutrition. *Food in Health and Disease, Scientific-Professional Journal of Nutrition and Dietetics*, 3(1), 38–43. <https://hrcak.srce.hr/126239>
- Shahidi, F., & Han, X. Q. (1993). Encapsulation of Food Ingredients. *Critical Reviews in Food Science and Nutrition*, 33(6), 501–547. <https://doi.org/10.1080/10408399309527645>
- Siemons, I., Politiek, R. G. A., Boom, R. M., van der Sman, R. G. M., & Schutyser, M. A. I. (2020). Dextrose equivalence of maltodextrins determines particle morphology development during single sessile droplet drying. *Food Research International*, 131, 108988. <https://doi.org/10.1016/j.foodres.2020.108988>
- Silva, K. A., Coelho, M. A. Z., Calado, V. M. A., & Rocha-LeAão, M. H. M. (2013). Olive oil and lemon salad dressing microencapsulated by freeze-drying. *LWT - Food Science and Technology*, 50(2), 569–574. <https://doi.org/10.1016/j.lwt.2012.08.005>
- Solans, C., Morales, D., & Homs, M. (2016). Spontaneous emulsification. In *Current Opinion in Colloid and Interface Science*. <https://doi.org/10.1016/j.cocis.2016.03.002>
- Souza, W. J., Santos, K. M. C., Cruz, A. A., Franceschi, E., Dariva, C., Santos, A. F., & Santana, C. C. (2015). Effect of Water Content, Temperature and Average Droplet Size on the Settling Velocity of Water-in-Oil-Emulsions. *Brazilian Journal of Chemical Engineering*, 32(02), 455–464. <https://doi.org/doi:10.1590/0104-6632.20150322s00003323>
- Stang, M., Schuchmann, H., & Schubert, H. (2001). Emulsification in High-Pressure Homogenizers. *Engineering in Life Sciences*, 1(4), 151. [https://doi.org/10.1002/1618-2863\(200110\)1:4<151::aid-elsc151>3.0.co;2-d](https://doi.org/10.1002/1618-2863(200110)1:4<151::aid-elsc151>3.0.co;2-d)
- Sudheera Polavarapu, Christine M. Oliver, Said Ajlouni, M. A. A. (2011). Physicochemical characterisation and oxidative stability of fish oil and fish oil-extra virgin olive oil microencapsulated by sugar beet pectin. *Food Chemistry*, 127(4), 1694–1705. <https://doi.org/10.1016/j.foodchem.2011.02.044>

- Sun-Waterhouse, D., Zhou, J., Miskelly, G. M., Wibisono, R., & Wadhwa, S. S. (2011). Stability of encapsulated olive oil in the presence of caffeic acid. *Food Chemistry*, 126(3), 1049–1056. <https://doi.org/10.1016/j.foodchem.2010.11.124>
- Tan, L. H., Chan, L. W., & Heng, P. W. S. (2005). *Effect of oil loading on microspheres produced by spray drying*. 22(May), 253–259. <https://doi.org/10.1080/02652040500100329>
- Tonon, R. V., Grosso, C. R. F., & Hubinger, M. D. (2011). Influence of emulsion composition and inlet air temperature on the microencapsulation of flaxseed oil by spray drying. *Food Research International*, 44(1), 282–289. <https://doi.org/10.1016/j.foodres.2010.10.018>
- Tonon, R. V., Pedro, R. B., Grosso, C. R. F., & Hubinger, M. D. (2012). Microencapsulation of Flaxseed Oil by Spray Drying: Effect of Oil Load and Type of Wall Material. *Drying Technology*, 30(13), 1491–1501. <https://doi.org/10.1080/07373937.2012.696227>
- Tontul, I., & Topuz, A. (2014). Influence of emulsion composition and ultrasonication time on flaxseed oil powder properties. *Powder Technology*, 264, 54–60. <https://doi.org/10.1016/j.powtec.2014.05.002>
- Velasco, J., Dobarganes, C., Holgado, F., & Márquez-Ruiz, G. (2009). A follow-up oxidation study in dried microencapsulated oils under the accelerated conditions of the Rancimat test. *Food Research International*, 42(1), 56–62. <https://doi.org/10.1016/j.foodres.2008.08.012>
- Velasco, J., M. C. Dobarganes, & G. Márquez-Ruiz. (2000). Application of the accelerated test Rancimat to evaluate oxidative stability of dried microencapsulated oils. *Grasas y Aceites*, 51(4), 261–267. <https://doi.org/10.3989/gya.2000.v51.i4.422>
- Viola, P., & Viola, M. (2009). Virgin olive oil as a fundamental nutritional component and skin protector. *Clinics in Dermatology*, 27(2), 159–165. <https://doi.org/10.1016/j.clindermatol.2008.01.008>
- Volker, S., Olaf B. & Helmar, S. (1998). Effect of Dynamic Interfacial Tension on the Emulsification Process Using Microporous , Ceramic Membranes. *Journal of Colloid and Interface Science*, 202(2), 334–340. <https://doi.org/https://doi.org/10.1006/jcis.1998.5429>
- Wangsakan, A., Chinachoti, P., & McClements, D. J. (2003). Effect of Different Dextrose Equivalent of Maltodextrin on the Interactions with Anionic Surfactant in an Isothermal Titration Calorimetry Study. *Journal of Agricultural and Food Chemistry*, 51(26), 7810–7814. <https://doi.org/10.1021/jf034052u>
- Wiesman, Z. (2009). The future of desert olive oil, and concluding remarks. *Desert Olive Oil Cultivation*, 387–394. <https://doi.org/10.1016/B978-0-12-374257-5.00018-X>
- Xu, S., Tang, Z., Liu, H., Wang, M., Sun, J., Song, Z., Cui, C., Sun, C., Liu, S., Wang, Z., & Yu, J. (2020). Microencapsulation of sea buckthorn (*Hippophae rhamnoides* L.) pulp oil by spray drying. *Food Science and Nutrition*, 8(11), 5785–5797. <https://doi.org/10.1002/fsn3.1828>
- Yakdhane, A., Labidi, S., Chaabane, D., Tolnay, A., Nath, A., Koris, A., & Vatai, G. (2021). Microencapsulation of Flaxseed Oil—State of Art. *Processes*, 9(2), 295. <https://doi.org/10.3390/pr9020295>
- Yang, X., Li, S., Yan, J., Xia, J., Huang, L., Li, M., Ding, H., & Xu, L. (2020). Effect of different combinations of emulsifier and wall materials on physical properties of spray-dried

- microencapsulated swida wilsoniana oil. In *Journal of Bioresources and Bioproducts* (Vol. 5, Issue 1, pp. 44–50). <https://doi.org/10.1016/j.jobab.2020.03.005>
- Yorulmaz, H. O., & Konuskan, D. B. (2017). Antioxidant activity, sterol and fatty acid compositions of Turkish olive oils as an indicator of variety and ripening degree. *Journal of Food Science and Technology*, 54(12), 4067–4077. <https://doi.org/10.1007/s13197-017-2879-y>
- Zanatta, V., Rezzadori, K., Penha, F. M., Zin, G., Lemos-Senna, E., Petrus, J. C. C., & Di Luccio, M. (2017). Stability of oil-in-water emulsions produced by membrane emulsification with microporous ceramic membranes. *Journal of Food Engineering*. <https://doi.org/10.1016/j.jfoodeng.2016.09.025>
- Zhao, X., & Tang, C. (2016). Food Hydrocolloids Spray-drying microencapsulation of CoQ 10 in olive oil for enhanced water dispersion , stability and bioaccessibility : In fl uence of type of emulsi fi ers and / or wall materials. *Food Hydrocolloids*, 61, 20–30. <https://doi.org/10.1016/j.foodhyd.2016.04.045>
- Zhou, P., & Labuza, T. P. (2007). Effect of water content on glass transition and protein aggregation of whey protein powders during short-term storage. *Food Biophysics*, 2(2–3), 108–116. <https://doi.org/10.1007/s11483-007-9037-4>
- Zhu, J., Li, X., Liu, L., Li, Y., Qi, B., & Jiang, L. (2022). Preparation of spray-dried soybean oil body microcapsules using maltodextrin: Effects of dextrose equivalence. *Lwt*, 154, 112874. <https://doi.org/10.1016/j.lwt.2021.112874>

Annex 2



Appendix- Figure 1: Rotor-stator homogenizer (DLAB D-160).



Appendix- Figure 2: Controlled-stress physica MCR92 rheometer (Anton Paar).



Appendix- Figure 3: Freeze drying machine.



Appendix- Figure 4: Spray drying machine.



Appendix- Figure 5: Picture of oil loaded dried microcapsules obtained by different drying methods. A: microcapsules obtained by freeze-drying, B: Microcapsules obtained by spray-drying.



Appendix- Figure 6: FRITSH laser Particle Sizer ANALYSETTE 22 NanoTec.



Appendix- Figure 7: External gelation experimental settlement.



Appendix- Figure 8: Malvern Zetasizer apparatus.



Appendix- Figure 9: Oil loaded sodium alginate beads



Appendix- Figure 8: Rancimat for oxidative stability measurement.

ACKNOWLEDGEMENT

I would like to thank myself for not giving up easily and for enduring all the challenges that I have faced during the long PhD journey. I am still on track even if a lot of destructions like depression, anxiety, uncertainty, judgement, loneliness etc. have come along to me to bring me down all the way. I didn't fail myself and thrived instead. I am proud of myself for who I became.

Firstly, let me express my special thanks to my supervisor, Dr András Koris for accepting me as a PhD student at the Hungarian University of Agriculture and Life Sciences (MATE) which brought me here, to a lovely city, Budapest. I am grateful to his continuous support.

Secondly, I would like to express my gratitude to my supervisor, Dr Krisztina Albert for her endless support, kindness, and understanding spirit during my PhD journey.

Third, I would like to express my gratitude to, Dr Arijit Nath that I have learned a lot from him. His encouragement made me believe in myself more.

I am delighted to be granted by Tempus Public Foundation (Stipendium Hungaricum Scholarship). I cannot thank them enough for their amazing support to make our student life easier in every possible way.

A special thanks to all my colleagues from the department of food process engineering, as well as the faculty of food sciences for helping me within their limits. I would also give a special thanks to all my lecturers, their contributions are sincerely appreciated and gratefully acknowledged.

Finally, I must say “thank you” to my husband, daughter, parents and family for their endless love and care for me. I couldn't have passed life exams without them. They are the reason that I am alive and want to live more.